EFFECT OF ROCK JOINT FREQUENCY AND APERTURE ON CERCHAR ABRASIVITY INDEX

RATCHAPON MINGKHWAN

A Thesis Submitted in Partial Fulfillment of the Requirements for the
Degree of Master of Engineering in Civil, Transportation
and Geo-resources Engineering
Suranaree University of Technology
Academic Year 2024

ผลของความถี่ของรอยแตกและช่องว่างของหินต่อดัชนีการสึกกร่อนเซอคาร์

นายรัชพล มิ่งขวัญ

วิทยานิพนธ์นี้เป็นส่วนหนึ่งของการศึกษาตามหลักสูตรปริญญาวิศวกรรมศาสตรมหาบัณฑิต
สาขาวิชาวิศวกรรมโยธา ขนส่ง และทรัพยากรธรณี
มหาวิทยาลัยเทคโนโลยีสุรนารี
ปีการศึกษา 2567

EFFECT OF ROCK JOINT FREQUENCY AND APERTURE ON CERCHAR ABRASIVITY INDEX

Suranaree University of Technology has approved this thesis submitted in partial fulfillment of the requirements for a Master's Degree.

Thesis Examining Committee

.....

(Assoc. Prof. Dr. Pornkasem Jongpradist)
Chairperson

.....

(Emeritus Prof. Dr. Kittitep Fuenkajorn)
Member (Thesis Advisor)

.....

(Asst. Prof. Dr. Prachya Tepnarong)
Member

.....

(Assoc. Prof. Dr. Yupaporn Ruksakulpiwat)
Vice Rector for Academic Affairs
and Quality Assurance

.....

(Assoc. Prof. Dr. Pornsiri Jongkol)
Dean of Institute of Engineering

รัชพล มิ่งขวัญ: ผลของความถี่ของรอยแตกและช่องว่างของหินต่อดัชนีการสึกกร่อนเซอคาร์ (EFFECT OF ROCK JOINT FREQUENCY AND APERTURE ON CERCHAR ABRASIVITY INDEX)
อาจารย์ที่ปรึกษา: ศาสตราจารย์ (เกียรติคุณ) ดร.กิตติเทพ เฟื่องขจร 118 หน้า

คำสำคัญ: จำนวนรอยต่อ/ช่องว่างรอยต่อ/แรงขูด/ปริมาตรการขูด

วัตถุประสงค์ของการศึกษานี้คือการศึกษาผลกระทบของรอยแตกของหินต่อค่าดัชนีการสึกกร่อนแบบเซอคาร์ ดำเนินการทดสอบโดยใช้หินทราย หินปูน และหินบะซอลต์ที่มีรอยแตกขนานกัน โดยผันแปรจำนวนรอยแตกตั้งแต่ 1, 2, 3 และ 4 รอยแตก และผันแปรระยะเปิดเผยของแต่ละรอยแตกตั้งแต่ 0, 0.3, 0.5 ถึง 0.8 มิลลิเมตร ซึ่งระยะห่างระหว่างรอยแตกมีค่าคงที่คือ 2 มิลลิเมตร ผลการทดสอบระบุว่าค่าดัชนีสึกกร่อนมีค่าลดลงเมื่อจำนวนรอยแตกและระยะเผยอเพิ่มขึ้น แรงขูดที่กระทำกับแท่งเหล็กสไตลัสขูดลดลงเมื่อปลายแท่งเหล็กสไตลัสขูดสัมผัสกับรอยแตก และมีผลมากขึ้นเมื่อระยะเปิดเผยอกว้างขึ้น นอกจากนี้แรงขูดยังมีค่าเพิ่มขึ้นเมื่อจำนวนรอยแตกเพิ่มขึ้น ปริมาตรร่องขูดมีค่าเพิ่มขึ้นเมื่อค่าดัชนีการสึกกร่อนลดลง เป็นสาเหตุมาจากเมื่อจำนวนรอยแตกมากจะแสดงค่าดัชนีการสึกกร่อนและพลังงานการขูดมีค่าน้อย แต่กลับมีปริมาตรร่องขูดมากกว่าเมื่อเทียบกับหินที่มีจำนวนรอยแตกน้อย

สาขาวิชา เทคโนโลยีธรณี
ปีการศึกษา 2567

ลายมือชื่อนักศึกษา .....
ลายมือชื่ออาจารย์ที่ปรึกษา .....

RATCHAPON MINGKHWAN: EFFECT OF ROCK JOINT FREQUENCY AND APERTURE ON CERCHAR ABRASIVITY INDEX.
THESIS ADVISOR: EMERITUS PROF. DR. KITTITEP FUENKAJORN, 118 PP.

Keywords: joint number, joint aperture, scratching force, scratching volume.

The objective of this study is to investigate the effect of rock joints on the CERCHAR abrasivity index (CAI). Sandstone, limestone, and basalt prepared to have parallel fractures with joint numbers varying from 1, 2, 3, to 4, and joint apertures of 0, 0.3, 0.5, to 0.8 mm are tested. The joint spacing is kept constant at 2 mm. The results indicate that the CAI value decreases with increasing joint frequencies and apertures. The scratching force exerted on the stylus pin is reduced when the pin tip subjected to the fracture. This is more pronounced as the aperture becomes larger. As the number of joints increases, the scratching force is increased. The scratching volume increases as CAI decreases, suggesting that highly fractured rocks show less CAI and less energy to scratch while yielding a higher scratching volume as compared to rock with lower fracture intensity.

School of Geotechnology
Academic Year 2024

Student's Signature .....
Advisor's Signature .....

ACKNOWLEDGEMENT

I wish to acknowledge the funding support from Suranaree University of Technology (SUT).

I would like to express thanks to Emeritus Prof. Dr. Kittitep Fuenkajorn, thesis advisor, who gave a critical review. I appreciate his encouragement, suggestions, and comments during the research period. I would like to express thanks to Assoc. Prof. Dr. Pornkasem Jongpradist and Asst. Prof. Dr. Prachya Tepnarong for their valuable suggestions and comments on my research works as thesis committee members. Grateful thanks are given to all staffs of Geomechanics Research Unit, Institute of Engineering who supported my work.

Finally, I most gratefully acknowledge my parents for all their support and encouragement throughout the period of this study.

Ratchapon Mingkhwan

TABLE OF CONTENTS

Page

TABLE OF CONTENTS (Continued)

Page

TABLE OF CONTENTS (Continued)

Page

TABLE OF CONTENTS (Continued)

Page

LIST OF TABLES

Table **Page**

LIST OF FIGURES

Figure **Page**

LIST OF FIGURES (Continued)

Figure **Page**

LIST OF FIGURES (Continued)

Figure **Page**

LIST OF FIGURES (Continued)

Figure **Page**

SYMBOLS AND ABBREVIATIONS

CAI	=	CERCHAR abrasivity index
σ_c	=	Uniaxial compressive strength
σ_t	=	Brazilian tensile strength
α	=	Empirical Constants of Joint aperture
β	=	Empirical Constants of Joint aperture
χ	=	Empirical Constants of Joint number
γ	=	Empirical Constants of Joint number
ω	=	Empirical Constants of Joint number and Joint aperture
τ	=	Empirical Constants of Joint number and Joint aperture
ϕ	=	Friction angle
I_S	=	Point load strength
EQC	=	Equivalent quartz content
CSE	=	CERCHAR specific energy
DSS	=	Direct Shear Strength
HRC	=	Pin Hardness
CV	=	Cofficient of Variation
W	=	Work done
V	=	Material removed volume or mean groove volume
d	=	Diameter of wear flat area of stylus tip
d_{sc}	=	Wear flat of stylus tip for saw cut surface specimen
N	=	Normal load
F	=	Horizontal force or ploughing force
d_n	=	Vertical displacement
d_s	=	Scratching distance
d	=	Wear flat width of stylus tip.

SYMBOLS AND ABBREVIATIONS (Continued)

T	=	Torque
c	=	Cohesion
e	=	Aperture
J_n	=	Joint Number
V_V	=	Pore volume of specimen
V_{total}	=	Specimen volume
H_M	=	Mohs hardness

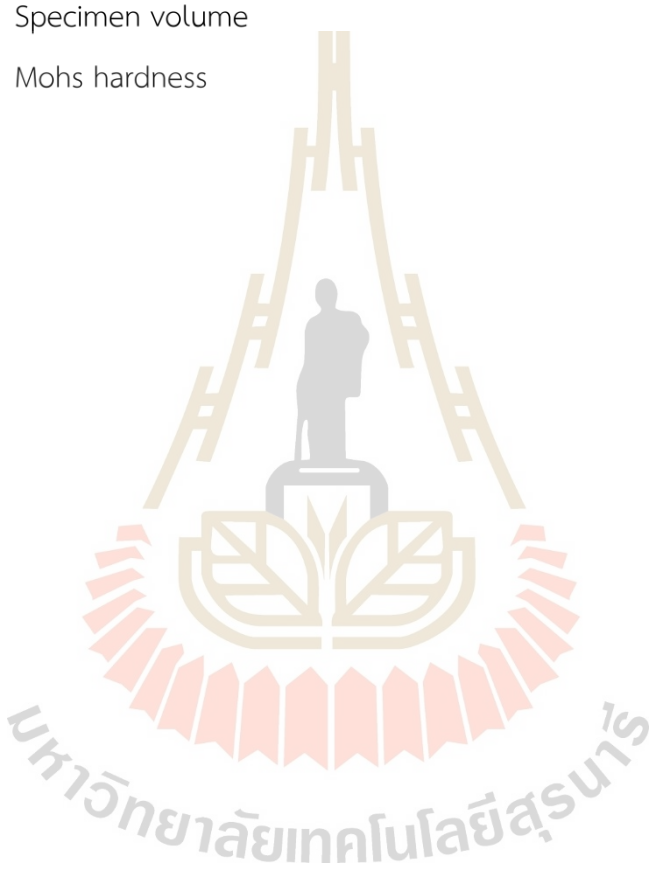

CHAPTER I

INTRODUCTION

1.1 Background and Rationale

CERCHAR abrasivity index (CAI) is widely used for evaluating the abrasion resistance of cutting tools. Its popularity is attributed to the method's simplicity, speed, and low cost Prieto, (2012); Ko, Kim, Son and Jeon, (2016); and Hamzaban, Karami and Rostami, (2013), which has driven extensive research to obtain various practical outcomes. The relationship of the CERCHAR abrasivity index (CAI) with various factors has been extensively developed, including testing length Al-Ameen and Waller, (1994); Plinninger, Käsling, Thuro and Spaun (2003); Yarail and Duru, (2016), velocity Kotsombat, Thongprapha and Fuenkajorn (2020); Plinninger, Kasling, and Thuro (2004), surface conditions Plinninger, et al., (2003); Thanadkha and Fuenkajorn (2022), mineral and rock compositions Kathancharoen and Fuenkajorn (2023), orientation, temperature and mechanical properties Hamzaban, Memarian and Rostami, (2013); Capik and Yilmaz, (2017); Alber, (2008); Deliormanli, (2012).

Despite extensive research on CAI, the current understanding does not fully account for all variables influencing it. In particular, the effects of joint frequency and aperture in rock are critical factors that remain underexplored. This study introduces a new concept that highlights the significance of these structural features on CAI when assessing tool wear. For instance, when a drill bit encounters a rock formation with a higher number of joints or wider apertures, these features significantly affect performance, leading to increased wear or reduced drilling efficiency. Understanding these effects is crucial for enhancing the predictive accuracy of CAI and optimizing drilling operations in geologically complex environments.

1.2 Research Objectives

The objective of the study is to investigate the effect of rock joint characteristics on CERCHAR abrasivity index under varying numbers of joints and joint apertures. Number of joints and their apertures are considered. Three rock types have been tested. Methematical relations between CAI and joint characteristics are developed.

1.3 Scope and Limitations

The scope and limitations of the research include as follows:

1) Three rock types are tested: sandstone from the Phu Phan formation and collected from Nakhon Ratchasima, limestone from the Khao Khad formation and collected from Saraburi and basalt from the Buriram formation and collected from Nakhon Ratchasima.

2) Number of joints are varing from 1-4 with constant joint spacing of 2 mm.

3) Joint aperture are rating from 0, 0.3, 0.5 and 0.8 mm.

4) CAI uses saw-cut surface.

5) The CERCHAR procedure follows ASTM D7625-22 standard practice.

6) Mineral compositions are determined by X-ray diffractometer.

7) Ploughing forces and grooves volume of CAI specimens are measured.

1.4 Research Methodology

The research methodology in Figure 1.1 includes literature review, sample preparation, CERCHAR testing, laser scan, X-ray diffraction analysis, mathematical relations, discussions and conclusions, and thesis writing.

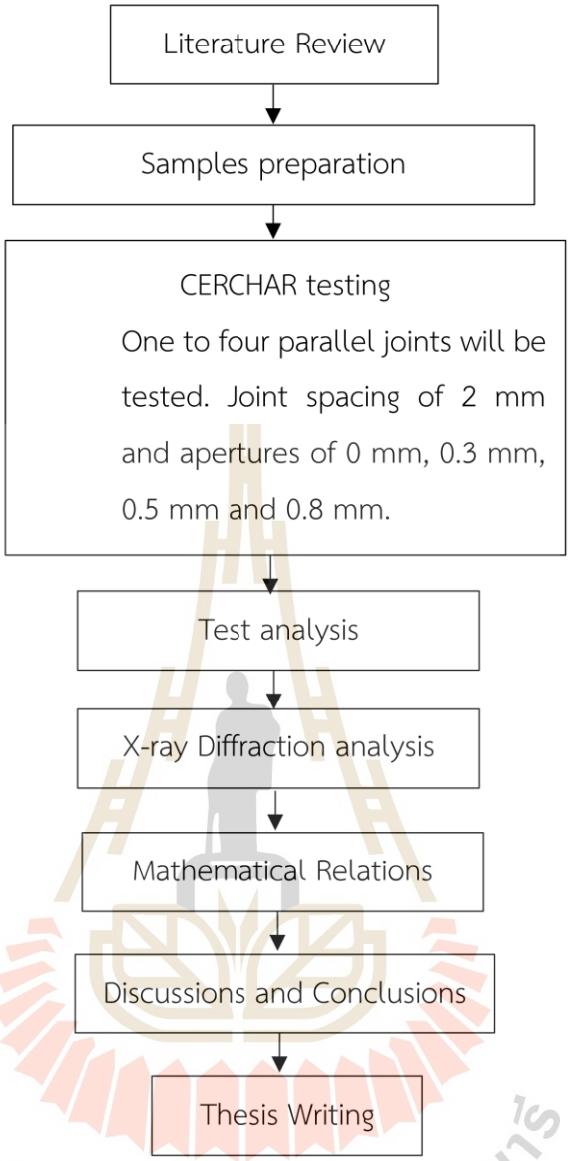

Figure 1.1 Research Methodology.

1.4.1 Literature Review

A literature review are carried out to study research about rock abrasiveness and joint discontinuity, CERCHAR testing, and effect factors on CAI. The sources of information are journals, technical reports, and conference papers.

1.4.2 Sample preparation

The rock specimens are cut and ground to produce saw-cut surface in accordance with the ASTM D7625-22 standard practice. Rectangular block specimen with nominal dimensions of 80×50×40 mm^3 are obtained with artificial fractures (saw-cut) normal to the test surfaces. The numbers of parallel joints are varied from 1 to 4, with joint apertures from 0 to 0.8 mm. The joint apertures are made by using filler gages placed between thin slaps of rock specimens to obtain a precise gap (aperture) between them.

1.4.3 CERCHAR testing

The testing are conducted to determine CAI of rock specimens with different joint numbers and spacing. The test procedure follows the ASTM D7625-22 standard practice with additional parameters vertical displacements and scratching force.

1.4.4 Test analysis

The Cerchar abrasivity Index (CAI) is determined as a function of joint numbers and joint apertures. The correlations between CAI and groove volume, obtained from surface scratching of the rock, are also examined. These correlations are analyzed for all rock joints and apertures. The findings reveal in the response of rock joints and apertures on CAI which provides insights into the processes that occur during excavation.

1.4.5 X-ray Diffraction analysis

In the X-ray diffraction (XRD) analysis, rock samples are finely ground to a powder with a particle size of 250 μm (mesh #60). The analysis results are utilized to assess the influence of mineral compositions on CAI. XRD analysis is conducted on the finely ground rock powder after CAI tests to determine the mineralogical composition, which is one of the key factors affecting the CAI.

1.4.6 Mathematical Relations

The mathematical relations are derived from the test results of CAI value, rock joint numbers and spacings to predict the CAI value as affected by rock joints on the CERCHAR abrasion index of three types of rock. Methematical relations between CAI and joint characteristics are developed.

1.4.7 Discussions and Conclusions

All activities, methods, and results are recorded and compiled in the thesis, including guidelines for continuing research results in the future.

1.5 Thesis content

This research thesis is divided into eight chapters. The first chapter includes background and rationale, research objectives, scope and limitations and research methodology. Chapter II presents results of the literature review to improve an understanding of CERCHAR testing. Chapter III describes sample preparation. Chapter IV describes the test method. Chapter V presents the experimental results. Chapter VI assesses the predictive capability of some rock, determine the effects of joint frequency and joint aperture on of rock and to assess the volume of rocks obtained from excavation. Chapter VII presents discussions, conclusions and recommendation for future studies.

CHAPTER II

LITERATURE REVIEW

This chapter gives a summary of literature review to understand the rock abrasiveness, CERCHAR testing researches and joint aperture and spacing.

2.1 Rock abrasiveness

The abrasiveness of rock is a significant factor affecting excavation tools during rock excavation. This factor results in loss of considerable costs due to wear and tear on the excavation tools. Various rock characteristics can influence the performance of excavation tools on the work site. It is crucial to gather information about the rock's characteristics in the area before commencing work (Thuro and Käsling, 2009). Rock abrasiveness depends on the types of rock and the presence of abrasive minerals within it. Consequently, various tests are developed and actively utilized for rock identification (Ghasemi, 2010).

Intensity and wear rate depend on several factors simultaneously acting in the interaction between the indenter and the rock (Labaš, Krepelka and Ivaničová, 2012). The most crucial factors include:

1. Types and properties of friction surfaces.
2. Operation regime of the cutting indenter (tool).
3. Properties of environment where the indenter operates.

2.2 CERCHAR testing

The CERCHAR test consists of three types: type one the original test developed by the CERCHAR center, type two version produced at the Colorado School of Mines (CSM) in the mid-1980s, and type three involved modification of (West's,1989) CERCHAR test (Rostami, Ozdemir, Bruland, & Dahl, 2005) (Figure 2.1). Type one and three are similar, as described by Plinninger, Käsling, Thuro, and Spaun (2003).

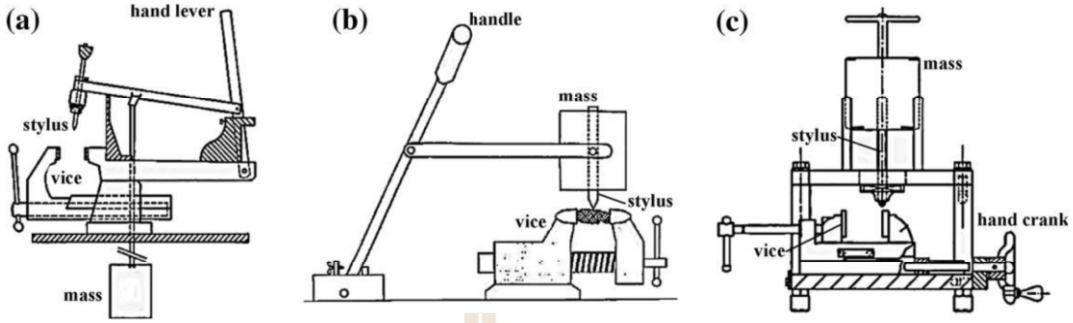

Figure 2.1 CERCHAR testing devices, CERCHAR Centre (a), CSM (b), West (c) (Rostami, Ozdemir, Bruland and Dahl, 2005).

The CERCHAR abrasivity test is a standardized procedure used to assess the abrasiveness or the abrasive potential of rocks and other geological materials (ASTM D7625-22). The CERCHAR scraping tool perpendicular to the specimen. The force applied is measured under vertical constant force of 70 N. Stylus scratches a groove of 10 mm in length on the rock surface. After scratching the wear on the stylus tip is measured in 0.1 mm units. The test apparatus includes a steel stylus with a Rockwell hardness of HRC 55, positioned perpendicular to the rock surface. Five individual tests are conducted on each specimen. CAI is calculated based on the average wear from the five tests. For saw-cut surfaces, the CAI is normalized to account for differences between saw-cut and natural rough surfaces.

2.2.1 Testing length

A longer length will cause more wear and tear. For better CAI estimation, multiple tests are performed on the same specimen with different test lengths (Plinninger et al., 2003) Of the 70% of pin wear occurring during the first millimeter of the test length, approximately 85% of the CAI occurs after 2 mm, and only 15% of the change in CAI is achieved at 8 mm, as shown in Figure2.2 (Al-Ameen and Waller, 1994).

.

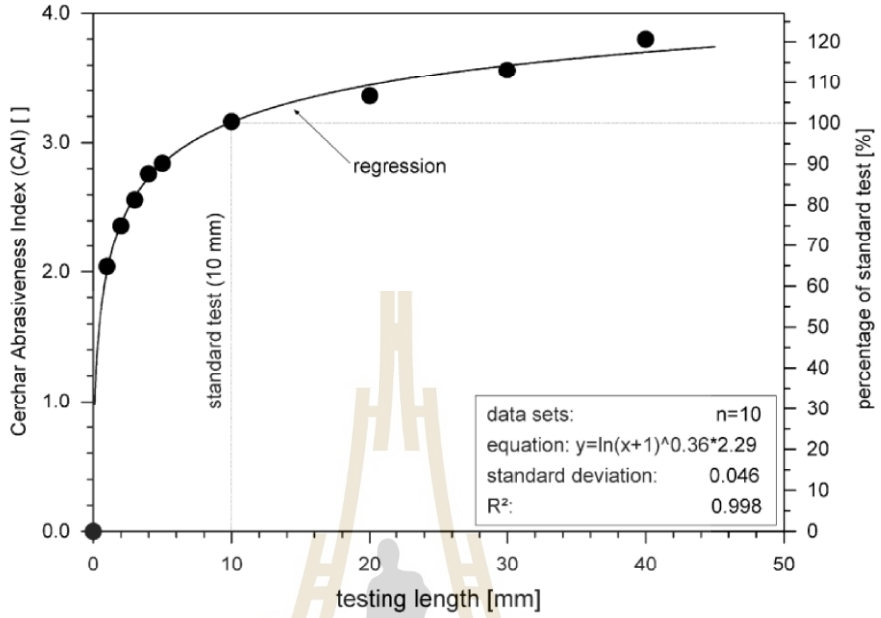

Figure 2.2. CAI versus length (Plinninger et al., 2003).

This method of extending the scratch length however is not beneficial. The deviation in CAI caused by changes in scratch length is not very significant when the variation in test length is kept between ± 0.5 mm (Plinninger, et al., 2003).

Scratches with lengths between 2 mm and 20 mm in 2 mm increments are analyzed separately by Yaralı and Duru (2016). It depends on the type of hardness of the stylus and various surface conditions (saw and rough cutting) and is summarized in Figure 2.3.

The test stylus wear does not end in a slide path of 10 mm, while the test stylus wear ends at a slide length of about 16 mm, and levels decrease. CAI is shown within the initial 2 mm of the scratch length. This continues to rise at an increasing rate until it reaches 16 mm and then decreases (Yarali and Duru, 2016). The evaluation results of the pin hardness and surface condition tests are shown in Table 2.1 and Figure 2.3.

Table 2.1. Evaluation results of pin hardness and surface condition tests for different scratch lengths (Yaralı and Duru, 2016).

Sample surface		Scratch length (mm)						
		2		10		15[a]		20
		(CAI)	(%)	(CAI)	(%)	(CAI)	(%)	(CAI)
Metamorphic rocks	SD	0.70	7.69	0.93	3.29	1.03	0.63	1.05
Sawn-cut	Avg	2.27	78.42	2.75	93.50	2.93	99.10	2.96
Rough	SD	0.93	6.44	1.45	1.00	1.52	0.22	1.53
	Avg	2.14	65.37	3.09	93.81	3.26	99.19	3.29
Smooth and rough	SD	0.81	6.57	1.18	1.54	1.27	0.38	1.29
	Avg	2.21	71.80	2.92	93.74	3.10	99.16	3.13
Sedimentary rocks	SD	0.26	6.17	0.49	4.18	0.56	0.54	0.57
Sawn-cut	Avg	1.45	63.01	2.01	86.37	2.28	97.79	2.33
Rough	SD	0.40	8.48	0.72	4.28	0.83	0.45	0.86
	Avg	1.45	58.60	2.16	84.99	2.48	97.70	2.54
Smooth and rough	SD	0.32	7.21	0.59	4.04	0.68	0.31	0.70
	Avg	1.45	60.63	2.09	85.62	2.38	97.72	2.43
Igneous rocks	SD	0.17	6.83	0.34	0.65	0.37	0.20	0.37
Sawn-cut	Avg	2.38	73.57	3.06	94.23	3.22	99.26	3.25
Rough	SD	0.46	6.53	0.38	2.32	0.42	0.62	0.43
	Avg	2.37	64.44	3.32	90.83	3.60	98.44	3.66
Smooth and rough	SD	0.81	6.57	1.18	1.54	1.27	0.38	1.28
	Avg	2.20	71.80	2.92	93.73	3.10	99.16	3.12

SD: Standard Deviation; Avg.: Average.

[a] Average of 14 and 16 mm scratch length.

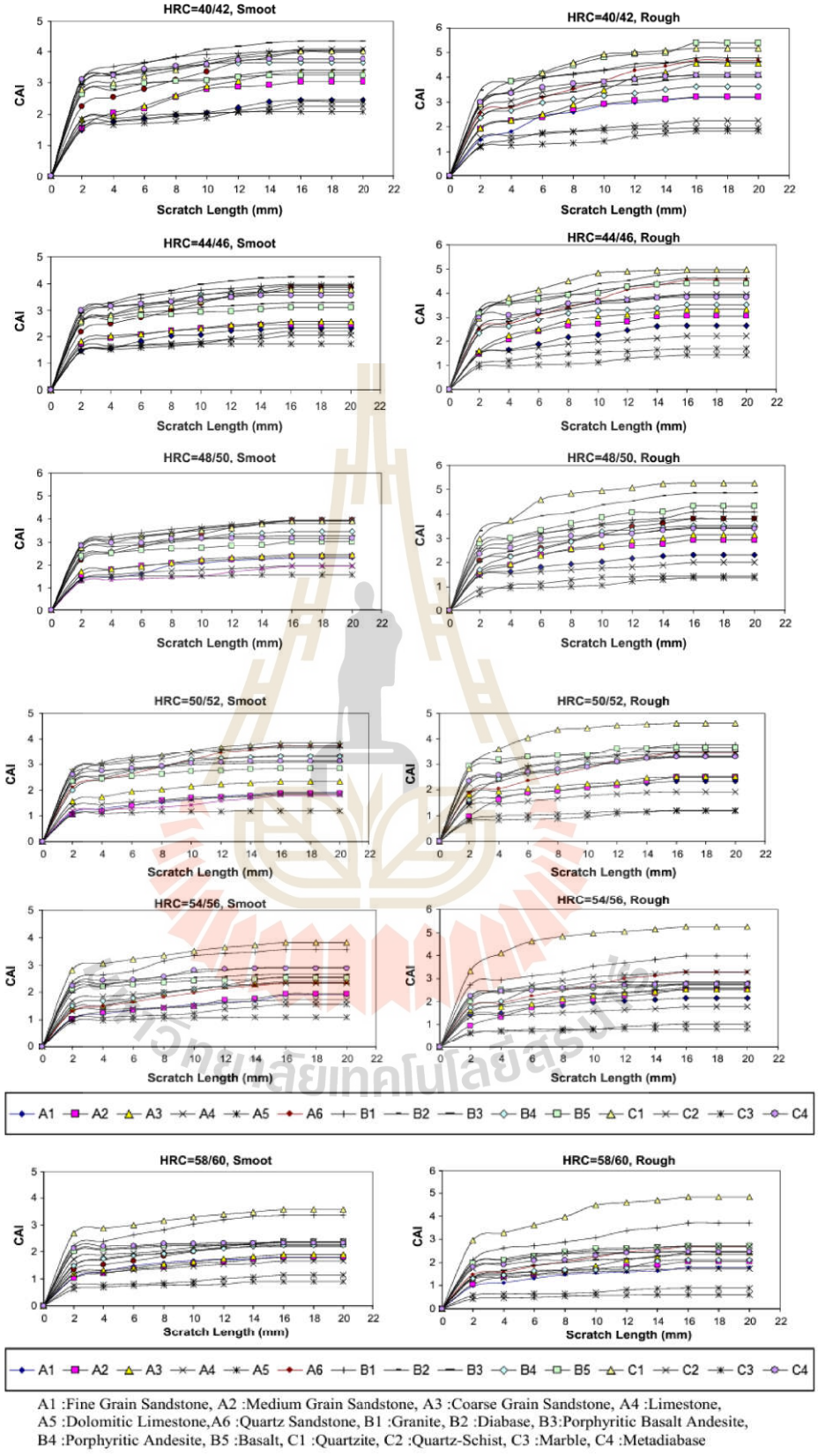

Figure 2.3. Results of pin hardness and surface condition tests (Yarali and Duru, 2016).

2.2.2 Stylus hardness

Michalakopoulos, Anagnostou, Bassanou and Panagiotou, (2005) tests 68 specimens with HRC 40 and HRC 55 and find that high stylus hardness shows the lower the CAI value corresponding to stylus hardness. CAI values exhibit substantial variation in response to changes in stylus hardness, rock type, and the geological origin of rocks. Generally, the average CAI decreases as the stylus hardness increases for all specimen hardness (Aydın, 2019). Yaralı and Duru, (2016) study the coefficient of variance (CV) or relative standard deviation to assess the distribution of CAI values in relation to stylus hardness. They use 6 stylus pin with Rockwell hardness ranging from HRC 40-42 to HRC 58-60. The results, shown in Figure 2.4, indicate that on sawn surfaces, the CV values for CAI ranged from 21.22 to 29.30, with the lowest CV values observed at HRC 54/56 for stylus hardness. On rough surfaces, the CV values ranged from 30.02 to 38.69, with the lowest values also occurring at HRC 54/56. The results suggest that the least variance in CAI measurements is dependent of stylus hardness, especially on sawn surfaces, and the significant of both stylus hardness and surface condition in minimizing measurement variance is significant.

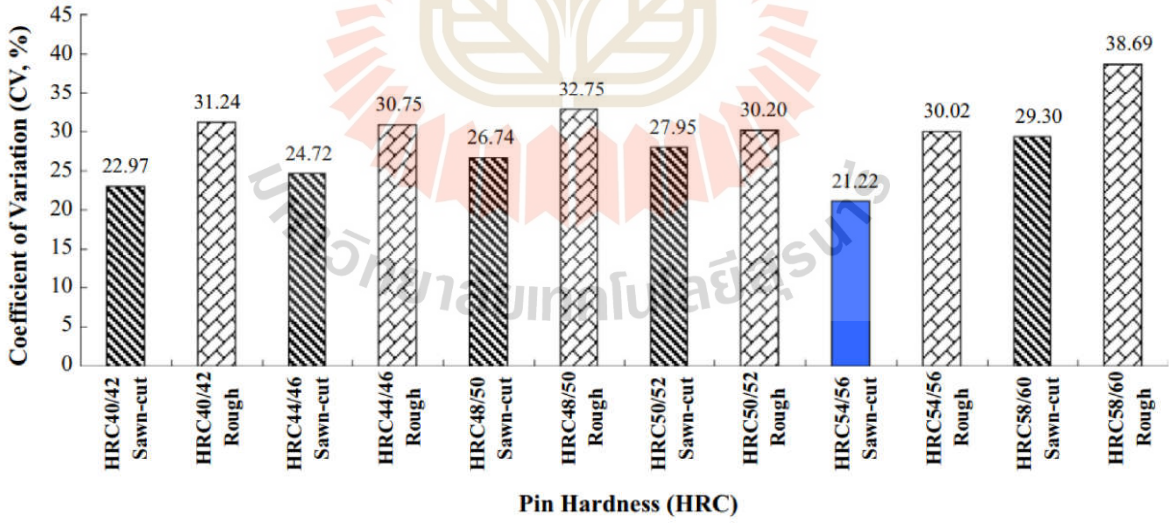

Figure 2.4 Coefficient of variation of CAI values measurement depends on pin hardness and surface condition of various samples (Yarali and Duru, 2016).

2.2.3 Material removal volume

Numerous researchers have examined the volumetric parameters involved in CERCHAR testing, with particular attention to both the wear volume of the stylus and the groove volume generated on the rock surface during the scratching process.

The wear volume of the stylus is typically calculated using the geometric formula for a cone, where the radius and height of the cone are taken as half the width of the worn stylus tip, as illustrated in Figure 2.5(a) Hamzaban, et al., (2019); Zhang and Konietzky, (2020). Conversely, the groove volume is determined by integrating the trapezoidal cross-sectional area along the scratching length, as depicted in Figure 2.5(b) Hamzaban, et al., (2019).

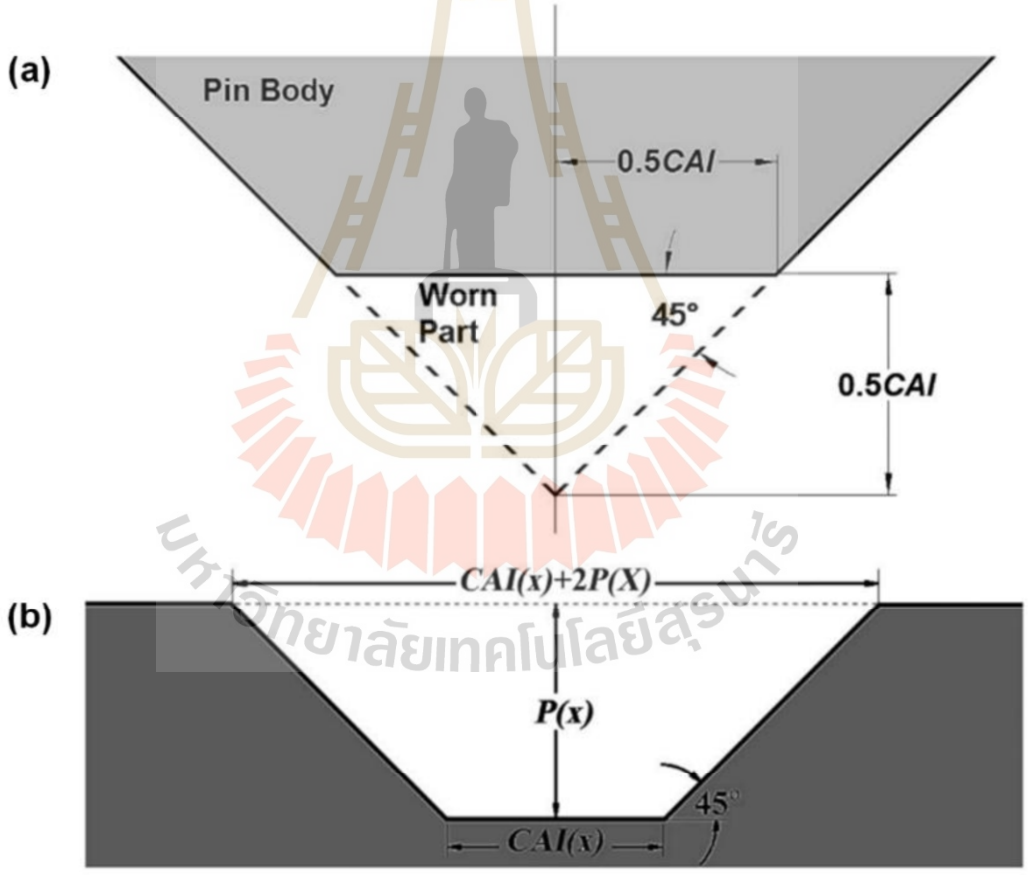

Figure 2.5 Geometry of worn pin tip (a) and cross section of scratch on sample Surface at a distance of x from beginning of motion path (b) (Hamzaban, et al., 2019).

The CAI is related to mean groove volume (V) as described by Kathancharoen and Fuenkajorn, (2023) who test 21 rocks, Their results are divided into two categories: clastic and crystalline rocks, which gives the CAI-V correlation curves as shown in Figures 2.6(a) and 2.6(b), and can be represented by the following equation.

$$CAI = \alpha \cdot (V)^{\beta} \quad (2.1)$$

where α and β are empirical constants that determine the relationship between CAI and V. An exception is porous basalts, which shows the opposite trend, where CAI increasing with increasing mean pore volume, possibly due to surface roughness that results in void formation. These rocks also have higher porosity, especially when compared to other rocks, except for clastic rocks. When grouping the rocks, crystalline rocks show a slightly stronger correlation between CAI and mean groove volume (R^2 of 0.452) as compared to the combined analysis of all rock types (R^2 of 0.391). In contrast, clastic rocks display a weak correlation, with R^2 of 0.039, indicating minimal association between mean groove volume and CAI in this group.

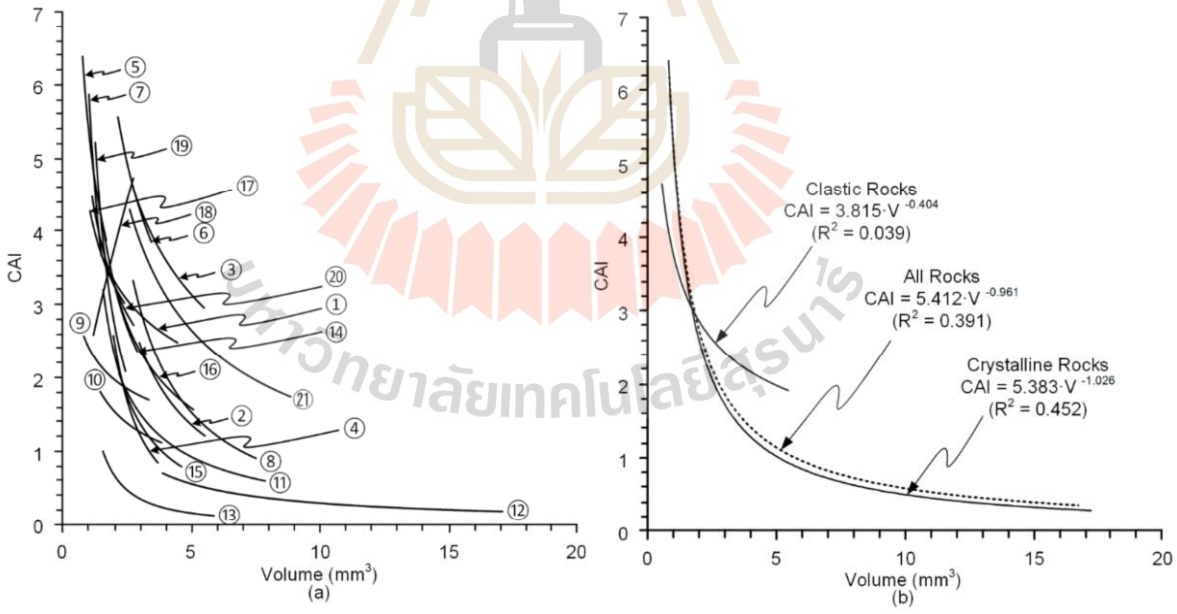

Figure 2.6 Correlation between CAI value and mean groove volume separated by rock types (a) and rock groups (b) (Kathancharoen and Fuenkajorn, 2023).

To further quantify the volume of material removed during the scratching process, a scanning electron microscope (SEM) is employed to analyze the rock surface post-scratch (Zhang and Konietzky, 2020). These volume parameters are crucial for the calculation of the scratch volume to wear ratio (SVWR) (Hamzaban et al., 2019) and the CERCHAR abrasion ratio (CAR), Zhang and Konietzky, (2020); Zhang, Konietzky, Song, and Zhang, (2020).

2.3 Rock properties

Rocks contain many factors that affect CAI values, including mineral compositions, hardness, grain size, and mechanical properties such as rock strength and hardness. (Beste, Lundvall and Jacobson, 2004).

2.3.1. Physical properties

The mineral compositions of a rock are related to its abrasiveness. Grain sizes of crystalline rocks with sharp edges are especially abrasive, (Feniak, 1944). The CAI value for a rough surface is higher than for a sawn cut surface. Hard rocks can be more abrasive than soft rock, (Rostami, et al. 2013). Suana and Peters, (1982) investigate the relationship between CERCHAR abrasivity index (CAI) and mineralogical and petrographic characteristics of rocks. Their study shows that grain size does not significantly influence the CAI, provided that the grain size falls within the range of 50 to 1000 microns. However, when grain sizes exceed 1 mm, a larger number of tests than the standard protocol recommends may be required to obtain a more accurate mean value. Despite this, their findings showed no discernible dependency of CAI values on grain size, with no significant variation observed between conducting 5 and 10 tests within the analyzed grain size range (Lassnig, Latal, and Klima, 2008). Kathancharoen and Fuenkajorn (2023) explain that mineral compesitions relate to volumetric hardness better than EQC. Both parameters have a positive linear relationship with CAI, as EQC and HV increase, CAI also increases. The correlation between CAI and EQC is moderate for all rocks (R^2 = 0.413), but stronger in specific rock groups: Clastic rocks (R^2 = 0.623) and Crystalline rocks (R^2 = 0.877 the highest correlation) (Figure 2.7). The correlation between CAI and HV is even stronger than the

EQC correlation. Clastic rocks (R^2 = 0.623), Crystalline rocks (R^2 = 0.893) and for all rocks (R^2 = 0.591)

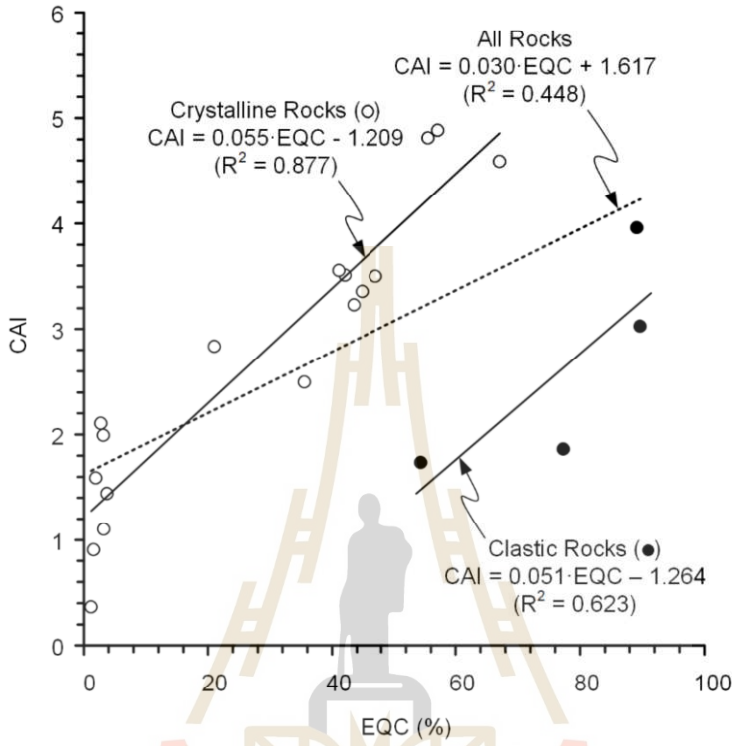

Figure 2.7 Correlation between CAI value and equivalent quartz contents (EQC) (Kathancharoen and Fuenkajorn, 2023).

When the HV of a rock is lower, the CAI also remains low or even zero, with an HV value of approximately 0.4 when the CAI is zero (Figure 2.8). This trend is consistent across all rock types. On the other hand, in the CAI-EQC relationship, when the EQC is zero, the CAI value can still exceed 1.2, indicating that CAI may remain high even in the absence of quartz content in some cases.

Zhang, Konietzky, et al. (2020) study factors affecting the CERCHAR abrasivity index with three rock types (granite, sandstone, and slate). They discover that the CAI value is not different between rough, sawn, and polished. They applied a stylus with a Rockwell hardness (HRC) of 54–56. Kotsombat, et al. (2020) explain that a lower scratching rate results in deeper grooves, a lower surface scraping force, and a lower CAI of the stylus pin. Thanadkha and Fuenkajorn, (2022) explain the difference between

a smooth surface and a rough surface. On rough surfaces the CAI value is higher than on smooth surfaces.

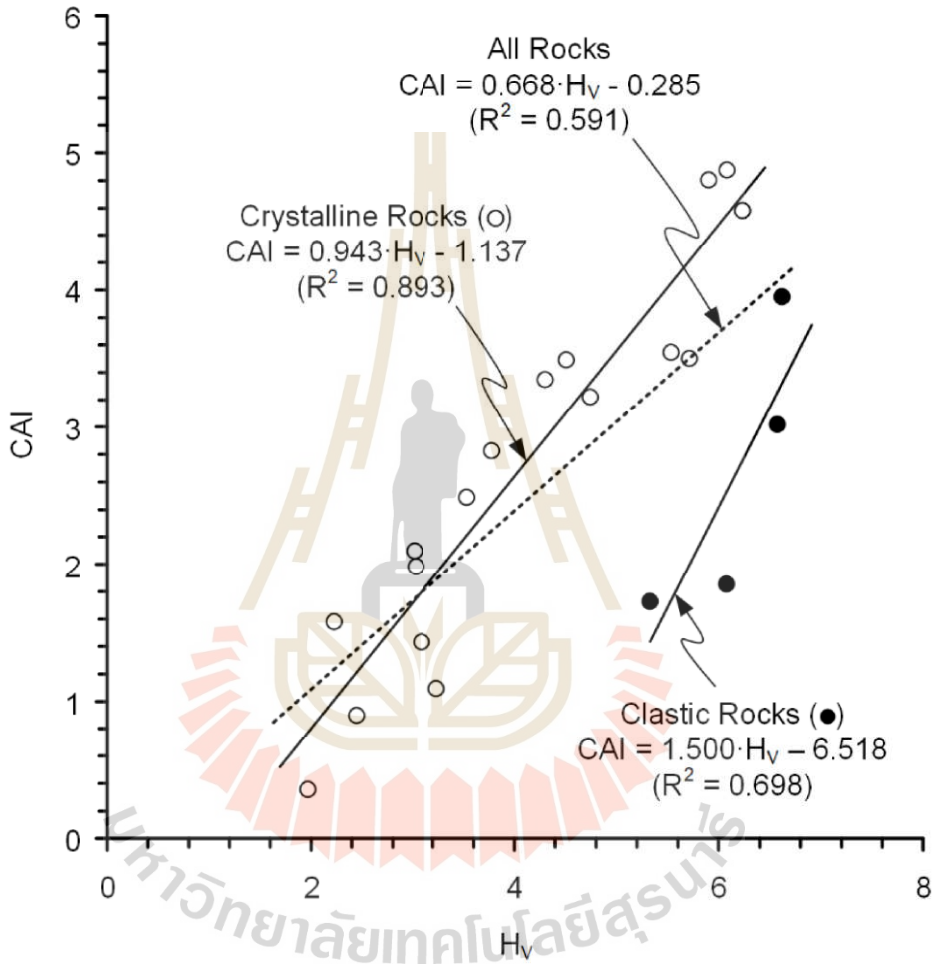

Figure 2.8 Correlation between CAI value and volumetric hardness (H_V) (Kathancharoen and Fuenkajorn, 2023).

2.3.2 Rock mechanical properties

Rock strength is significant factors affecting the value of CAI. Many researchers in this context consider several mechanical properties, including rock strength and rock hardness.

2.3.2.1 Strength of rock

Strength parameters such as uniaxial compressive strength, Brazilian tensile strength, and point load strength (IS) significantly influence the CAI values as proposed by Capik and Yilmaz, (2017). More researchers confirm this influence by identifying a strong linear relationship between CAI and both compressive strength and Brazilian tensile strength, as indicated by high coefficients of determination. Er and Tuğrul, (2016); Sirdesai, Aravind and Panchal, (2021).

Hamzaban, et al. (2014) study the new CERCHAR abrasivity testing device that determines friction force and penetration into rock surfaces. They discover a new parameter that explains the relationship between rock and stylus pin and the abrasiveness of rock. The CAI increases with the rise in uniaxial compressive strength, point load strength, Brazilian tensile strength, Schmidt rebound hardness, and the equivalent quartz content (EQC) (Capik and Yilmaz, 2017) (Figure 2.9). Alber, (2008) study CAI under stress. This indicates higher CAI values under confining pressure on the specimen within a triaxial test and demonstrates that the CAI is stress-dependent.

Deliormanli, (2012) study the relationship between strength and CAI value on soft rock using the methods of uniaxial compressive strength, direct share strength, Bohme abrasion, and wide wheel abrasion values. (Figures 2.10 and 2.11).

Kathancharoen and Fuenkajorn, (2023) explain that rock strength is significant factors affecting the value of CAI. Many researchers in this context consider several mechanical properties, including Young's modulus and Poisson’s ratio. It indicates that both values affect the CAI of clastic rocks, but in crystalline rocks there is no effect on CAI. Therefore, it is predicted that in clastic rocks there may be some significant factors affecting the CAI value. The relationship between CAI and triaxial properties, particularly adhesion force and friction angle (Figures 2.12 and 2.13), in clastic rocks both values had an effect on CAI, whereas in crystalline rocks the effect on CAI was less, limiting the study's conclusions.

2.3.2.2 Hardness of rock

There are many methods to determine the hardness of rocks, such as Shore hardness, Schmidt hardness, Vickers hardness, and others. Many researchers find

a relationship between CAI and Shore hardness, with R^2 values greater than 0.74 Er and Tuğrul, (2016); Lee, Jeong and Jeon, (2012); Ozdogan, Deliormanli and Yenice, (2018).

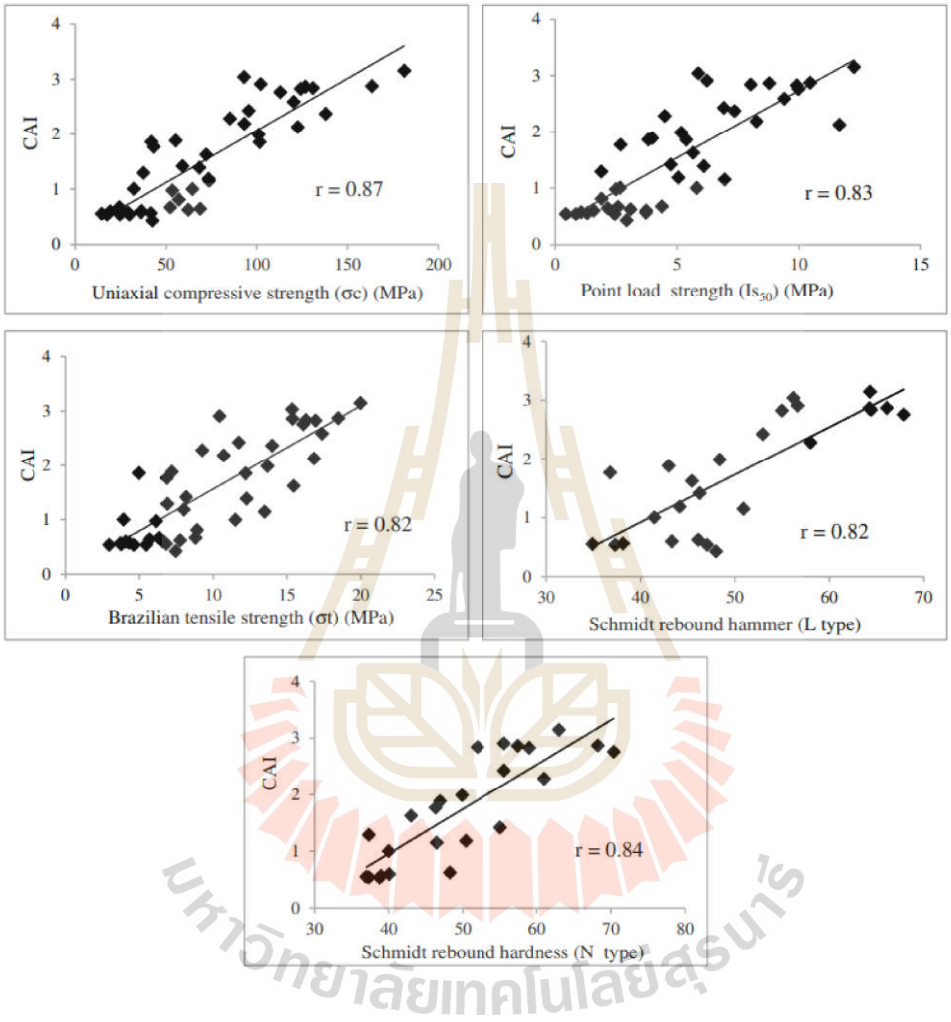

Figure 2.9 Relationships between CAI and mechanical properties of rock (Capik and Yilmaz, 2017).

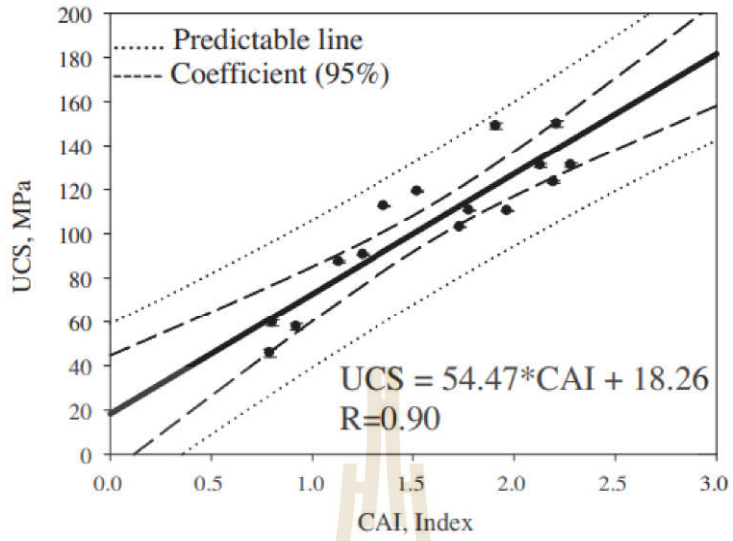

Figure 2.10 Scatter and relation graph of UCS versus CAI (Deliormanli, 2012).

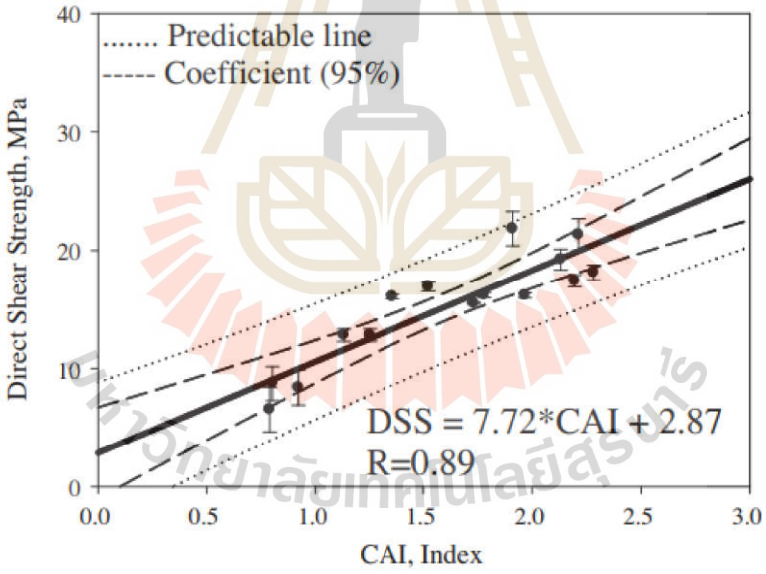

Figure 2.11 Scatter and relation graph of DSS versus CAI (Deliormanli, 2012).

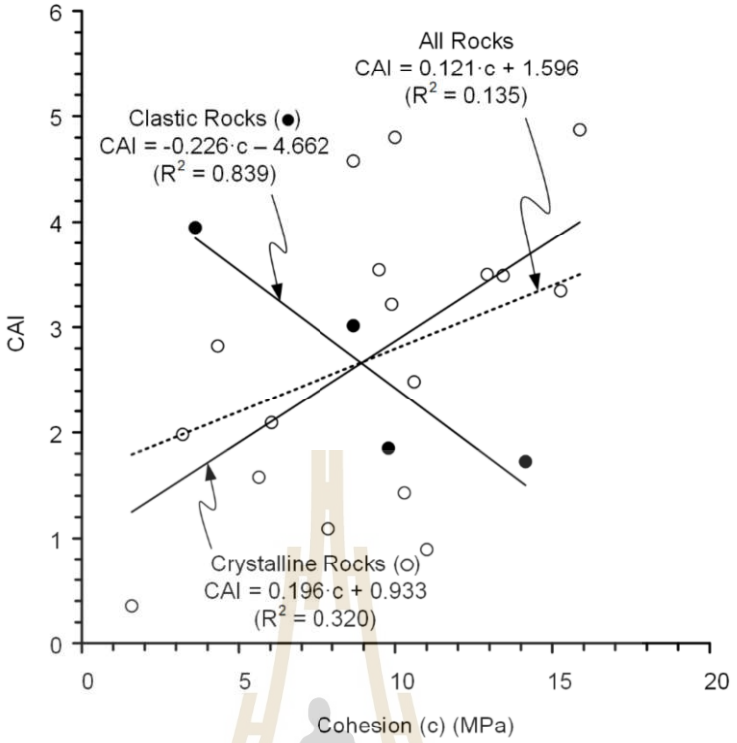

Figure 2.12 Correlation between CAI value and rock cohesion (c) (Kathancharoen and Fuenkajorn, 2023).

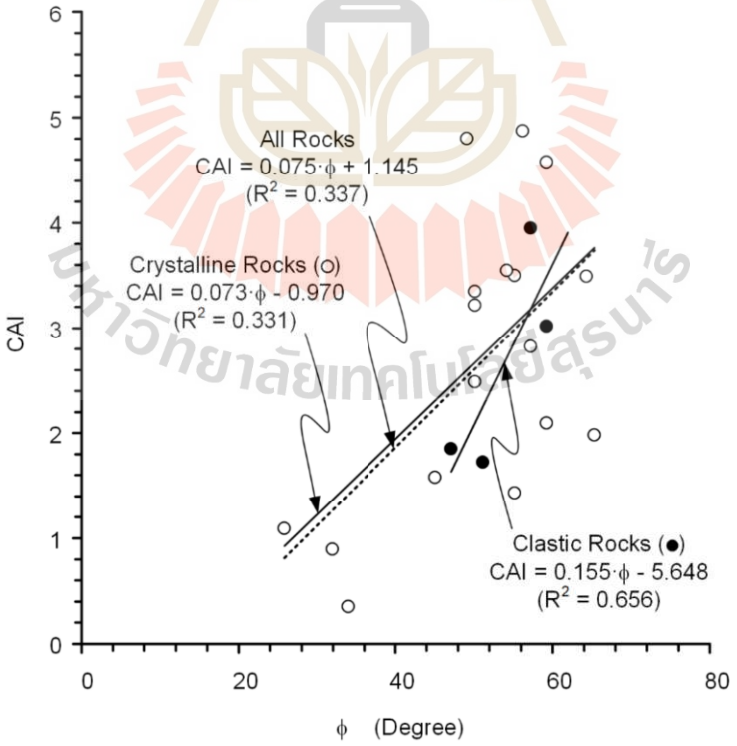

Figure 2.13 Correlation between CAI value and friction angle (ϕ) (Kathancharoen and Fuenkajorn, 2023).

CHAPTER III

SAMPLE PREPARATION

3.1 Introduction

This chapter provides a detailed description of the rock samples used in this study. Tests are conducted on three rock types to investigate the effects of different testing parameters.

3.2 Rock sample preparation

This study examines three rock types: Khao Khad limestone, Phu Phan sandstone, and Buriram basalt. The mineral compositions of these rocks, determined through XRD analysis, are detailed in Table 3.1, which are widely exposed in northeastern Thailand. The rock specimens are cut and ground to create saw-cut surfaces following the ASTM D7625-22 standard practice. Rectangular block specimens with nominal dimensions of 80 × 50 × 40 mm^3 are prepared, featuring artificial fractures (saw-cuts) perpendicular to the test surfaces (Figure 3.1).

Table 3.1 details mineral compositions of three rock type obtained from XRD analysis.

Rock Type	Code	Mineral Compositions
Phu Phan sandstone	Kpp	77.10% Quartz, 8.35% Chlonite, 5.08% Glauconite, 4.72% Kaolinite, 1.80% Illite, 1.29% Feldspar, 1.12% Mica, 0.40% Montmorillonite, 0.09% Magnetite, 0.04% Calcite
Buriram basalt	Qbs	34.81% Anorthite,19.97 % Albite, 16.19% Orthoclase, 12.25% Chlorite, 7.35 % Muscovite, 4.97% Calcite, 3.07% Kaolinite, 1.37% Hematite, 0.03% Quartz
Khao Khad limestone	Pkd	93.54% Calcite, 2.77% Dolomite, 0.95% Montmorillonite, 0.85% Quartz, 0.71% Feldspar, 0.64% Chalcopyrite, 0.48% Fluorite, 0.05% Kaolinite

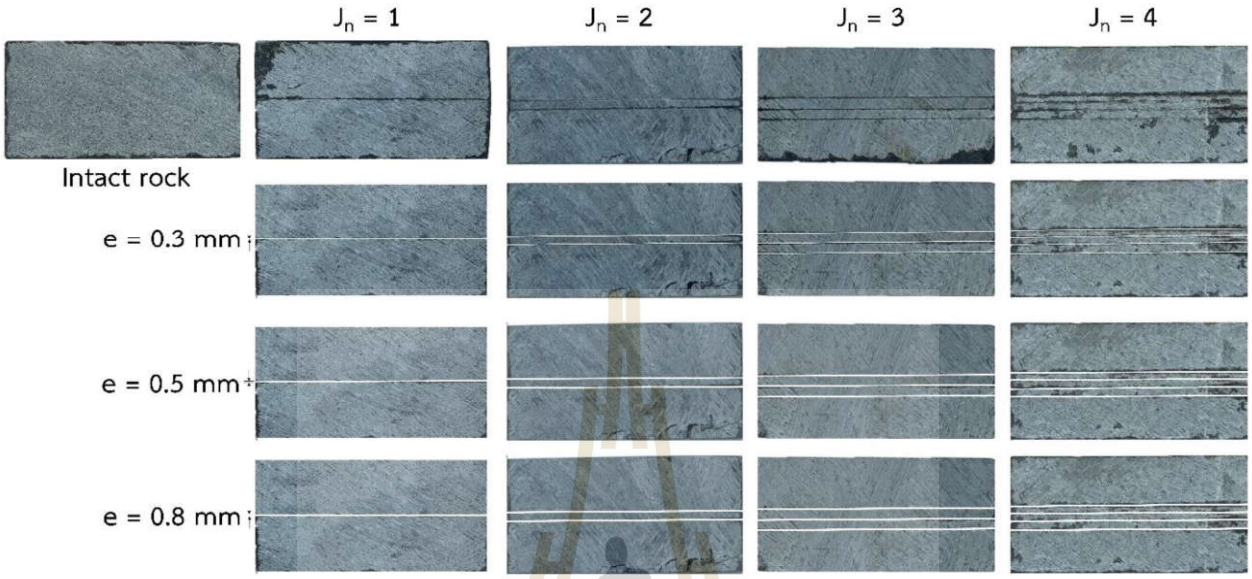

Figure 3.1 Some specimens used in CERCHAR testing for Khao Khad limestone.

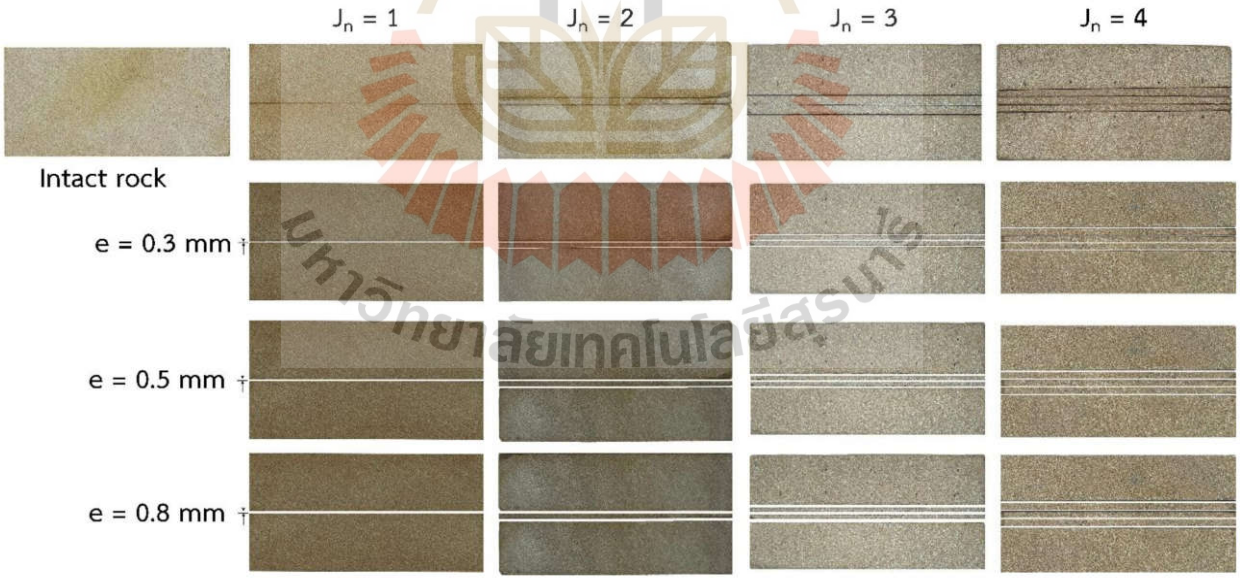

Figure 3.2 Some specimens used in CERCHAR testing for Phu-Phan sandstone.

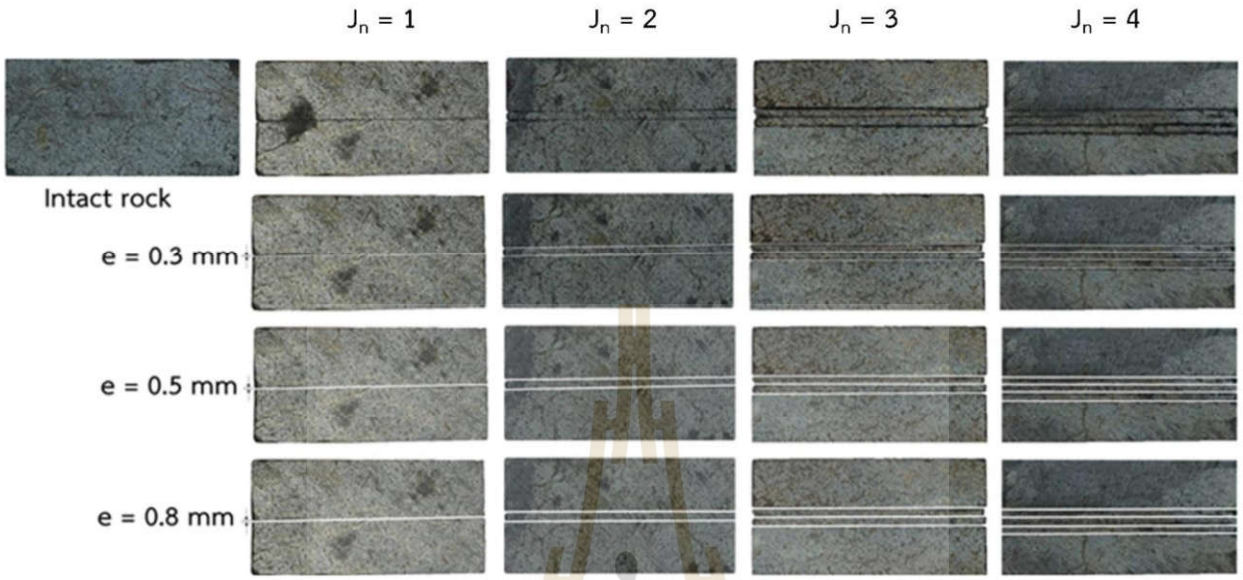

Figure 3.3 Some specimens used in CERCHAR testing for Buriram basalt.

The number of parallel joints ranges from 1 to 4, with joint apertures varying between 0 and 0.8 mm (Table3.2). The joint apertures are created using filler gauges placed between thin rock slabs to achieve precise gaps (apertures). These slabs are then bonded together while maintaining the desired joint apertures and spacing.

The specimens are prepared with three different characteristics for joint and different apertures. Each case is shown in Table 3.2 and is described below.

Case I: specimens are prepared to study intact rock on saw-cut surface,

Case II: One joint specimen are prepared to study the effect of parallel joints are varied joint apertures from 0 to 0.8 mm, **Case III**: Two parallel joints specimens with two joint frequencies are used in this case and varied joint apertures from 0 to 0.8 mm, **Case VI**: Three joints parallel joints with three joint frequencies are used in this case and varied joint apertures from 0 to 0.8 mm, **Case V**: Four parallel joints with four joint frequencies are used in this case and varied joint apertures from 0 to 0.8 mm. The multiple joint specimens use joint spacing of 2 mm

Table 3.2 Specimens prepared for numbers of parallel joints varied from 1 to 4, with joint apertures from 0 to 0.8 mm.

Cases	Joint number	e (mm)	Specimens
I	J_0	-	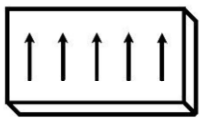
II	J_1	0 0.3 0.5 0.8	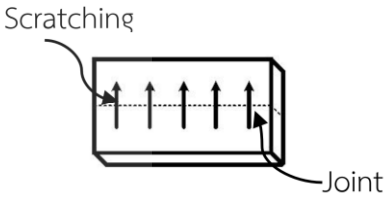
III	J_2	0 0.3 0.5 0.8	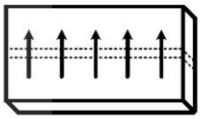
IV	J_3	0 0.3 0.5 0.8	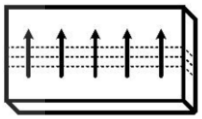
V	J_4	0 0.3 0.5 0.8	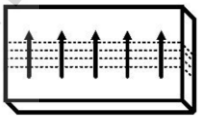

CHAPTER IV

TEST APPARATUS AND METHODS

4.1 Introduction

Presented in this chapter are test apparatus and test methods for determining CERCHAR abrasivity index (CAI). Additional parameters include ploughing force and mean groove volume. Methods for determining effect of rock joint and aperture of rock specimens on CAI are also described.

4.2 CERCHAR test

The CERCHAR abrasivity test used have follows the ASTM D7625-22 standard. This test is a widely recognized method for evaluating the abrasiveness or abrasive potential of rocks and other geological materials, as shown in Figure 4.1. Figure 4.2 presents the schematic drawing of the CERCHAR device and shows the torque wrench that are used to determine the rotation torque to scratch the steel stylus. They are used to calculate ploughing force and determine mean groove volume to assess effect of rock joint and rock aperture. Steel stylus pin with rockwell hardness of 55 ± 1 (Figure 4.3) are used with 90 degrees conical tip. Equations for calculating the CAI are shown in Eq (4.1) and Eq (4.2).

Figure 4.1 Device based on West CERCHAR apparatus West, (1989) with additional torque (Kathancharoen and Fuenkajorn, 2023).

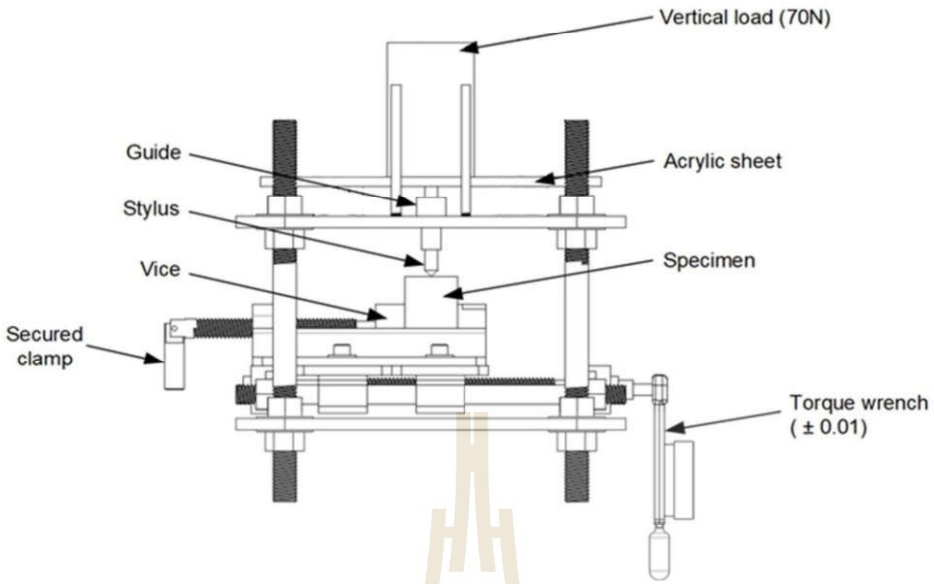

Figure 4.2 Schematic drawing of CERCHAR device used in this study. (Kathancharoen and Fuenkajorn, 2023).

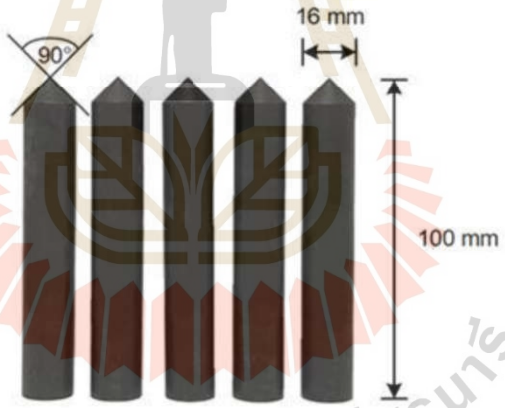

Figure 4.3 Example steel stylus pin with rockwell hardness of 55 ± 1 HRC for CERCHAR testing.

For each saw-cut rock surface specimen, scratching is repeated 5 times. Each time with a new stylus on a new scratch location. Wear flat width (d) of stylus tip is used to calculate CAI as follows:

$$CAI = d \times 10 \quad (4.1)$$

where CAI is CERCHAR abrasivity index for natural surface, d is diameter of wear flat area of stylus tip with an accuracy of 0.01 mm. If saw cut specimen is tested, wear flat of stylus tip is calculated from:

$$d = 1.14\ d_{sc} \tag{4.2}$$

where d_{sc} is wear flat of stylus tip for saw cut surface specimen performed in this study.

The schematic drawing of wear flat width of the stylus tip is shown in Figure 4.4. The wear tip is measured using a stereomicroscope (Nikon SMZ745T) at a magnification of 50x. The variables added beyond the standard suggestions in this study are shown in Figure 4.4.

The vertical displacement is measured by using the digital displacement gages with a precision of 0.001 mm to measure groove depth during scratching. The horizontal force applied on the steel stylus can be calculated from torque on the crank using load torque required for driving a ball screw equation from Nidec corporation as shown in Eq. (4.3).

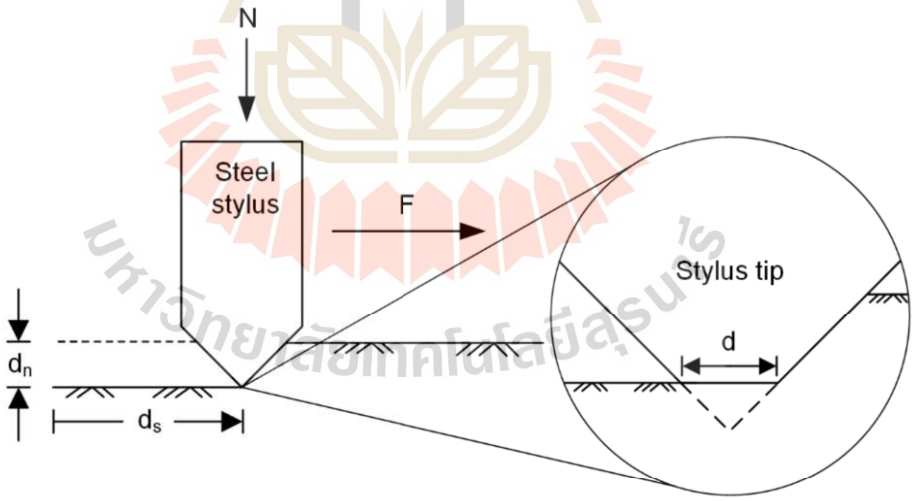

Figure 4.4 Steel stylus test variables, N is normal load (N), F is horizontal force (N), dn is vertical displacement (mm), ds is scratching distance (mm), and d is wear flat width of stylus tip (Kathancharoen and Fuenkajorn, 2023).

$$F = 2\pi T/P \text{ (N)} \quad (4.3)$$

where F is ploughing force (N), T is torque (N•m) and P is screw pitch (0.001 m). Rock surface after CAI testing have been laser-scanned to observe groove shape and to calculate the groove volume. The measurements are made to the nearest 0.001 mm. The torque for moving the specimen to scratch the steel stylus could be obtained from the torque wrench, the additional torque measuring device from the West apparatus, with an accuracy of 0.01 N•m is shown in Figure 4.5.

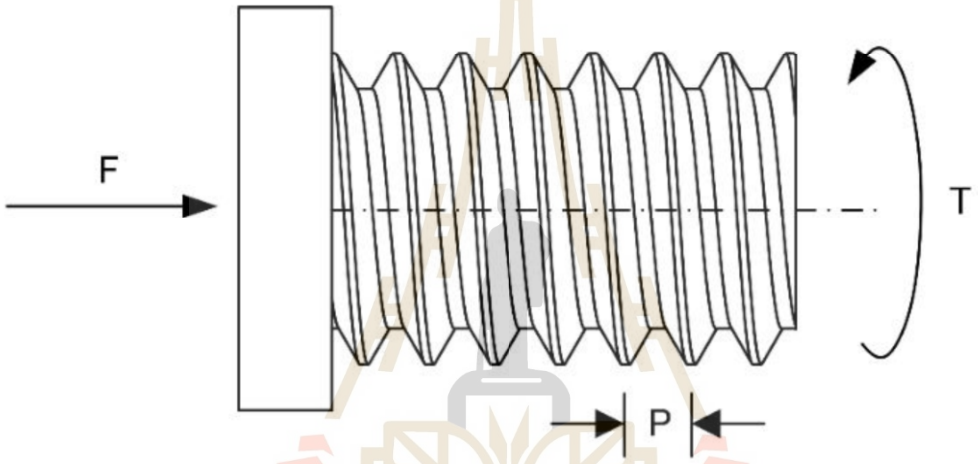

Figure 4.5 Force diagram used to convert torque (T) to horizontal force (F) (Kathancharoen and Fuenkajorn, 2023).

4.3 X-ray diffraction

Post-test CERCHAR specimens are ground to produce powder particles that pass through a #60 mesh. Approximately 5 to 10 grams of the powder are then analyzed using an X-ray diffractometer. The Topaz software is employed to determine the weight percentages of the mineral compositions, as shown in Figure 4.6.

Figure 4.6 X-ray diffraction Bruker, D8 advance (Center for Scientific and Technology Equipment University of Technology).

CHAPTER V

TEST RESULTS

5.1 Introduction

Laboratory test results are presented in this chapter. The CERCHAR abrasivity index tests reveal the effects of number of joints and joint apertures. Scratching groove volume on the specimens, and energy required to produce groove volumes under different joint characteristics are also described.

5.2 CERCHAR abrasivity index

Table 5.1 summarizs the CAI values obtained from intact rocks and those with different characteristics of joints for all rock types. It can be clearly seen that intact Buriram basalt (strong rock) tends to show larger abrasiveness than those obtained from softer rocks (limestone and sandstone). This is also true when the rock contain joints. Appendix A shows the stylus tips measured from the three intact rocks.

5.2.1 Effect of number of joints

The CAI values are plotted as a function of number of joints (J_n) in Figures 5.1 through 5.3 for the three rock types. They are also compared with those of the intact rocks. For all tested rocks, CAI's steadily decrease as J_n increases. Each data point in the diagrams represents mean and standard deviation values. The existence of even one joint can signifyingly reduce the CAI values for each rock type. Appendixs B though E give stylus tips after scratching the specimen surfaces with one though four joints.

5.2.2 Effect of joint apertures

As shown in Figures 5.1 though 5.3, CAI's decrease notably when the joint apertures (e) increase. This is true for all tested rocks. Different joint apertures tend to show similar reduction trend of CAI's as the number of joints (J_n) increases. The

reduction of CAI's with increasing joint apertures (e) is larger for basalt (strong rock) than those observed from limestone and sandstone (softer rocks).

Table 5.1 Results of CERCHAR testing of all rock types and joint characteristics.

Number of joints (J_n)	Aperture (e) (mm)	CAI		
		Rock type		
		Khao Khad limestone	Phu Phan sandstone	Buriram basalt
0 (Intact rock)	-	1.75	2.27	2.47
1	0	1.47	1.63	1.99
	0.3	1.37	1.56	1.51
	0.5	1.17	1.20	1.45
	0.8	0.96	1.04	1.09
2	0	1.36	1.41	1.74
	0.3	1.13	1.08	1.30
	0.5	1.02	0.96	1.26
	0.8	0.94	0.83	0.87
3	0	1.25	1.34	1.71
	0.3	1.10	0.95	1.06
	0.5	0.95	0.88	1.02
	0.8	0.75	0.73	0.87
4	0	0.87	1.23	1.70
	0.3	0.75	0.72	1.00
	0.5	0.60	0.69	0.77
	0.8	0.51	0.57	0.67

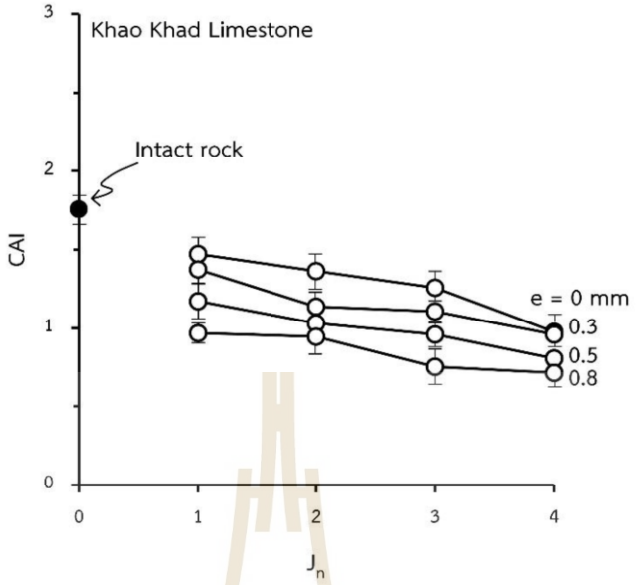

Figure 5.1 CAI as a function of joint numbers with different aperture for Khao Khad limestone.

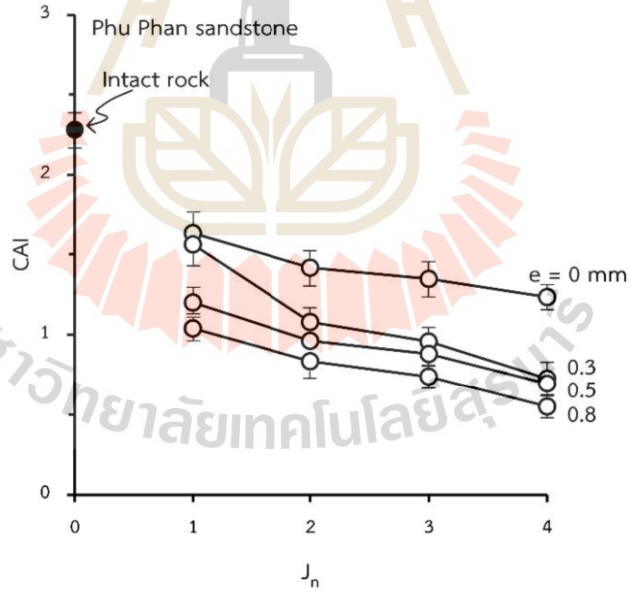

Figure 5.2 CAI as a function of joint numbers with different aperture for Phu Phan sandstone.

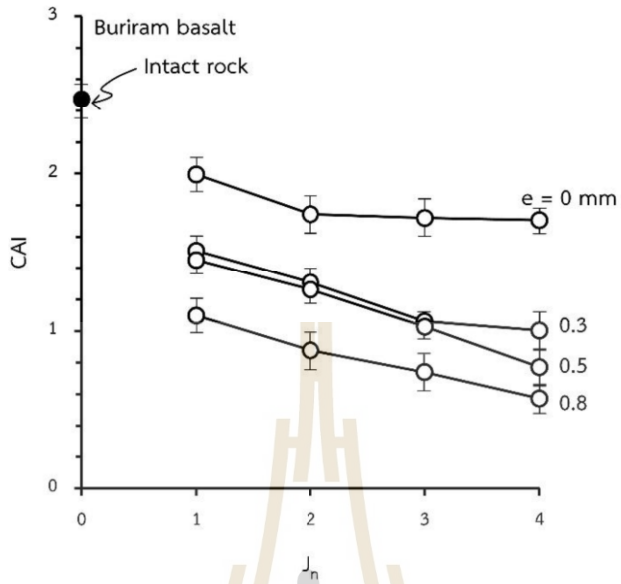

Figure 5.3 CAI as a function of joint numbers with different aperture for Buriram basalt.

5.3 Lateral force

Figures 5.4 through 5.6 show the lateral forces as a function of scratching distance for different numbers of joints and apertures. They are compared with those of the intact specimen (no joint). The curves shown here are the average of the five scratching tests. Individual scratching results for different joint characteristics are given in Appendix F, by the force at each contact point is determined based on the peak value recorded during each effect event between the rock surface and the stylus.

The method to obtain the representative curves from the five individual scratching is presented in the next chapter (Analysis of the results). Both joint apertures and their numbers strongly affect the scratching force, particularly for sandstone and basalt. For Khao Khad limestone the effects of joint aperture and joint number are small (Figure 5.4). Larger joint number and aperture induce larger scratching force on the rock surfaces for sandstone and basalt (Figures 5.5 and 5.6).

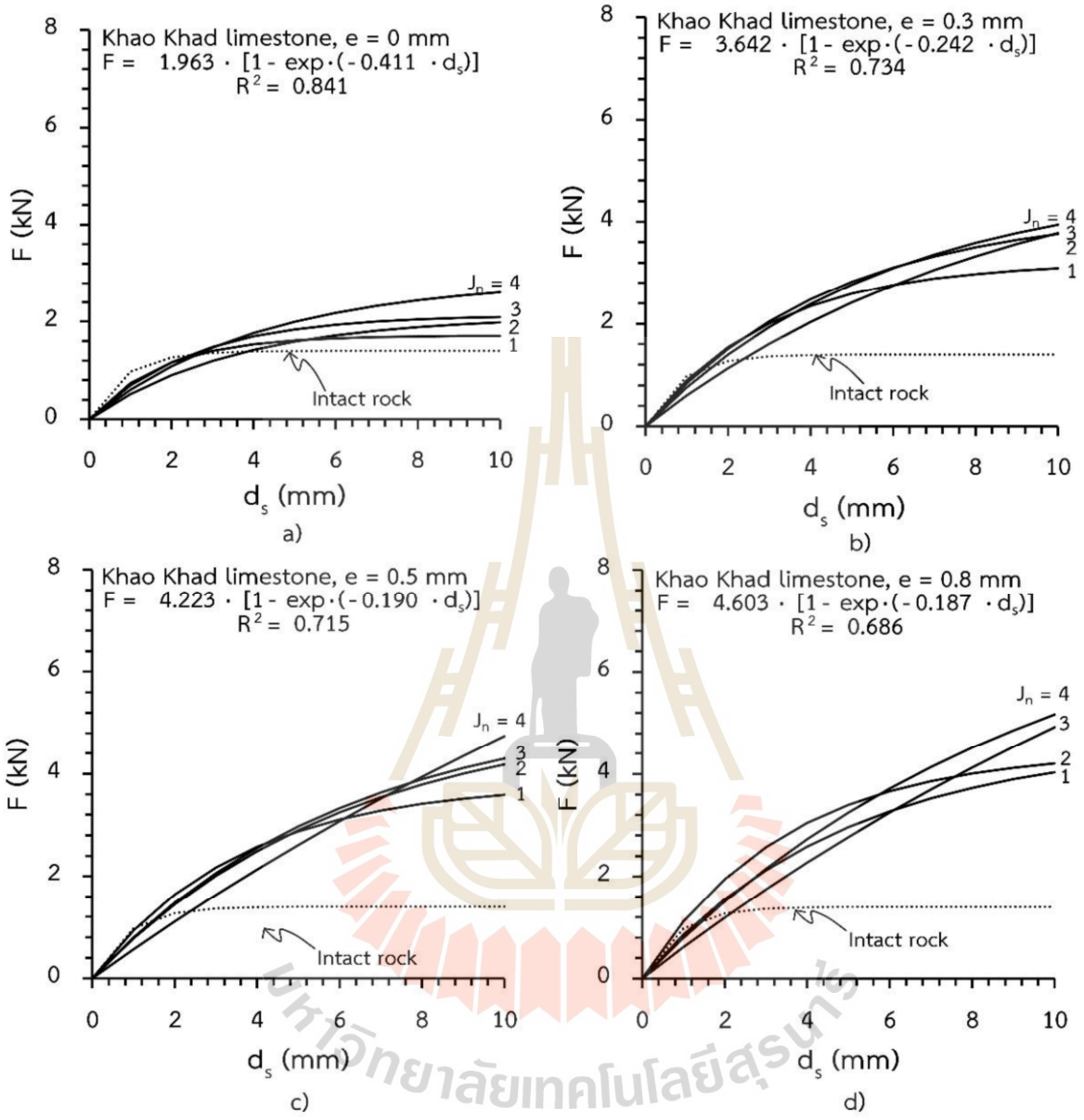

Figure 5.4 Lateral force as a function scratching displacement (d_s) for Khao Khad limestone for apertures of 0 (a), 0.3 (b), 0.5 (c) and 0.8 mm (d) with different number of joints (J_n).

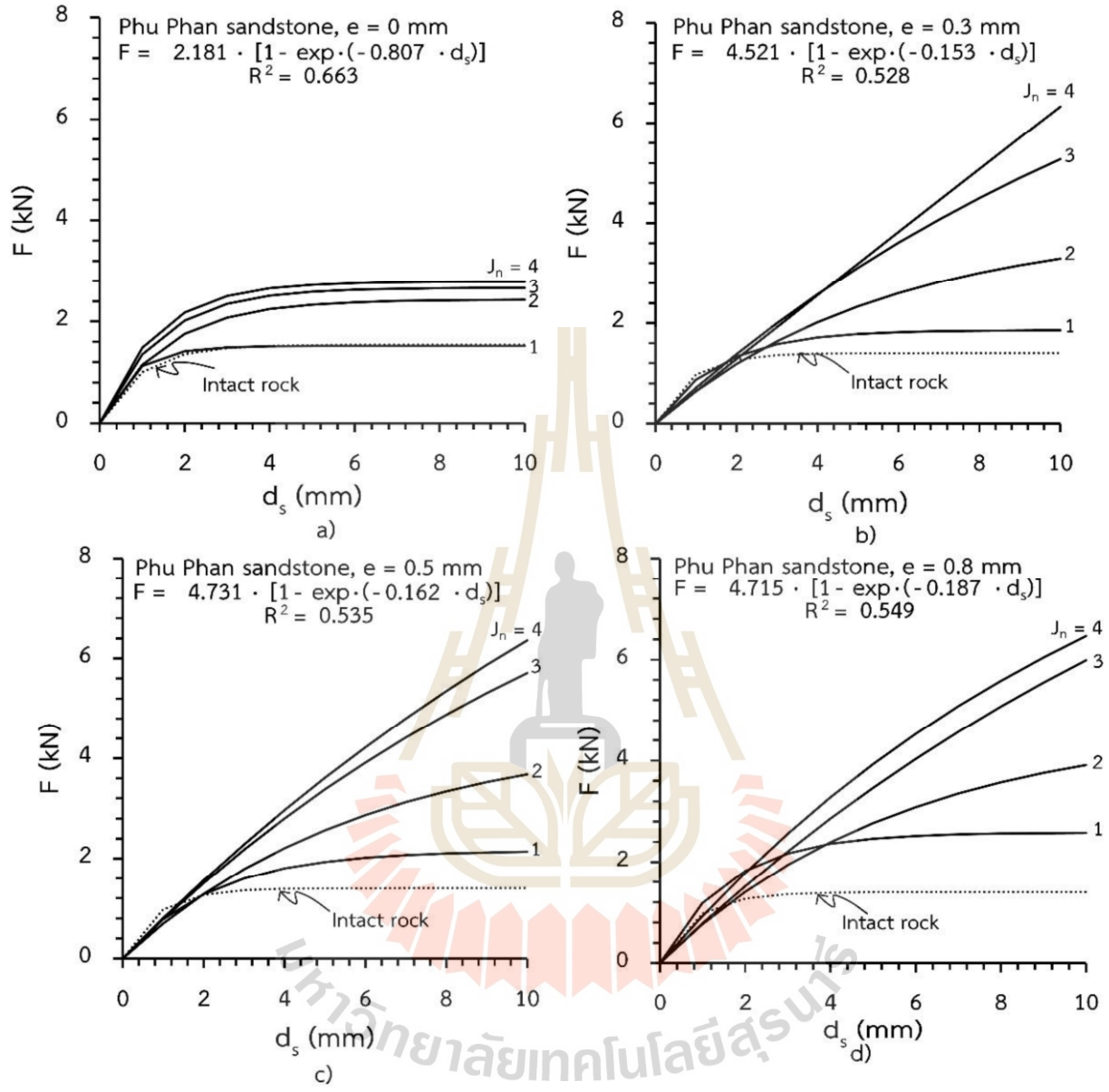

Figure 5.5 Lateral force as a function scratching displacement (d_s) for Phu Phan sandstone for apertures of 0 (a), 0.3 (b), 0.5 (c) and 0.8 mm (d) with different number of joints (J_n).

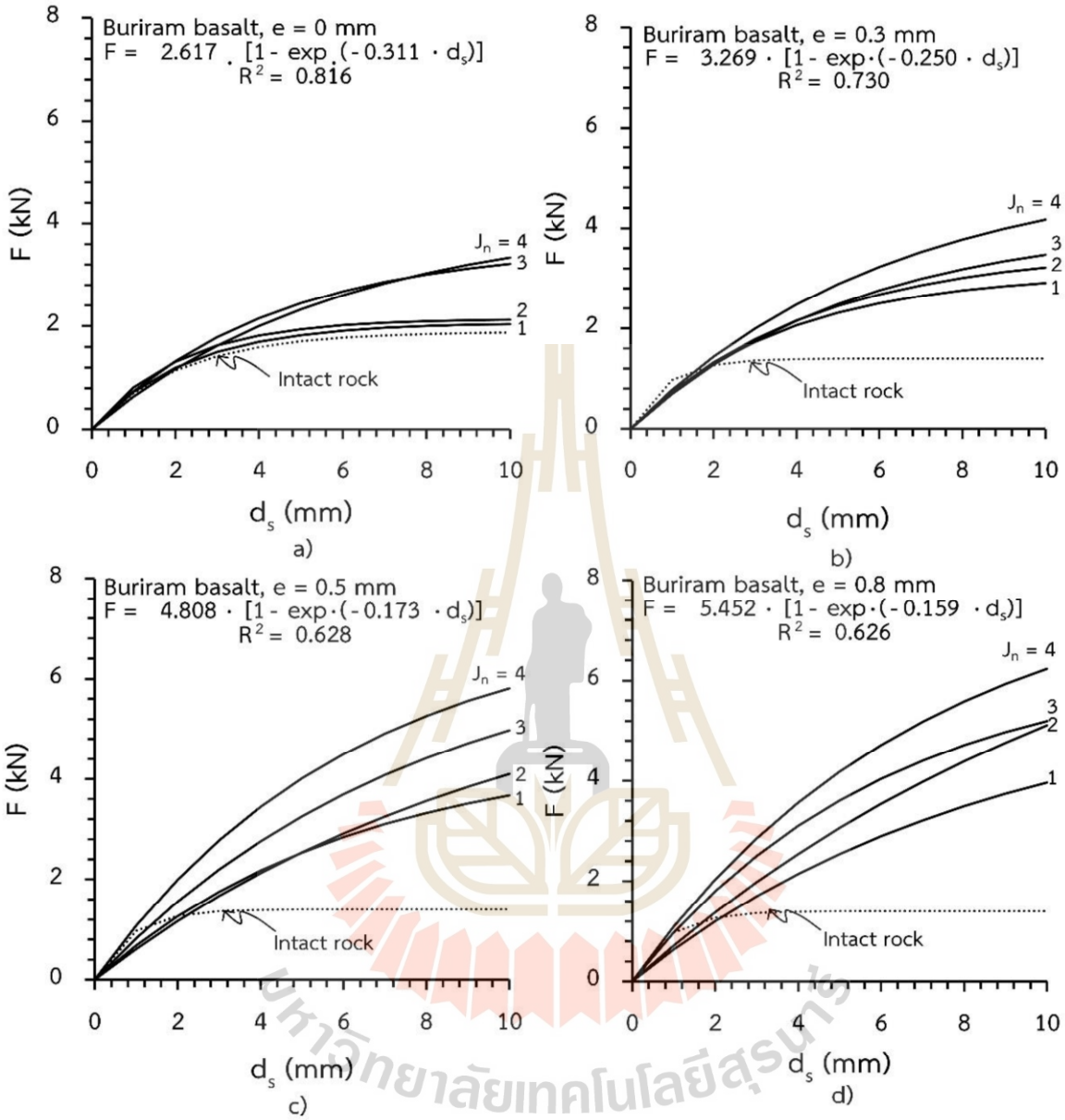

Figure 5.6 Lateral force as a function scratching displacement (d_s) for Buriram basalt for apertures of 0 (a), 0.3 (b), 0.5 (c) and 0.8 mm (d) with different number of joints (J_n).

5.4 Groove volume

Table 5.2 summarizes the average groove volumes measured from specimen surfaces under different joint characteristics for all tested rocks. The results from scratching intact rocks are also presented. Detailed images of individual scratching tests are given in Appendix G. For all tested rocks, the scratching volumes increase with joint numbers and apertures (Figure 5.7).

Table 5.2 Groove volumes for all rock types and joint characteristics.

Number of joints (J_n)	Aperture (e) (mm)	V (mm^3)		
		Rock type		
		Khao Khad limestone	Phu Phan sandstone	Buriram basalt
0 (Intact rock)	-	1.14	1.58	2.49
1	0	1.12	3.68	2.85
	0.3	3.01	5.89	3.87
	0.5	11.78	13.34	10.75
	0.8	16.05	21.61	13.78
2	0	1.92	9.09	3.08
	0.3	10.36	20.03	11.02
	0.5	21.05	39.21	29.16
	0.8	32.74	46.92	38.15
3	0	5.25	11.87	3.89
	0.3	16.90	25.95	14.87
	0.5	40.44	48.20	34.60
	0.8	50.99	59.19	47.72
4	0	14.71	20.67	13.85
	0.3	20.26	28.81	18.37
	0.5	47.65	52.99	42.57
	0.8	54.63	66.31	51.21

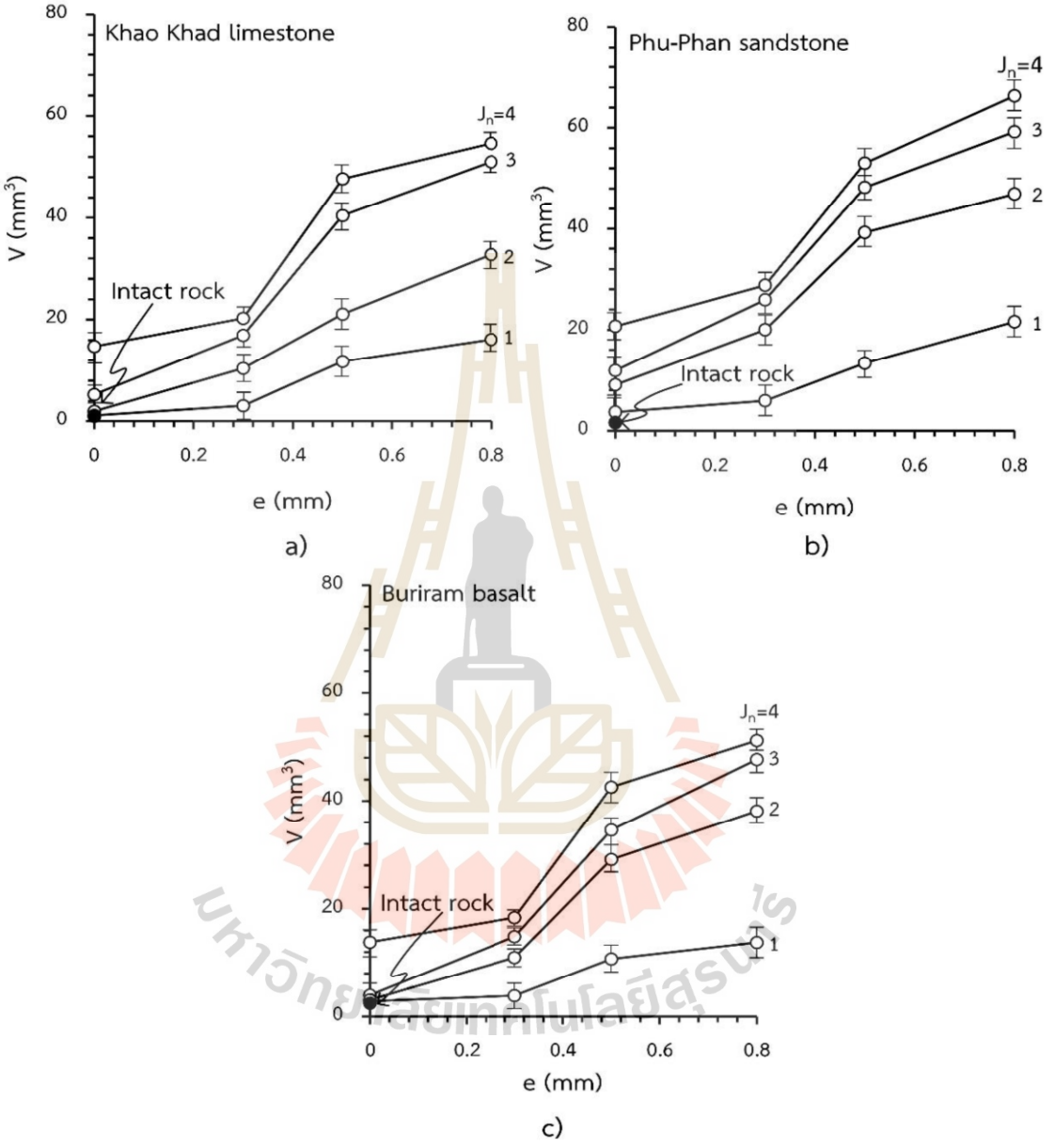

Figure 5.7 Groove volume as a function of joint aperture for different numbers of joints for Khao Khad limestone (a), Phu Phan sandstone (b) and Buriram basalt (c).

CHAPTER VI
ANALYSIS OF RESULTS

6.1 Introduction

The objective of this chapter is to determine the relationship between CAI and joint characteristics. The effects of joint numbers and joint apertures on CAI are quantitatively derived. This allows predicting the CAI values as affected by the joint variables occurring beyond those used in this study. The work and CERCHAR specific energy exerting on the jointed rocks are also derived to compare with those of the intact ones that have been widely performed elsewhere.

6.2 Correlation between CAI and joint apertures

Figure 6.1 plots CAI as a function of joint aperture (e) for all tested rock specimens. Each data point in the diagram represents the average CAI values obtained from five stylus pins. For all rock types CAI's decrease linearly with increasing joint apertures. This holds ture for all joint numbers. The decrease of CAI can be represented by:

$$CAI=\alpha \cdot e+\beta \quad (6.1)$$

where α and β are empirical constants. Their numerical values are given in Table 6.1. Good correlations are obtained ($R2 > 0.9$). The parameter α represents the negative slope of the linear relation. Each rock type tends to show similar values of α for different joint numbers. Strong rock (basalt) shows higher values of α than the softer ones (limestone and sandstone). This implies that the effects of joint apertures are more pronounced in the strong rocks than in the softer ones. The parameter β represents the intercept of the linear curves. The fewer joint numbers yield the higher β values where intact rocks show the highest value as shown by solid data point for

compassion. In addition, strong rock (basalt) gives higher β values than the softer ones (limestone and sandstone).

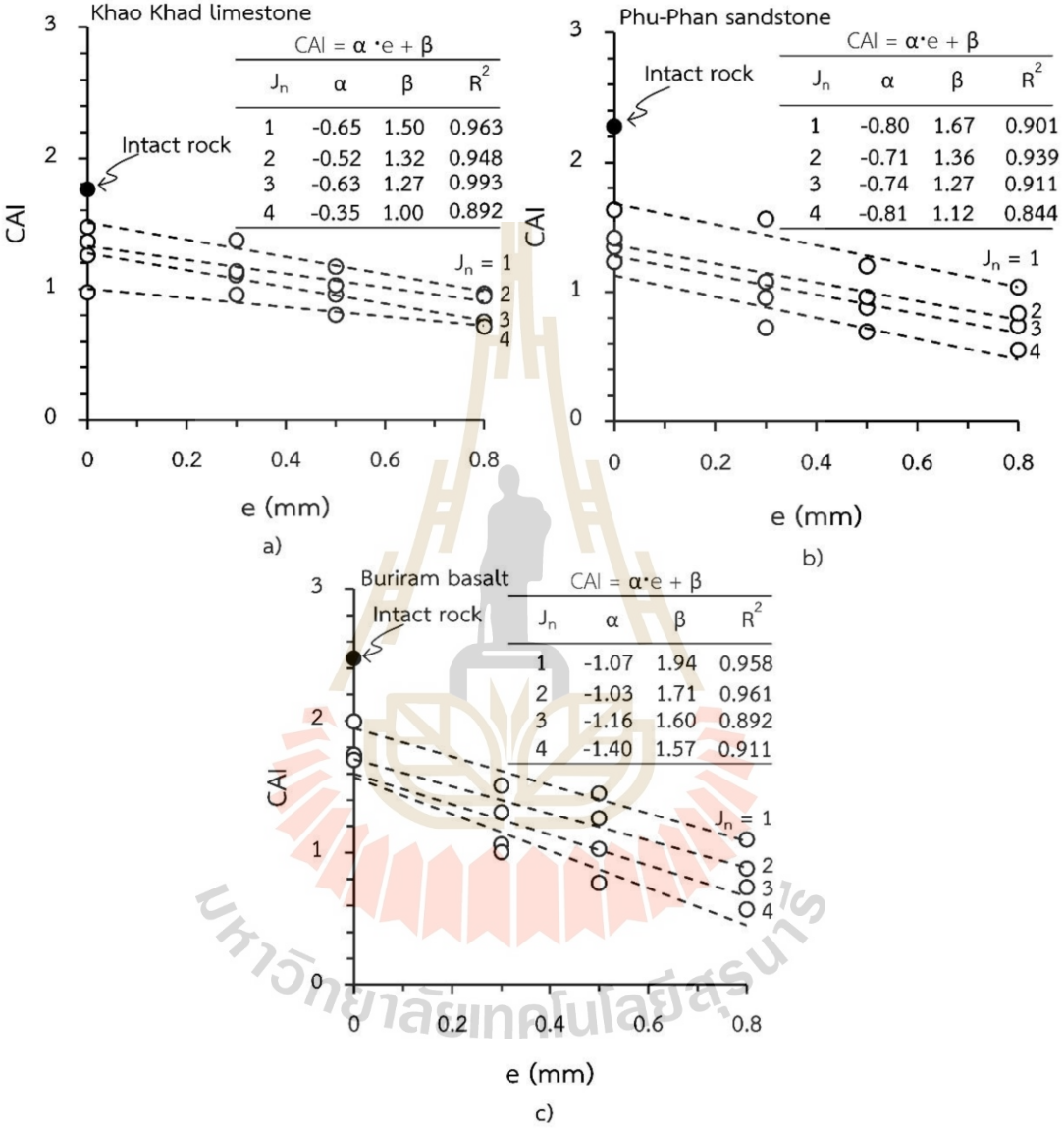

Figure 6.1 CAI as a function of joint aperture (e) for different numbers of joints (J_n) for Khao Khad limestone (a), Phu Phan sandstone (b) and Buriram basalt (c).

Table 6.1 CAI and joint apertures for all rock types.

Number of joints (J_n)	Aperture (e) (mm)	CAI = $\alpha \cdot e + \beta$								
		Rock type								
		Khao Khad limestone			Phu Phan sandstone			Buriram basalt		
0 (Intact rock)	-	α	β	R^2	α	β	R^2	α	β	R^2
	-	-	-	-	-	-	-	-	-	-
1	0 0.3 0.5 0.8	-0.65	1.51	0.963	-0.80	1.67	0.901	-1.07	1.94	0.958
2	0 0.3 0.5 0.8	-0.52	1.32	0.948	-0.71	1.36	0.939	-1.03	1.71	0.961
3	0 0.3 0.5 0.8	-0.63	1.27	0.993	-0.73	1.27	0.911	-1.16	1.60	0.892
4	0 0.3 0.5 0.8	-0.35	1.00	0.892	-0.81	1.12	0.844	-1.40	1.57	0.911

6.3 Correlation between CAI and joint numbers

CAI's are presented as a function of joint numbers (J_n) in Figure 6.2 They decrease linearly as J_n increases. No significant trend of the decreasing rates has been observed. This is probably due to intrinsic variability of the rocks. Strong rock (basalt) nevertheless tends to show higher curve than the softer ones (sandstone and limestone). The CAI for intact rock is shown as a solid point in the diagram (at J_n = 0) for comparison. The linear curve can be represented by:

$$CAI = \chi \cdot J_n + \gamma \quad (6.2)$$

where χ and γ are empirical constants, with their numerical values provided in Table 6.2. A good correlation is observed ($R^2 > 0.9$), except for strong rock (basalt of aperture 0 mm), which has the lowest correlation with $R^2 > 0.7$.

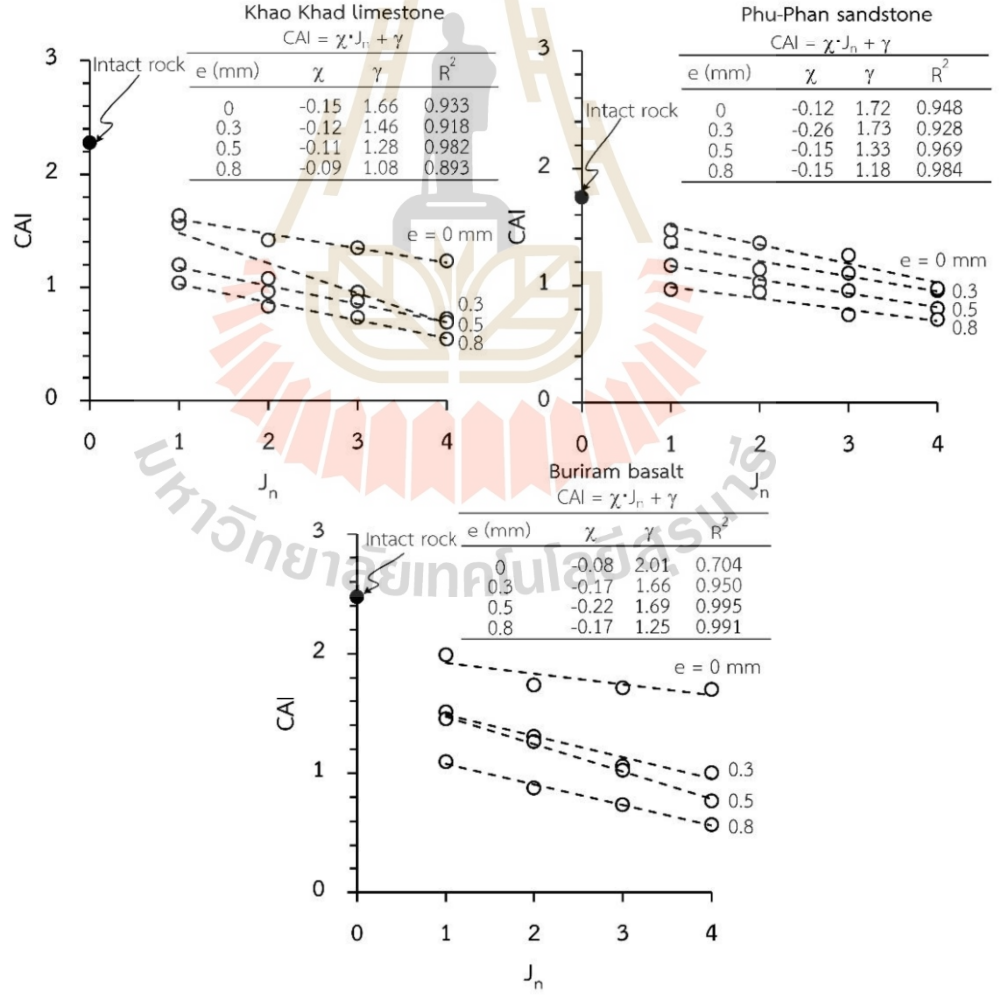

Figure 6.2 CAI as a function of joint numbers (J_n) for different apertures (e) for Khao Khad limestone (a), Phu Phan sandstone (b) and Buriram basalt (c).

Table 6.2 CAI and joint numbers for all rock types.

Number of joints (J_n)	Aperture (e) (mm)	CAI = $\chi \cdot J_n + \gamma$								
		Rock type								
		Khao Khad limestone			Phu Phan sandstone			Buriram basalt		
0 (Intact rock)	-	χ	γ	R^2	χ	γ	R^2	χ	γ	R^2
		-	-	-	-	-	-	-	-	-
1	0 0.3 0.5 0.8	-0.15	1.66	0.933	-0.12	1.72	0.948	-0.08	2.01	0.704
2	0 0.3 0.5 0.8	-0.12	1.46	0.918	-0.26	1.73	0.928	-0.17	1.66	0.950
3	0 0.3 0.5 0.8	-0.11	1.28	0.982	-0.15	1.33	0.969	-0.22	1.69	0.995
4	0 0.3 0.5 0.8	-0.09	1.08	0.893	-0.15	1.18	0.984	-0.17	1.25	0.991

6.4 Lateral force and scratching distance

An exponential equation is proposed to represent the lateral force (F) as a function of scratching distance (d_s). The primary objective is to calculate the specific energy of the stylus pin along the scratching distance. Similar form of the equation has been used by Kathancharoen and Fuenkajorn, (2023) for ten types of intact rocks.

$$F = a \cdot [1 - \exp \cdot (-b \cdot d_s)] \quad (6.3)$$

where a and b are empirical constants. Their numerical values are given in Table 6.3. Good correlations are obtained ($R^2 > 0.7$).

Table 6.3 Empirical constants (a and b) in equation (6.3).

Number of joint (J_n)	Aperture (e) (mm)	$F = a \cdot [1 - \exp \cdot (-b \cdot d_s)]$								
		Rock type								
		Khao Khad limestone			Phu Phan sandstone			Buriram basalt		
		a	b	R^2	a	b	R^2	a	b	R^2
0 (Intact rock)	-	1.40	-1.19	0.967	1.54	-1.05	0.961	2.06	-0.42	0.895
1	0	1.78	-0.56	0.867	1.51	-1.34	0.911	2.14	-0.85	0.861
	0.3	3.21	-0.32	0.907	1.86	-0.63	0.856	3.11	-2.87	0.944
	0.5	3.81	-0.28	0.893	2.16	-0.44	0.875	4.58	-10.75	0.872
	0.8	4.64	-0.20	0.824	2.58	-0.61	0.946	5.76	-13.78	0.826
2	0	2.11	-0.27	0.834	2.43	-0.64	0.897	1.89	-2.49	0.794
	0.3	5.56	-0.11	0.818	3.96	-0.17	0.900	4.12	-11.02	0.844
	0.5	14.0	-0.04	0.891	4.53	-0.16	0.894	6.57	-29.16	0.765
	0.8	12.5	-0.05	0.859	4.72	-0.17	0.906	9.24	-38.15	0.842
3	0	2.13	-0.39	0.712	2.66	-0.70	0.901	4.12	-3.89	0.764
	0.3	4.80	-0.17	0.867	10.26	-0.07	0.830	5.21	-14.87	0.773
	0.5	5.20	-0.16	0.849	10.86	-0.07	0.896	6.88	-34.60	0.822
	0.8	4.45	-0.28	0.846	12.81	-0.06	0.829	6.44	-47.72	0.792
4	0	2.86	-0.23	0.799	2.78	-0.75	0.956	3.57	-13.85	0.793
	0.3	4.22	-0.22	0.860	11.11	-0.03	0.923	6.30	-18.37	0.866
	0.5	5.37	-0.16	0.880	19.266	-0.04	0.888	7.26	-42.57	0.922
	0.8	7.96	-0.10	0.895	186.45	-0.09	0.930	8.22	-51.21	0.919

Figures 6.3 through 6.5 plot the lateral force as a function of scratching distance. The intact rocks shown the lowest force for all rock types. The larger joint numbers and apertures require the higher lateral force along the scratching length. The forces reach maximum at the end of the scratching length. Joint frequency (J_n) tends to have stronger effect on rock abrasiveness than the joint aperture (e).

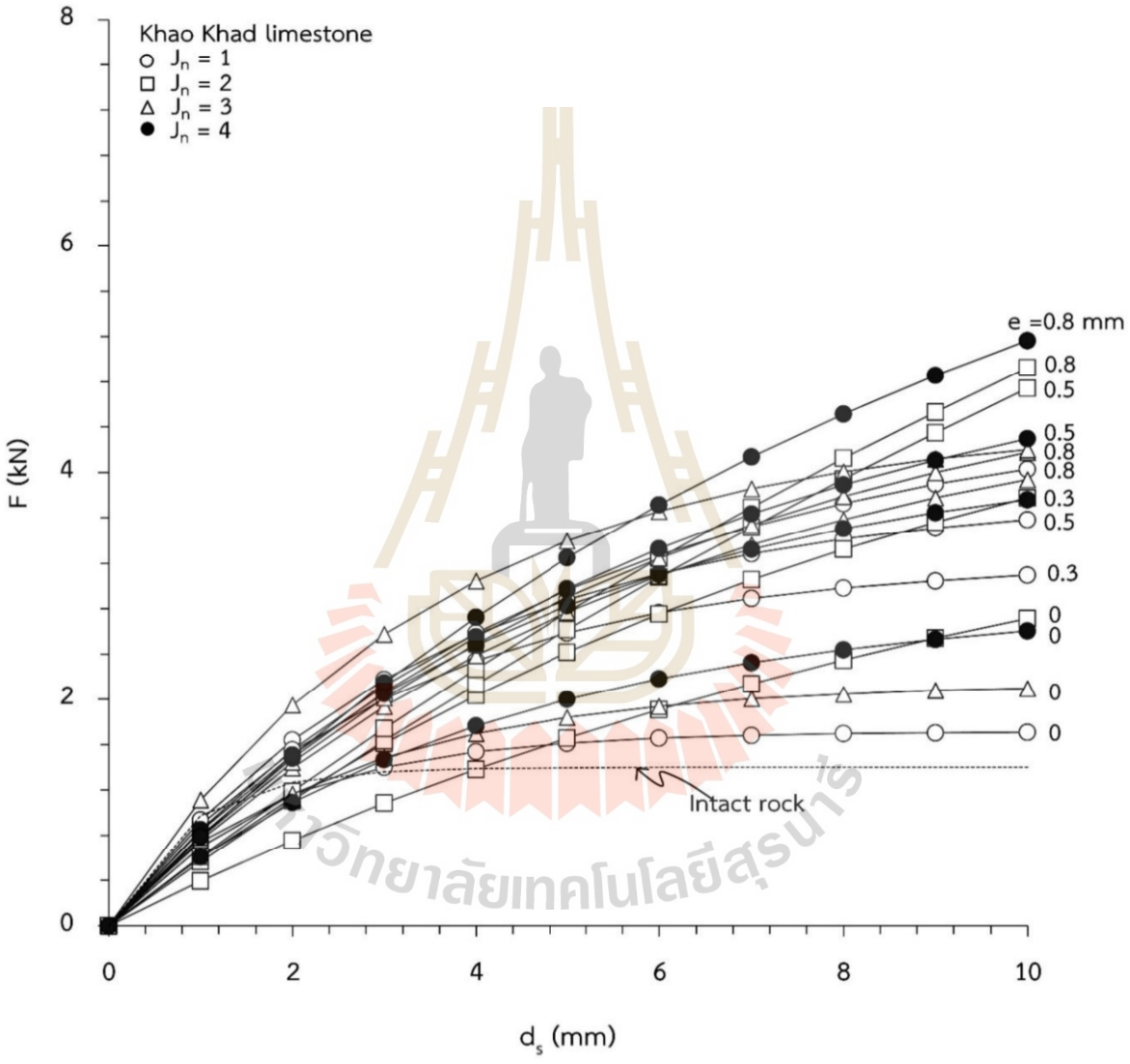

Figure 6.3 Lateral force as a function of scratching distance (d_s) of for different joint numbers and apertures for Khao Khad limestone.

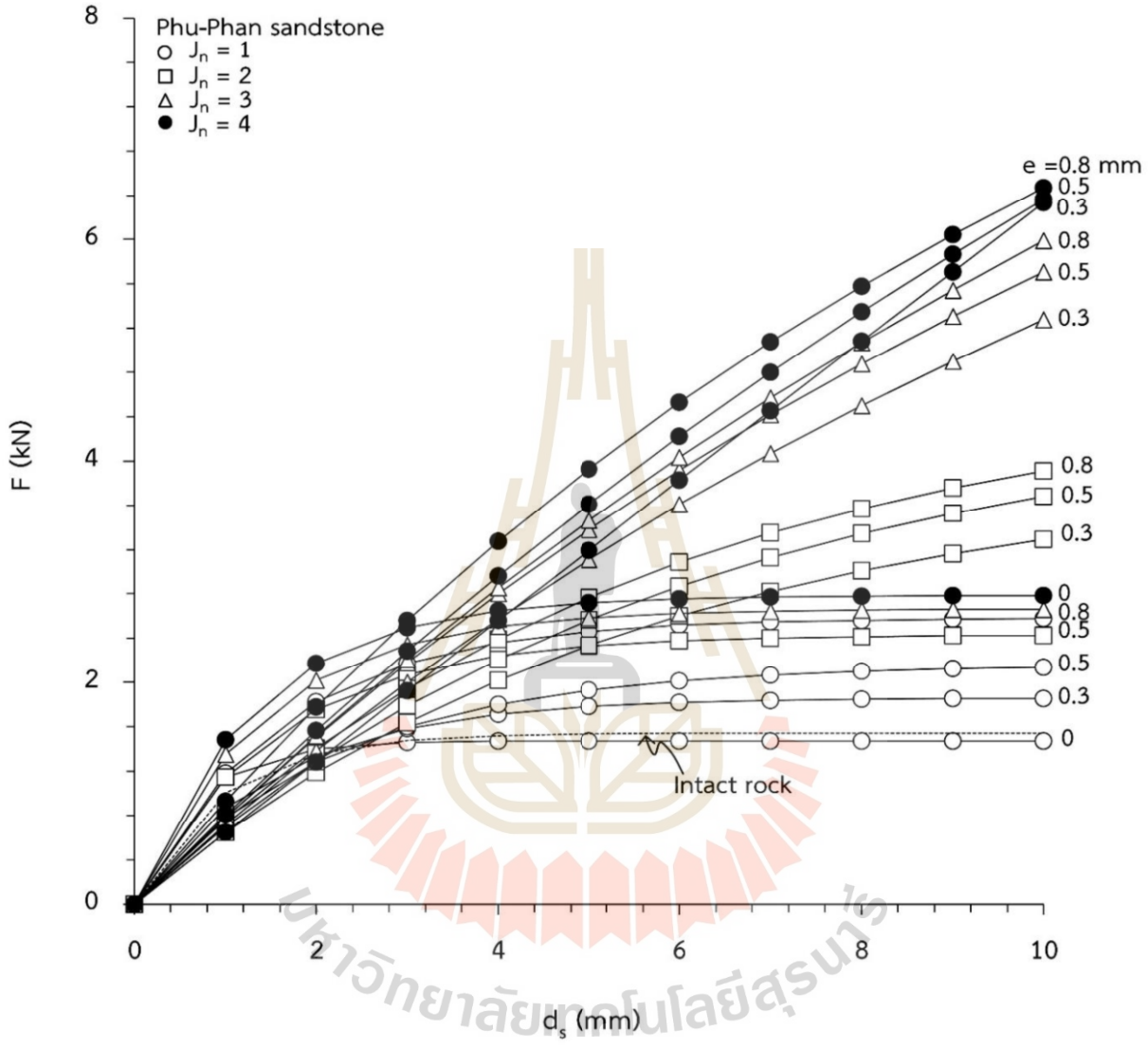

Figure 6.4 Lateral force as a function of scratching distance (d_s) of for different joint numbers and apertures for Phu Phan sandstone.

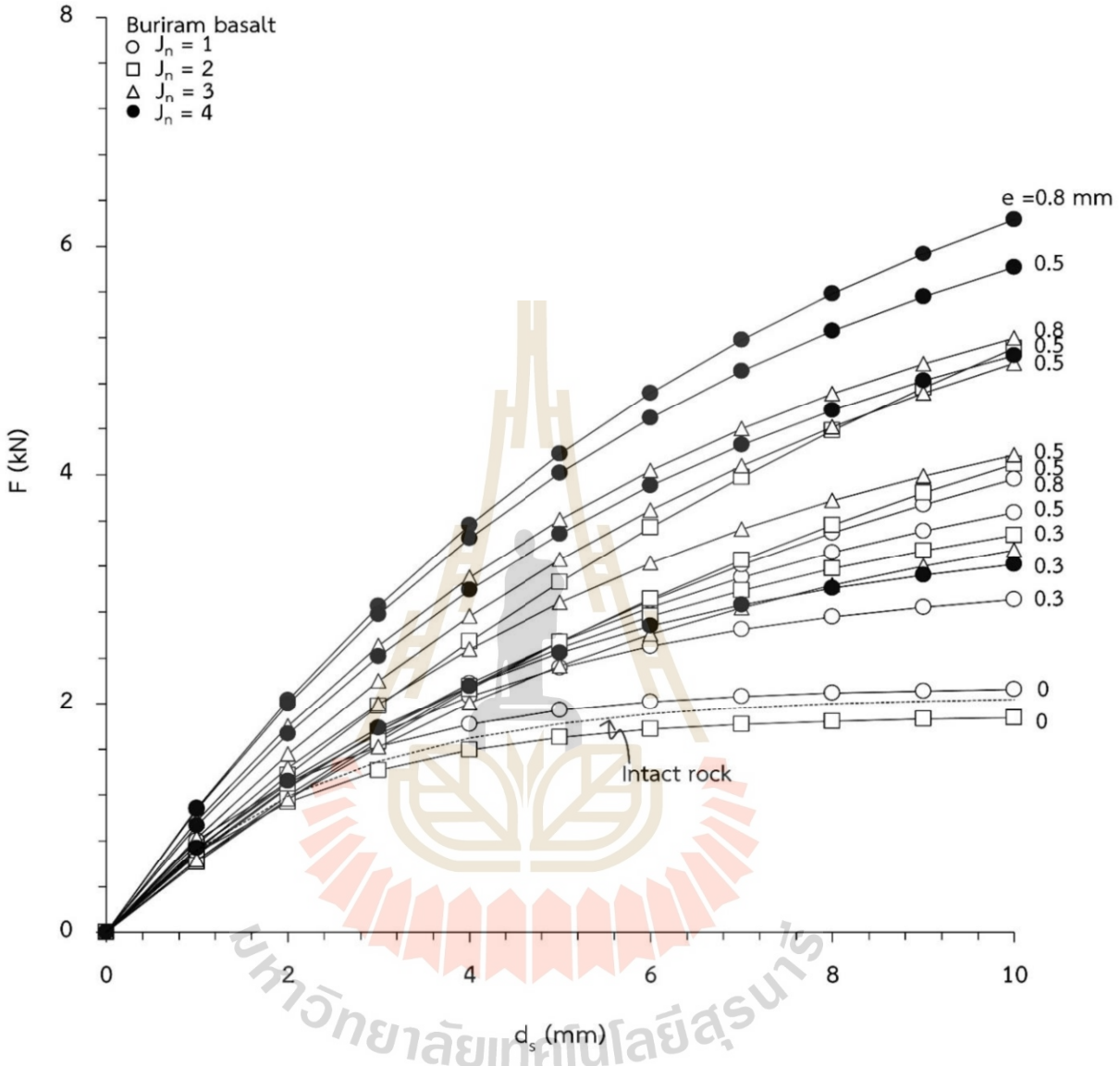

Figure 6.5 Lateral force as a function of scratching distance (d_s) of for different joint numbers and apertures for Buriram basalt.

6.5 Correlation between scratching groove volume (v) and joint number (J_n) and aperture (e)

The groove volume is affected by both joint number (J_n) and aperture (e). The number of joints increases the groove volume. This relationship can be expressed by the liner equation:

$$V = \omega J_n + \tau \quad (6.4)$$

where ω and τ are empirical constants, with their numerical values provided in Table 6.4.

Table 6.4 Empirical constants (ω and τ) in equation (6.4).

Number of joint (J_n)	Aperture (e) (mm)	$V = \omega \cdot J_n + \tau$								
		Rock type								
		Khao Khad limestone			Phu Phan sandstone			Buriram basalt		
0 (Intact rock)	-	ω	τ	R^2	ω	τ	R^2	ω	τ	R^2
		-	-		-	-		-	-	
1	0 0.3 0.5 0.8	2.76	-2.81	0.820	5.37	-2.10	0.956	3.40	-2.68	0.667
2	0 0.3 0.5 0.8	2.19	2.86	0.620	7.46	1.50	0.893	4.11	0.73	0.850
3	0 0.3 0.5 0.8	6.58	6.42	0.976	12.79	6.45	0.873	12.64	-0.20	0.964
4	0 0.3 0.5 0.8	9.48	9.67	0.933	14.63	11.91	0.925	15.25	2.13	0.961

The scratching groove volume however decreases as the joint aperture increases. This holds true for all tested rock shown in Figures 6.6. Note that the groove volume considered here is only from the scratching of the intact portion of the rock between the joints, excluding the joint apertures.

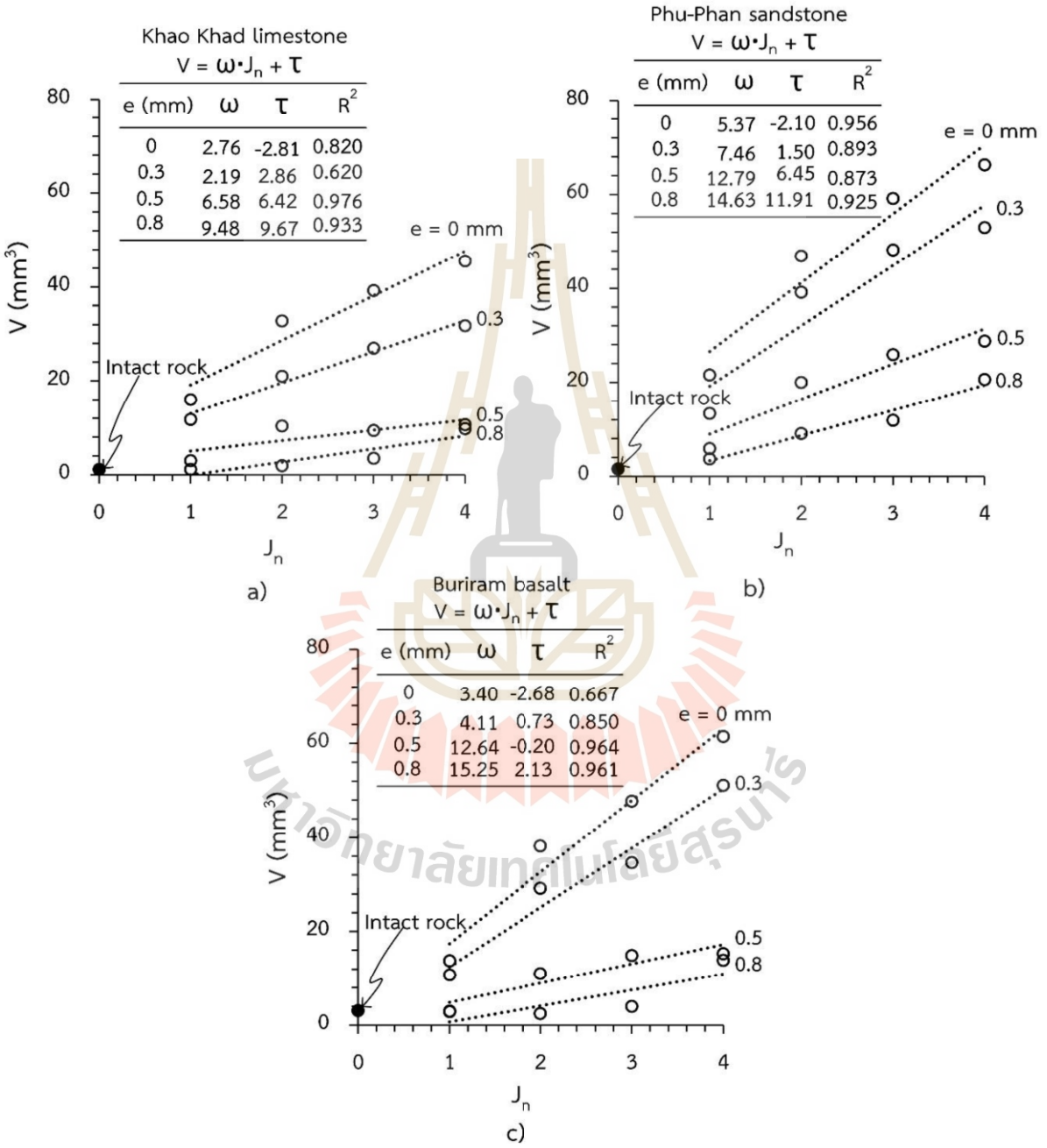

Figure 6.6 Groove volume as a function of joint numbers (J_n) for different apertures (e) for Khao Khad limestone (a), Phu Phan sandstone (b) and Buriram basalt (c).

6.6 Work and energy

Analysis in this study involves calculating the specific energy required for scratching, known as the CERCHAR specific energy (CSE), as proposed by Hamzaban, Memarian, and Rostami, (2018).

CSE is calculated by comparing the work (energy) used for scratching with the volume of the groove created on the intact rock surface excluding the joints. The fundamental equation for calculating the work is as follows (Zhang, Konietzky, and Frühwirt, 2020).:

$$W = \int_{d_s=0}^{10} F \cdot d_S \tag{6.5}$$

The work (W) is calculated based on the lateral force as a function of scratching displacement (F-ds) over a scratching distance of 10 millimeters. The specific energy can be calculated using the following equation (Zhang, Konietzky et al., 2020).

$$CSE = \frac{W}{V} = \frac{\int_{d_s=0}^{10} F \cdot d_s}{V} \tag{6.6}$$

The results of calculation are given in Table 6.5. CSE values as a function of joint CAI are plotted as a function of CAI in Figures 6.7 through 6.9.

The energy required to scratching the jointed rock per unit groove volume increases exponentially with CAI, where the greater joint numbers (J_n) use the lower scratching energy. Basalt (strong rock) shows higher CSE and CAI values than sandstone and limestone (softer rocks). For all tested rocks, wider joint apertures require lower specific energy to scratch.

Table 6.5 Results of work and energy for all rock types and joint characteristics.

Number of joints (J_n)	Aperture (e) (mm)	Rock type					
		Khao Khad limestone		Phu Phan sandstone		Buriram basalt	
0 (Intact rock)	-	W (J)	CSE (J/mm^{-1})	W (J)	CSE (J/mm^{-1})	W (J)	CSE (J/mm^{-1})
		11.76	10.29	12.93	8.13	40.85	13.23
1	0	11.39	10.12	25.81	6.99	34.42	11.49
	0.3	26.24	8.70	30.32	5.14	25.12	8.72
	0.5	94.79	8.04	51.83	4.00	61.16	5.68
	0.8	79.63	4.9	86.48	3.88	70.52	5.11
2	0	15.92	8.26	40.62	5.06	22.37	8.95
	0.3	56.98	5.50	101.51	4.46	70.35	6.38
	0.5	109.92	5.22	139.98	3.56	92.81	3.20
	0.8	122.028	3.72	165.61	3.52	122.11	3.18
3	0	16.81	4.79	33.84	3.78	17.87	4.48
	0.3	37.50	4.51	98.33	3.51	47.14	3.16
	0.5	39.10	1.45	127.87	2.84	69.11	1.99
	0.8	42.43	0.95	207.85	2.65	59.44	1.24
4	0	31.75	3.33	23.75	2.78	29.33	2.11
	0.3	32.53	3.23	80.29	2.14	30.72	2.00
	0.5	35.20	1.02	113.57	2.13	68.24	1.33
	0.8	35.58	0.77	141.75	1.14	57.79	0.94

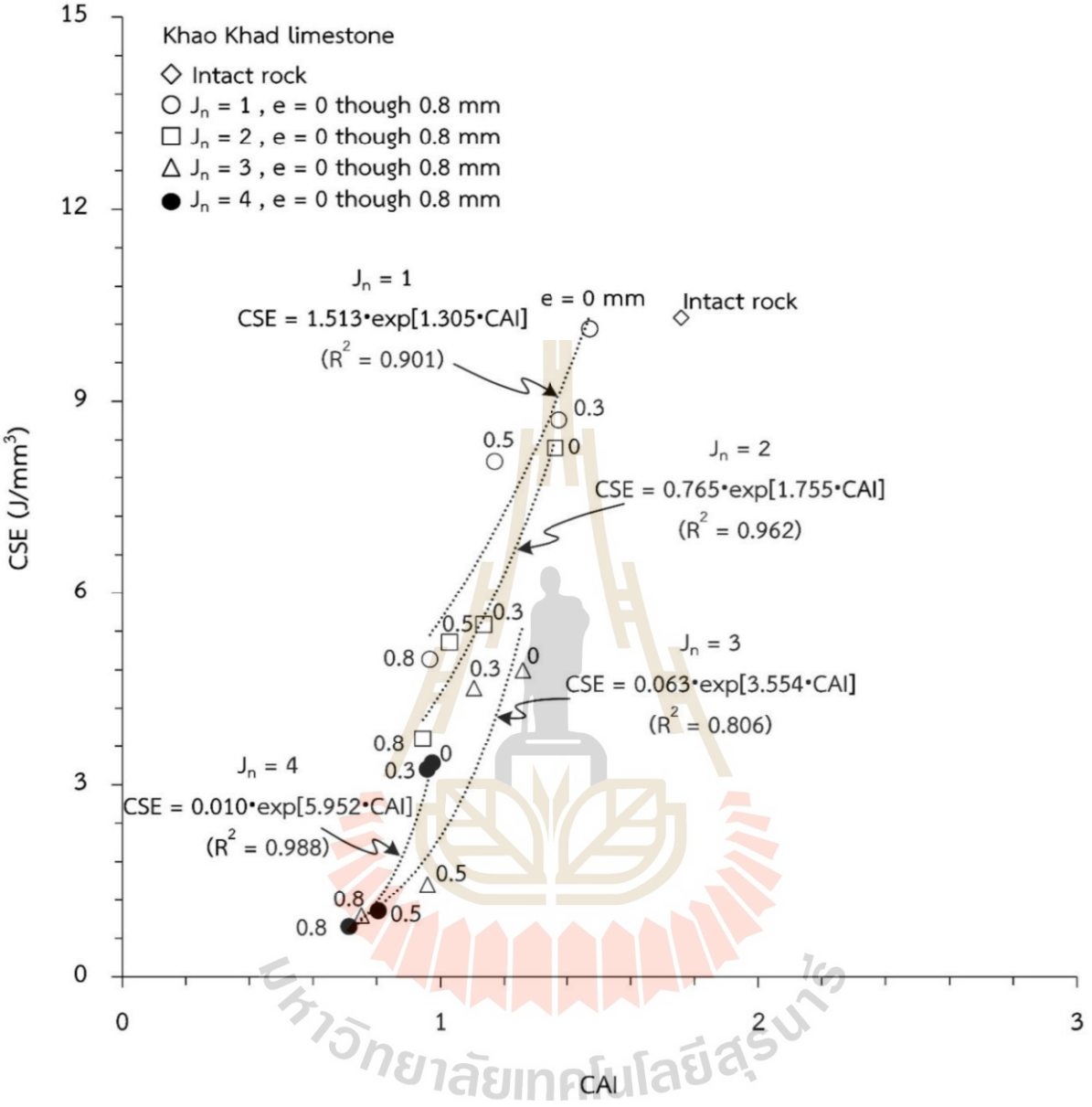

Figure 6.7 Correlation between CSE and CAI for all rock type for Khao Khad limestone.

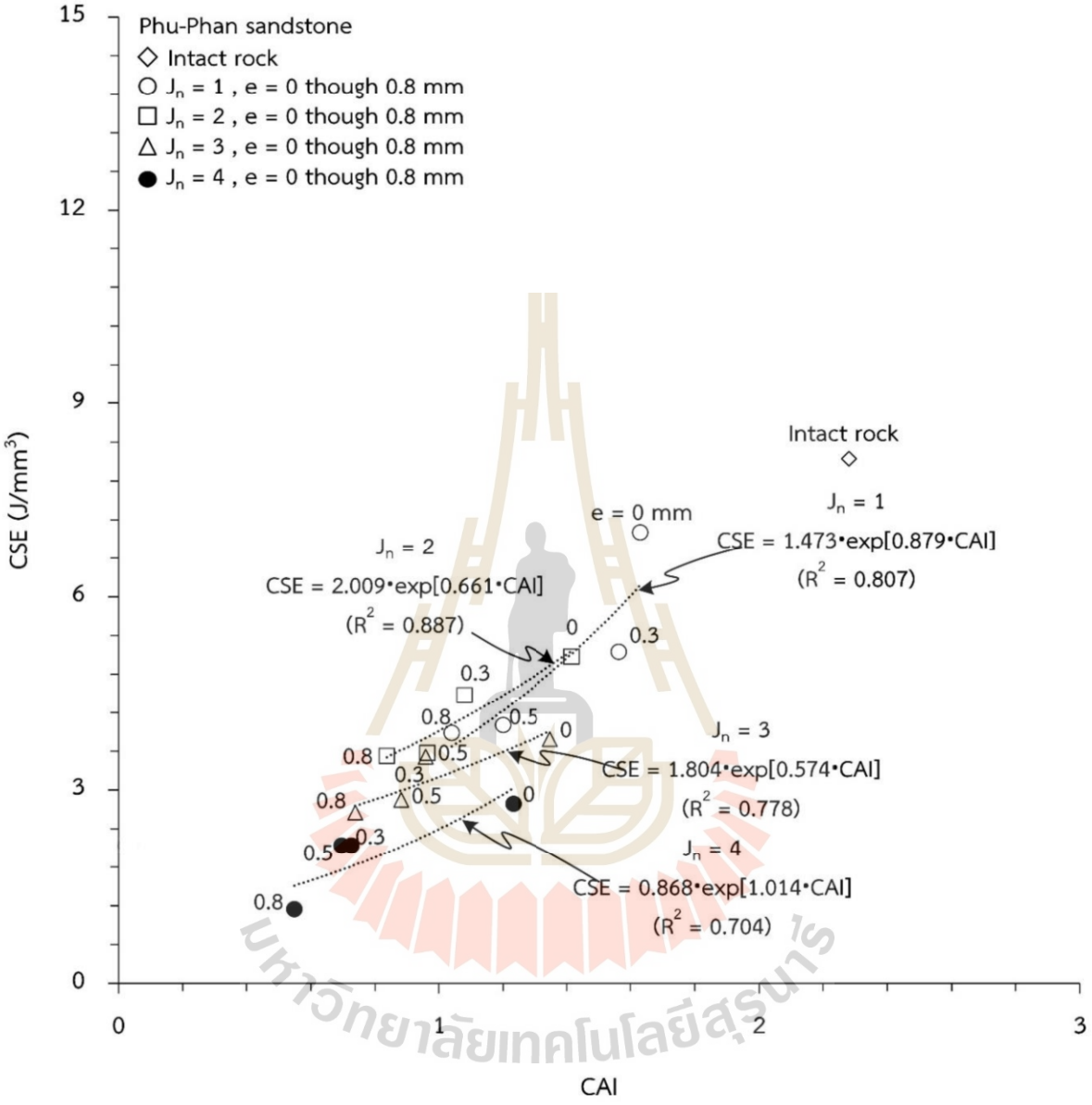

Figure 6.8 Correlation between CSE and CAI for all rock type for Phu Phan sandstone.

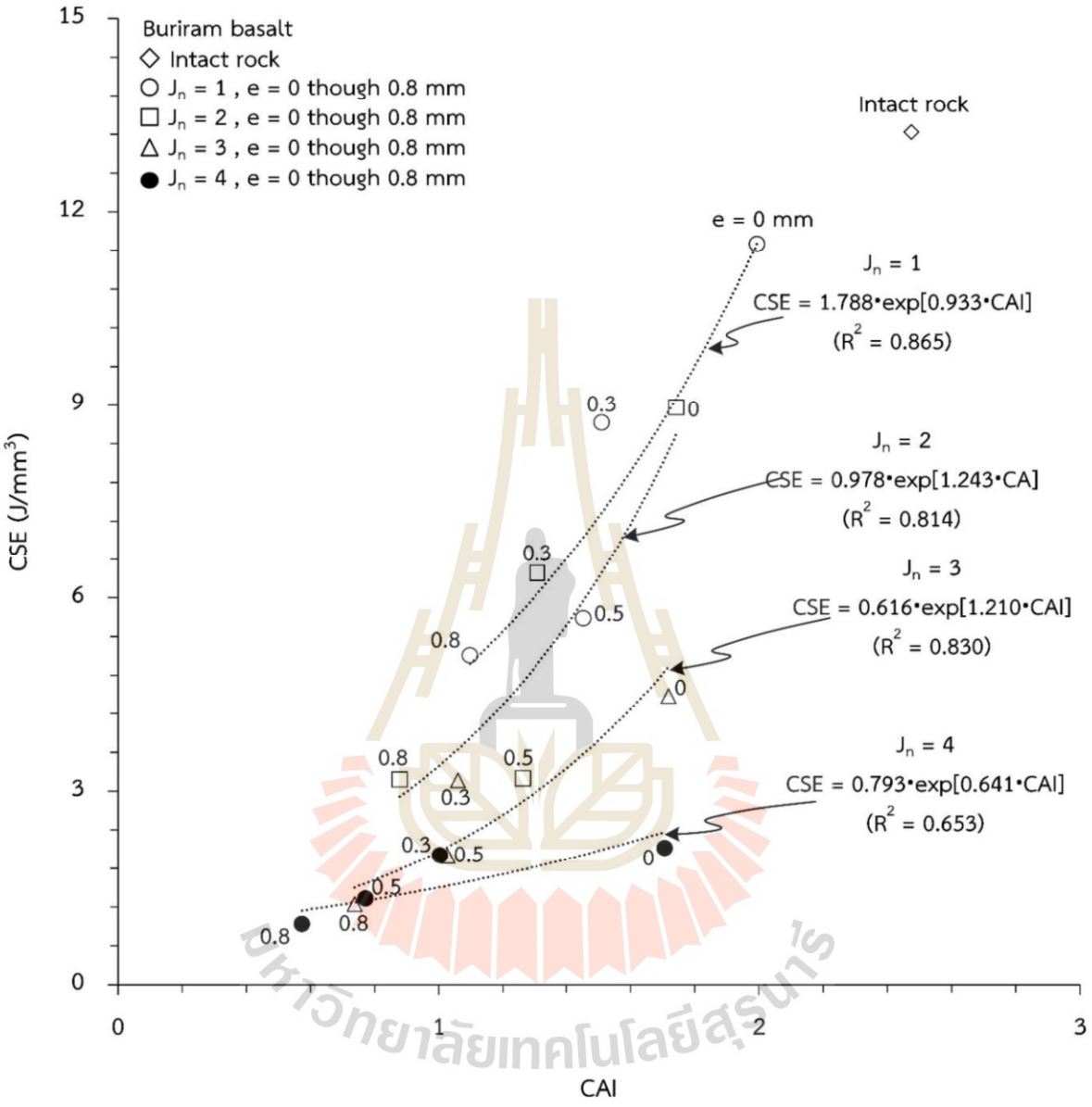

Figure 6.9 Correlation between CSE and CAI for all rock type for Buriram basalt.

CHAPTER VII
DISCUSSIONS, CONCLUSIONS AND RECOMMENDATIONS FOR FUTURE STUDIES

7.1 Discussions

The CAI values decrease as a result of both Jn and e. This reduction is attributed to the stylus tip entering the joint apertures during the test, which led to a smaller abrasion of the stylus. The stylus tip did not maintain contact with the entire rock surface over the 10 mm distance, resulting in a reduction of abrasion.

Sandstone and basalt show higher CAI values than limestone. This is because of the dependence of CAI on rock strength, as indicated by previous studies elsewhere Thanadkha and Fuenkajorn, (2022) and Kathancharoen and Fuenkajorn, (2023). They report strengths of 81.43 MPa for sandstone, 79.17 for basalt and 54.61 for limestone. Hard rock gives greater CAI values and shows large effect of joint characteristics than the softer ones.

The force measured during scratching increases with Jn and e. Higher numbers of joints and larger apertures require higher force to scratch the rock surface. This is due to the stylus encountering the gaps created by larger apertures, causing additional resistance. When the stylus passes through a large gap, it drops and requires more force to step up to continue scratching. The larger gap (aperture) results in a higher scratching force. This implies that an excavating tool may show less wear if it cuts through fractured rocks as compared to the intact ones. Larger scratch volumes are obtained when the number of joints is increased. This effect is more pronounced in strong rock (basalt), as compared to the softer rock, and hence resulting in a higher CAI value. The roles of joint apertures are, however, opposite. Lager apertures lead to a reduction of scratching volume. This is because as the aperture increases the intact

portions of the rock surface reduce as the total scratching distance is maintained constant at 10 mm as specified by the ASTM standard practice.

Regardless of joint number and aperture the CERCHAR specific energy (CSE) increases with CAI. This observation is similar to those of intact rocks performed elsewhere. The CSE-CAI relations show small effect of Jn and e for softer rocks (limestone and sandstone). The Jn and e effects are significant for the CSE-CAI relation of strong rock (basalt). This implies that for strong rock under the same CAI value the increases of Jn and e can notably reduce the energy to cut their surfaces.

The results obtained here are limited to the condition at which the scratching direction is normal to the joint traces with one joint set. The effect of the angles between scratching direction and joint line has not been investigated. In addition, the dip angle of the simulated joints is limited to 90°. The effect of dip angle has not been investigated.

7.2 Conclusions

The results of testing and analyses obtained here can be concluded as follows.

1) Number of joint and aperture can decrease the wear of stylus pin (CAI) while increasing the scratching force and groove volume.

2) The effects of joint aperture and joint number on CAI and ploughing force pronounce more in strong rock (basalt) than in soft rock (limestone). This results in a reduction of lower cutting energy.

3) The groove volume increases more rapidly for larger numbers of joints, as compared to smaller number of joints.

4) The effect of joint aperture on groove volume is more significant in soft rock than in the stronger one.

5) Soft rocks show less effect on CSE-CAI relation than does the stronger ones.

7.3 Recommendations for future studies

Scope and limitations of the test variables in the study lead to

recommendations for future studies as follows.

1) A variety of rocks with a wide range of compressive strengths should be tested to confirm the conclusion drawn in this study.

2) The effect of joint orientations and dip angles in relation to the scratching abrasives should be investigated.

3) This study is limited to testing on smooth rock and joint surfaces. The effect of roughness of rock surface and joint wall should be investigated. Effect of pore pressure in joint should be incorporated into the future study.

REFERENCES

Al-Ameen. SI., & Waller, MD. (1994). The influence of rock strength and abrasive mineral content on the CERCHAR abrasive index. *Engineering Geology*, *36*(3), 293–301.

American Society for Testing and Materials. (2022). *Annual Book of ASTM Standards: Standard Test Method for Laboratory Determination of Abrasiveness of Rock Using the CERCHAR Method* (Vol. 04.09). West Conshohocken, PA: ASTM International.

Aydın, H. (2019). Investigating the effects of various testing parameters on CERCHAR abrasivity index and its repeatability. *Wear*, *418-419*, 61-74.

Alber, M. (2008). Stress dependency of the CERCHAR abrasivity index (CAI) and its effects on wear of selected rock cutting tools. *Tunnelling and Underground Space Technology*, *23*(4), 351-359.

Beste, U., Lundvall, A., & Jacobson, S. (2004). Micro-scratch evaluation of rock type a means to comprehend rock drill wear. *Tribology International*, *37*(2), 203-210.

Capik, M., & Yilmaz, A. O. (2017). Correlation between CERCHAR abrasivity index, rock properties, and drill bit lifetime. *Arabian Journal of Geosciences*, *10*(15), 1-12.

Dahl, F., Bruland, A., Jakobsen, P. D., Nilsen, B., & Grøv, E. (2012). Classifications of properties influencing the drillability of rocks, based on the NTNU/SINTEF test method. *Tunnelling and Underground Space Technology*, *28*(1), 150-158.

Deliormanlı, A. H. (2012). CERCHAR abrasivity index (CAI) and its relation to strength and abrasion test methods for marble stones. *Construction and Building Materials*, *30*, 16-21.

Er, S., & Tuğrul, A. (2016). Estimation of CERCHAR abrasivity index of granitic rocks in Turkey by geological properties using regression analysis. *Bulletin of*

Engineering Geology and the Environment, 75(3), 1325-1339.

Feniak, M.W. (1944). Grain sizes and shapes of various minerals in igneous rocks. *American Mineralogist Journal of Earth and Planetary Materials*, *29*(11-12), 415-421.

Ghasemi, A. (2010). Study of CERCHAR abrasivity index and potential modifications for more consistent measurement of rock abrasion. *Master Thesis*, Pennsylvania State University.

Hamzaban, MT., Memarian, H., & Rostami, J. (2014). Continuous monitoringof pin tip wear and penetration into rock surface using a new CERCHAR abrasivity testing device. *Rock Mechanics and Rock Engineering*, *47*(2), 689–701.

Hamzaban, M. T., Memarian, H., & Rostami, J. (2018). Determination of scratching energy index for CERCHAR abrasion test. *Journal of Mining and Environment*, *9*(1), 73-89.

Hamzaban, M., Karami, B., & Rostami, J. (2019). Effect of pin speed on CERCHAR abrasion test results. *Journal of Testing and Evaluation*, *47*(1), 121-139.

Kathancharoen, N., & Fuenkajorn, K. (2023). Effects of mechanical and mineralogical properties on CERCHAR abrasivity index and specific energy of some thai rocks. *Engineering & Applied Science Research*, *50*(5), 478-489.

Ko, T. Y., Kim, T. K., Son, Y., & Jeon, S. (2016). Effect of geomechanical properties on Cerchar Abrasivity Index (CAI) and its application to TBM tunnelling. *Tunnelling and Underground Space Technology*, *57*(1), 99-111.

Kotsombat, T., Thongprapha, T., & Fuenkajorn, K. (2020). Scratching rate effects on CERCHAR abrasiveness index of sandstones. *Proceedings of Academicsera International Conference* (pp. 6-9). Thailand.

Labaš, M., Krepelka, F., & Ivaničová, L. (2012). Assessment of abrasiveness for research of rock cutting. *Acta Montanistica Slovaca*, *17*(1), 65-73.

Lassnig, K., Latal, C., & Klima, K. (2008). Impact of grain size on the CERCHAR abrasiveness test. *Geomechanics and Tunnelling, 1*(1), 71-76.

Lee, S., Jeong, H.-Y., & Jeon, S. (2012). Determination of Rock Abrasiveness using CERCHAR Abrasiveness Test. *Tunnelling and Underground Space Technology*, *22*(4), 284-295.

Michalakopoulos T.N., Anagnostou V.G., Bassanou M.E., & Panagiotou G.N. (2005) The influence of steel styli hardness on the CERCHAR abrasiveness index value. *International Journal of Rock Mechanics & Mining Sciences*, *43*, 321-327.

Ozdogan, M. V., Deliormanli, A. H., & Yenice, H. (2018). The correlations between the CERCHAR abrasivity index and the geomechanical properties of building stones. *Arabian Journal of Geosciences, 11*(20).

Plinninger, R., Käsling, H., Thuro, K., & Spaun, G. (2003). Testing conditions and geomechanical properties influencing the CERCHAR abrasiveness index (CAI) value. *International Journal of Rock Mechanics and Mining Sciences*, *40*(2), 259-263.

Plinninger, R. J., Kasling, H., & Thuro, K. (2004). Wear prediction in hardrock excavation using the CERCHAR abrasiveness index (CAI). *EUROCK 2004 & 53rd Geomechanics Colloquium*, Schubert (ed.). 1-6.

Prieto, L. (2012). The CERCHAR abrasivity index's applicability to dredging rock. *Proceedings of the Western Dredging Association (WEDA XXXII) Technical Conference and Texas A&M University (TAMU 43) Dredging Seminar* (pp. 212-219). San Antonio, Texas: WEDA.

Rostami, J., Ozdemir, L., Bruland, A., & Dahl, F. (2005). Review of issues related to Cerchar abrasivity testing and their implications on geotechnical investigations and cutter cost estimates. *Proceedings of the Rapid Excavation and Tunnelling Conference (RETC)* (pp. 738-751). Seattle, Washington: SME.

Rostami, J., Ghasemi, A., Alavi Gharahbagh, E., Dogruoz, C., & Dahl, F. (2013). Study of dominant factors affecting CERCHAR abrasivity index. *Rock Mechanics and Rock Engineering*, *47*(5), 1905-1919.

Sirdesai, N. N., Aravind, A., & Panchal, S. (2021). Impact of rock abrasivity on TBM cutter-discs during tunnelling in various rock formations. *Proceedings of the Advances in Mechanical Engineering* (pp. 527-534). Singapore: Springer.

Suana, M., & Peters, T. (1982). The CERCHAR abrasivity index and its relation to rock mineralogy and petrography. *Rock Mechanics, 15*(1), 1-8.

Thanadkha, P., & Fuenkajorn, K. (2022). Correlation between cerchar abrasivity index of smooth and rough rock fractures. *In Academicsera International Conference* (pp. 8-12). Kuala Lumpur, Malaysia.

Thuro K., & Käsling H., (2009). Classification of the abrasiveness of soil and rock. *Geomechanics And Tunnelling, 2*(2), 179–188.

Yaralı, O., & Duru, H. (2016). Investigation into effect of scratch length and surface condition on CERCHAR abrasivity index. *Tunnelling and Underground Space Technology*, *60*(36), 111-120.

Zhang, G., & Konietzky, H. (2020). CERCHAR Abrasion Ratio (CAR) as a New Indicator for Assessing Rock Abrasivity, Rock–Stylus Interaction and Cutting Efficiency. *Rock Mechanics and Rock Engineering, 53*(7), 3363-3371.

Zhang, G., Konietzky, H., & Frühwirt, T. (2020). Investigation of scratching specific energy in the CERCHAR abrasivity test and its application for evaluating rock-tool interaction and efficiency of rock cutting. *Wear, 448-449*(1).

Zhang, G., Konietzky, H., Song, Z., & Zhang, M. (2020). Study of CERCHAR abrasive parameters and their relations to intrinsic properties of rocks for construction. *Construction and Building Materials, 244*(1).

APPENDIX A

CAI RESULTS FOR INTACT ROCK

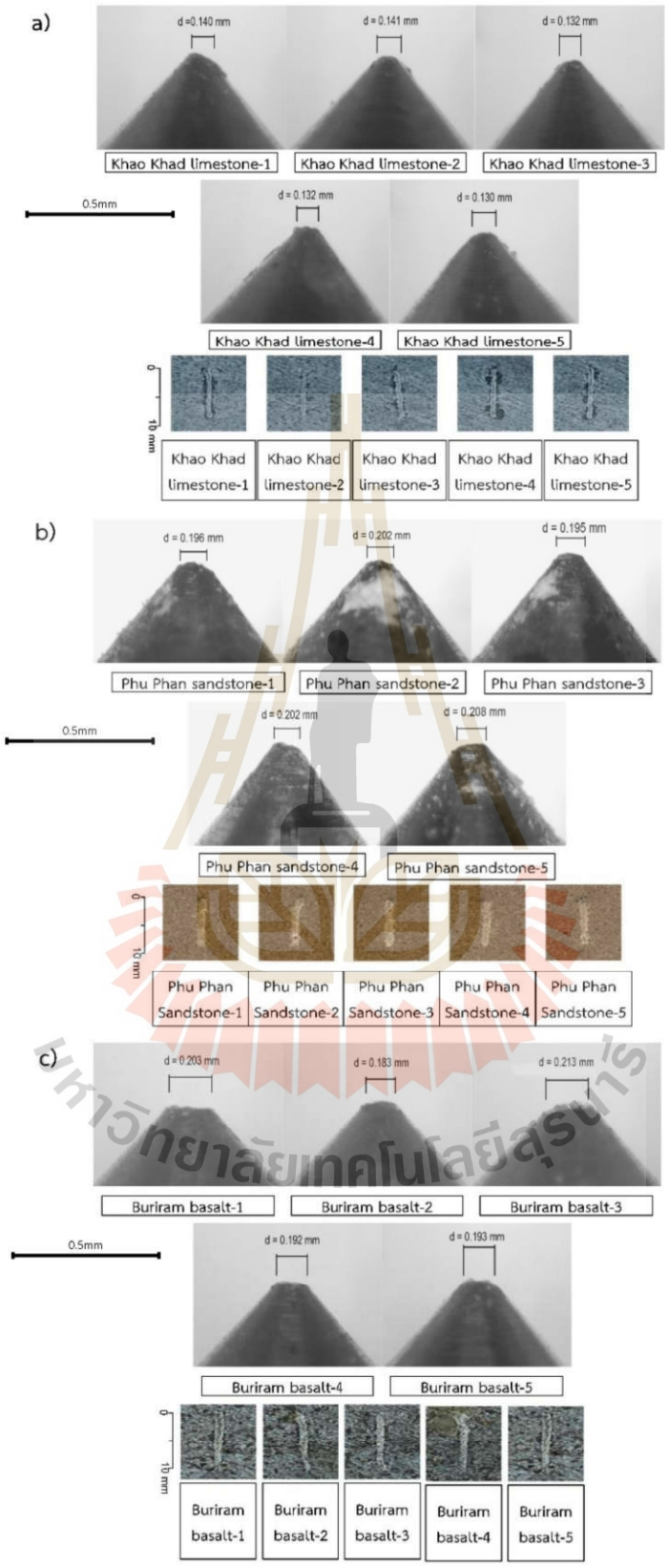

Figure A.1 Stylus tips after CERCHAR testing and scratching trace after testing on intact rock

APPENDIX B

CAI RESULTS FOR ONE JOINT WITH DIFFERENT APERTURES

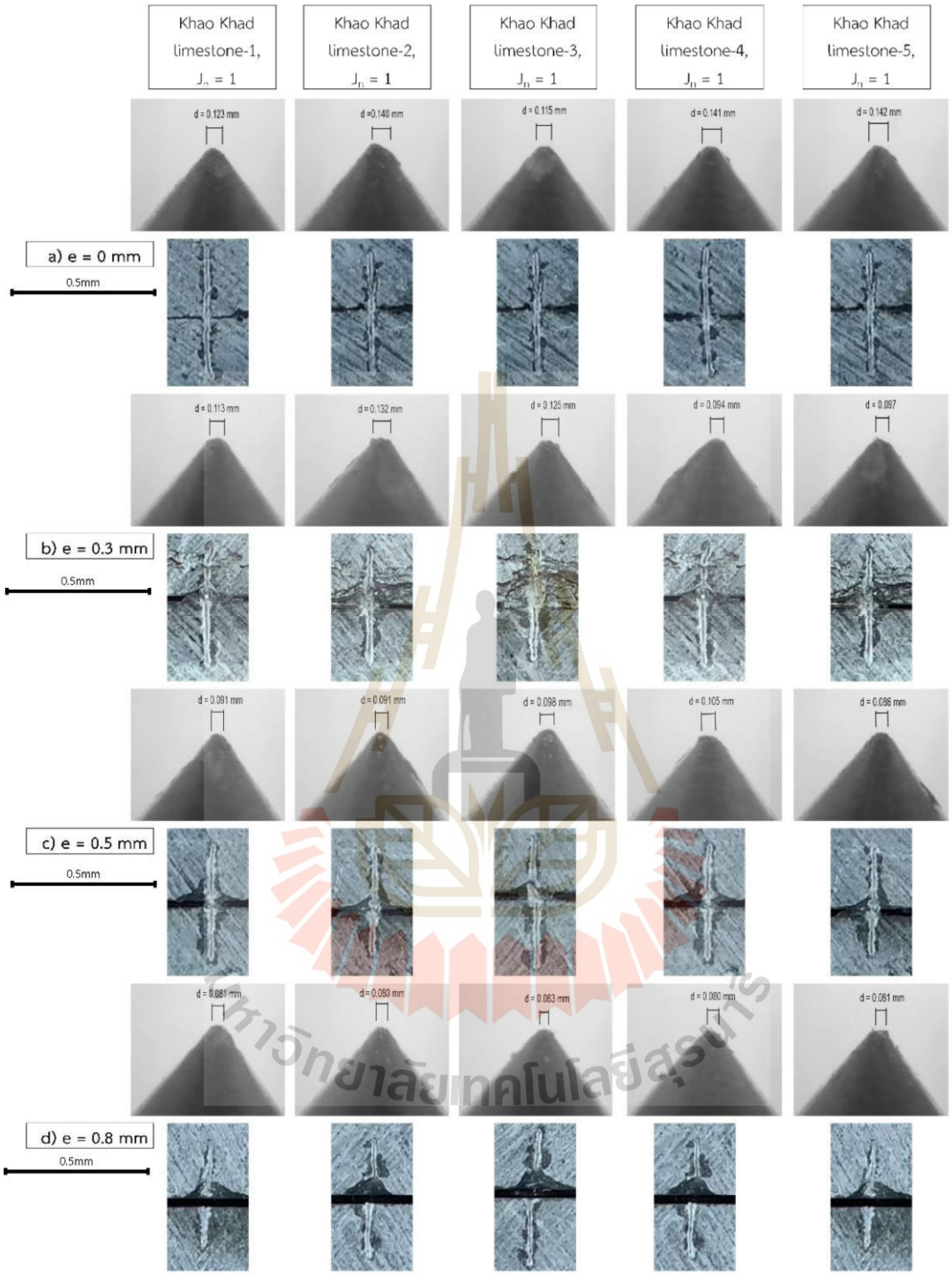

Figure B.1 CAI results for one joint with different apertures of Khao Khad limestone for apertures of 0 mm (a), 0.3 mm (b), 0.5 mm (c) and 0.8 mm (d).

Figure B.2 CAI results for one joint with different apertures of Phu Phan sandstone for apertures of 0 mm (a), 0.3 mm (b), 0.5 mm (c) and 0.8 mm (d).

.

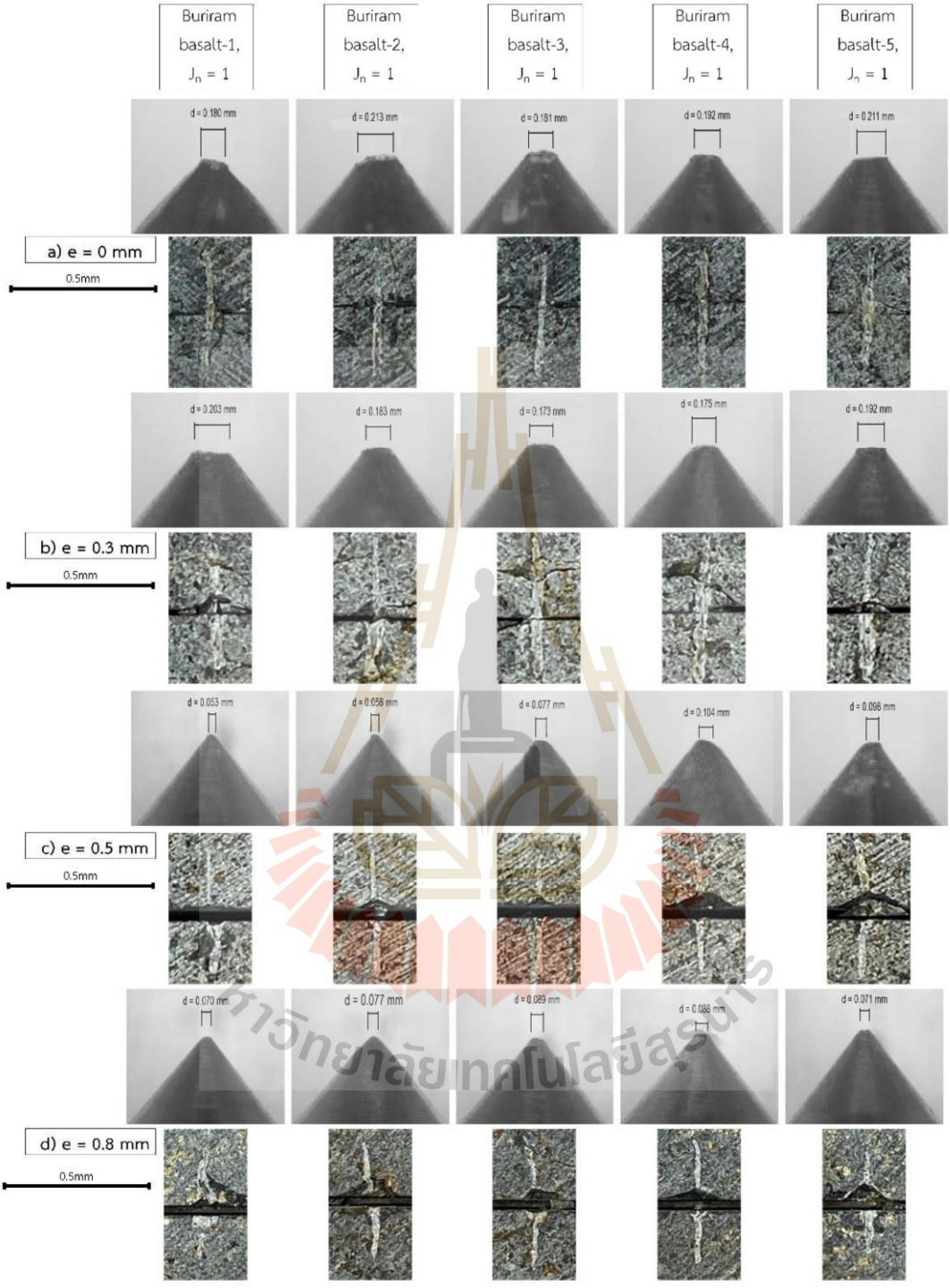

Figure B.3 CAI results for one joint with different apertures of Buriram basalt for apertures of 0 mm (a), 0.3 mm (b), 0.5 mm (c) and 0.8 mm (d).

.

APPENDIX C

CAI RESULTS FOR TWO JOINTS WITH DIFFERENT APERTURES

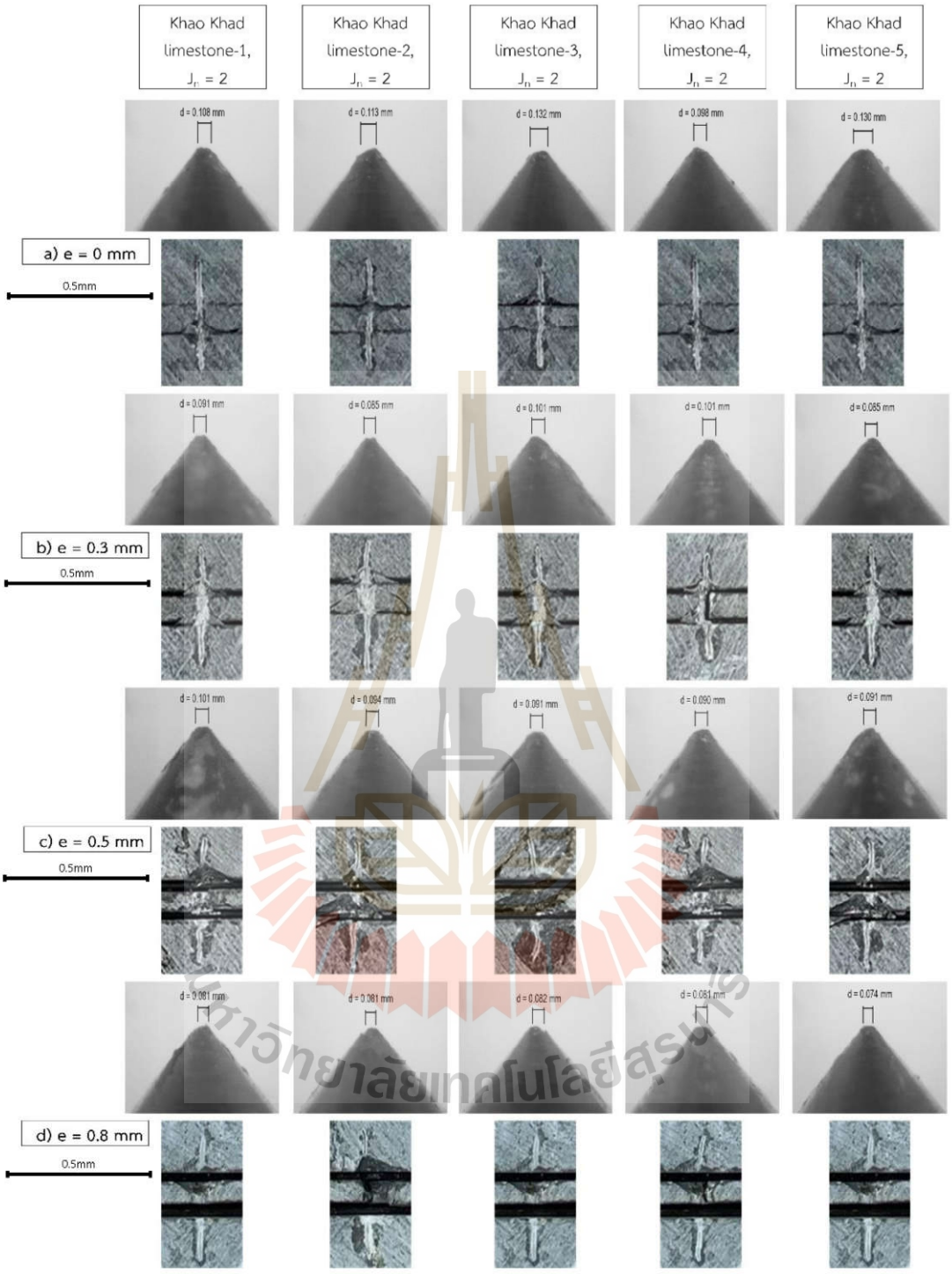

Figure C.1 CAI result for two joints with different aperture of Khao Khad limestone for aperture of 0 mm (a), 0.3 mm (b), 0.5 mm (c) and 0.8 mm (d).

Figure C.2 CAI result for two joints with different aperture of Phu Phan sandstone for aperture of 0 mm (a), 0.3 mm (b), 0.5 mm (c) and 0.8 mm (d).

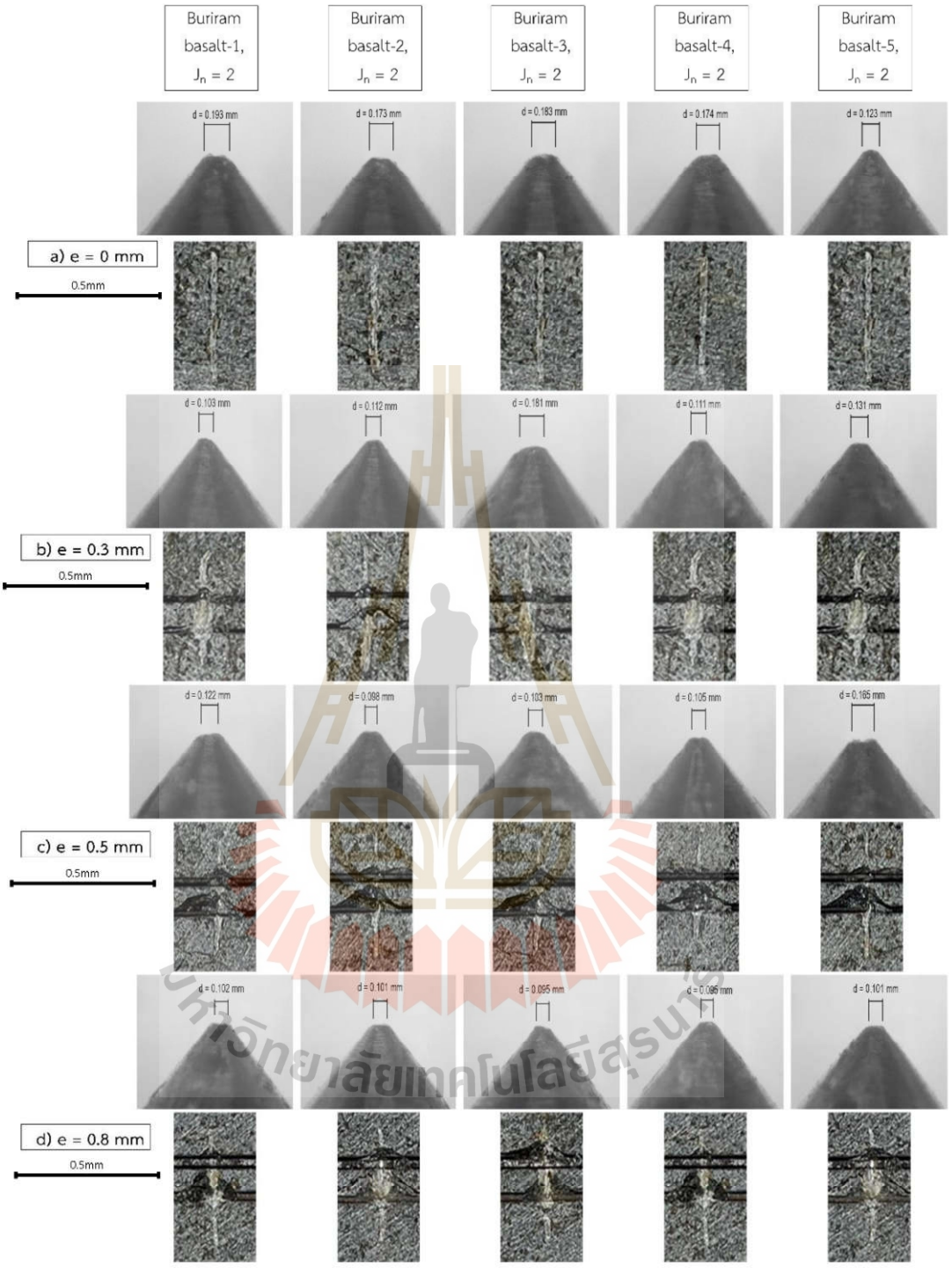

Figure C.3 CAI result for two joints with different aperture of Buriram basalt for aperture of 0 mm (a), 0.3 mm (b), 0.5 mm (c) and 0.8 mm (d).

APPENDIX D

CAI RESULTS FOR THREE JOINTS WITH DIFFERENT APERTURES

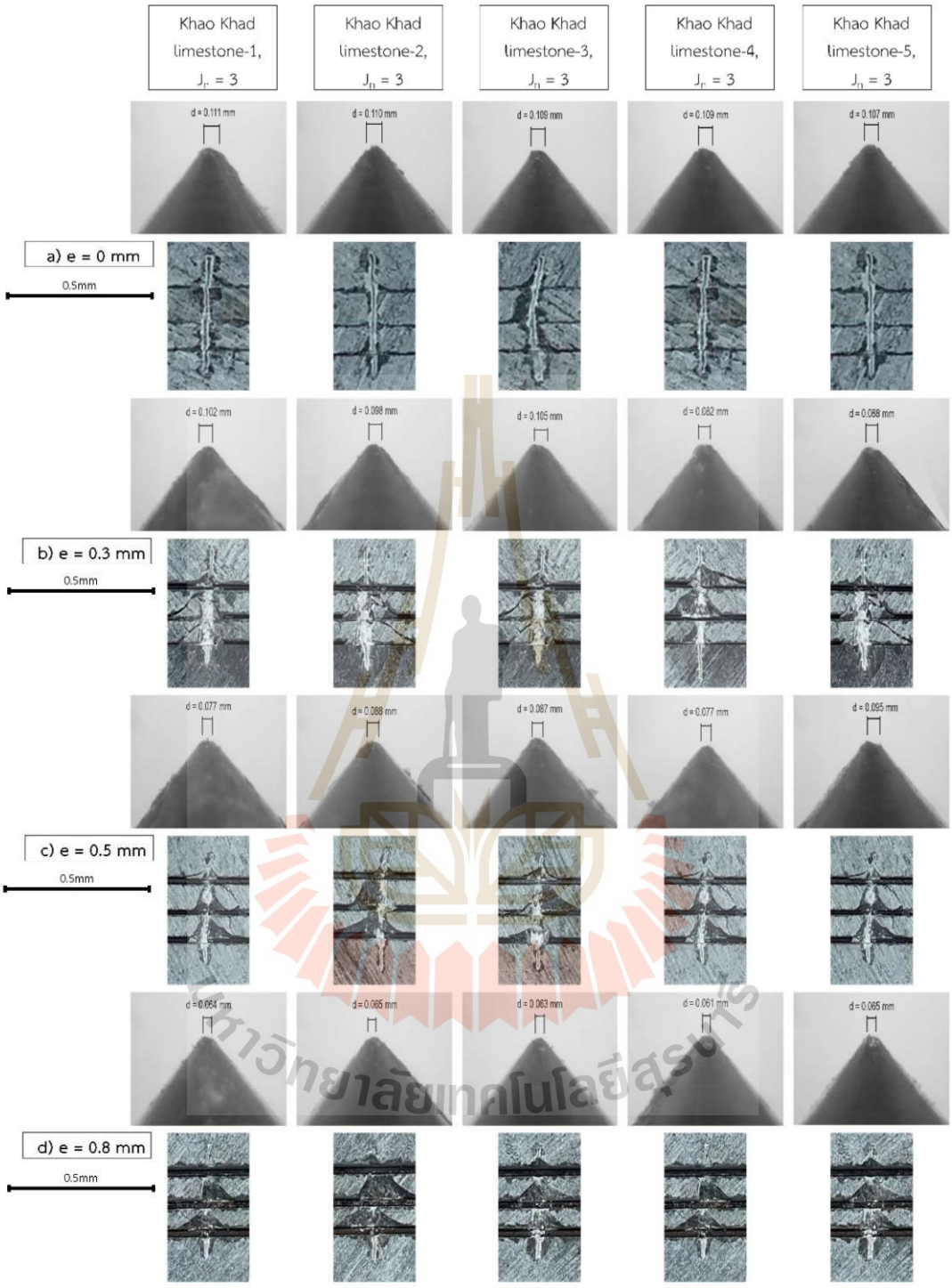

Figure D.1 CAI result for three joints with different aperture of Khao Khad limestone for aperture of 0 mm (a), 0.3 mm (b), 0.5 mm (c) and 0.8 mm (d).

Figure D.2 CAI result for three joints with different aperture of Phu Phan sandstone for aperture of 0 mm (a), 0.3 mm (b), 0.5 mm (c) and 0.8 mm (d).

.

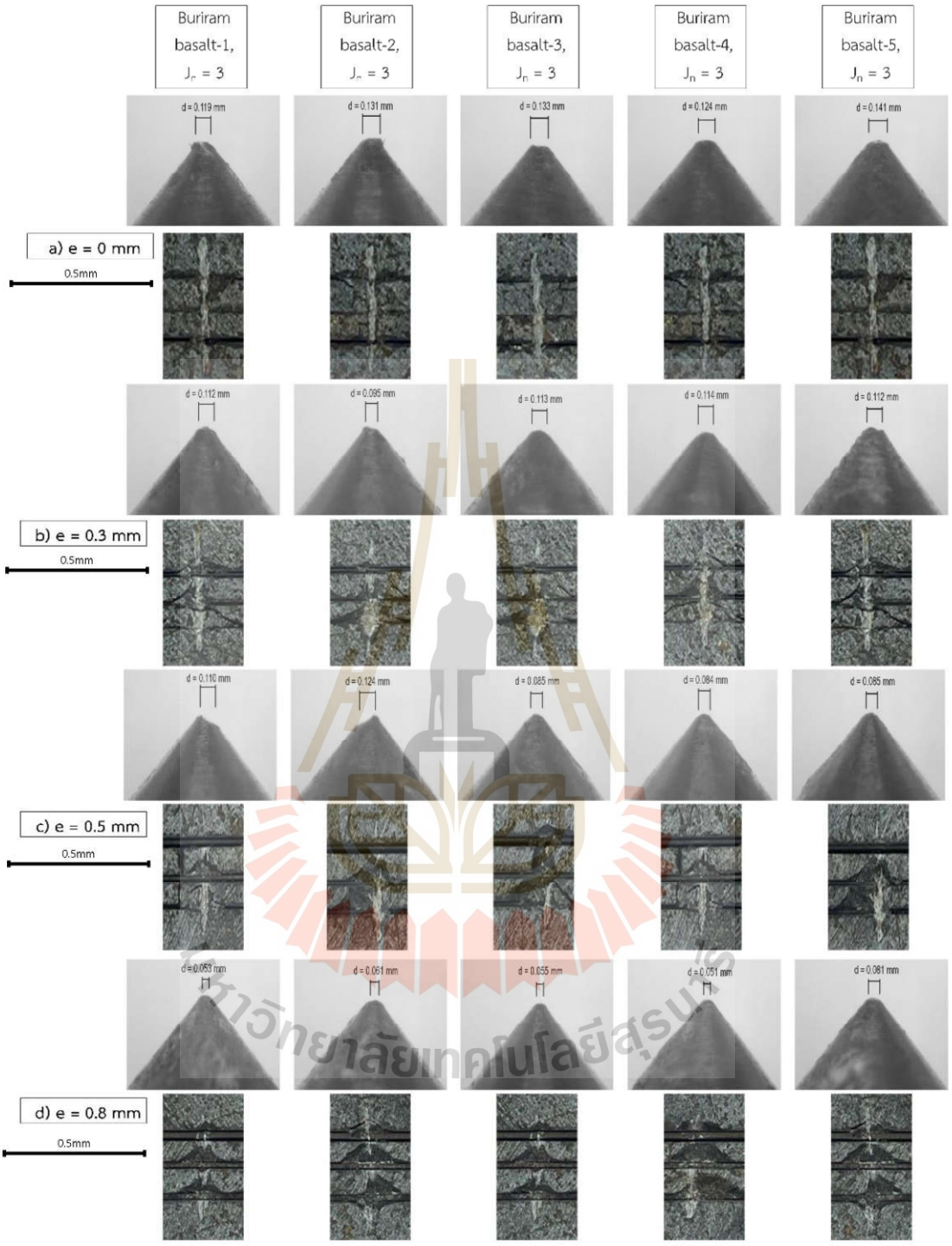

Figure D.3 CAI result for three joints with different aperture of Buriram basalt for aperture of 0 mm (a), 0.3 mm (b), 0.5 mm (c) and 0.8 mm (d).

.

APPENDIX E

CAI RESULTS FOR FOUR JOINTS WITH DIFFERENT APERTURES

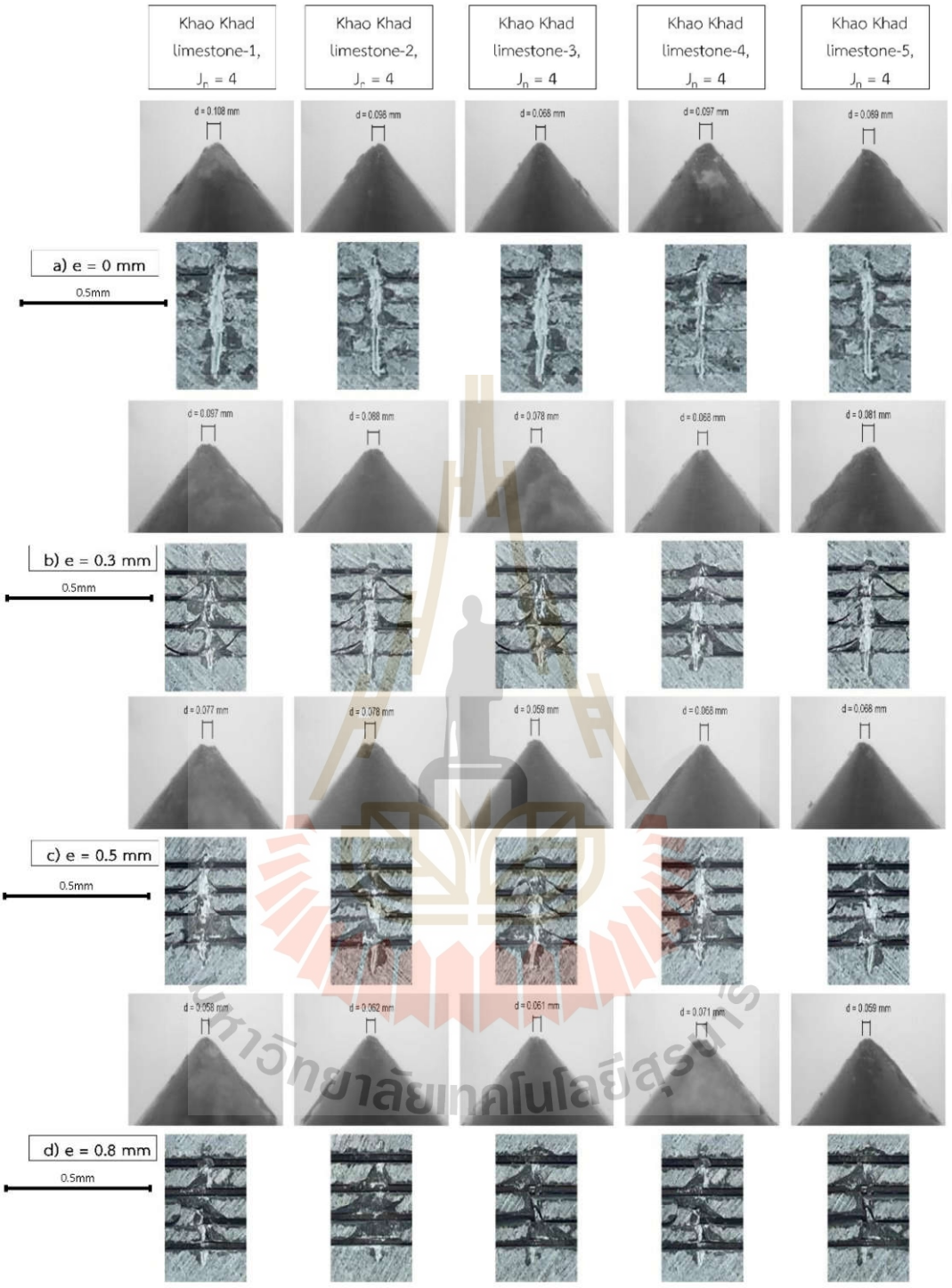

Figure E.1 CAI result for four joints with different aperture of Khao Khad limestone for aperture of 0 mm (a), 0.3 mm (b), 0.5 mm (c) and 0.8 mm (d).

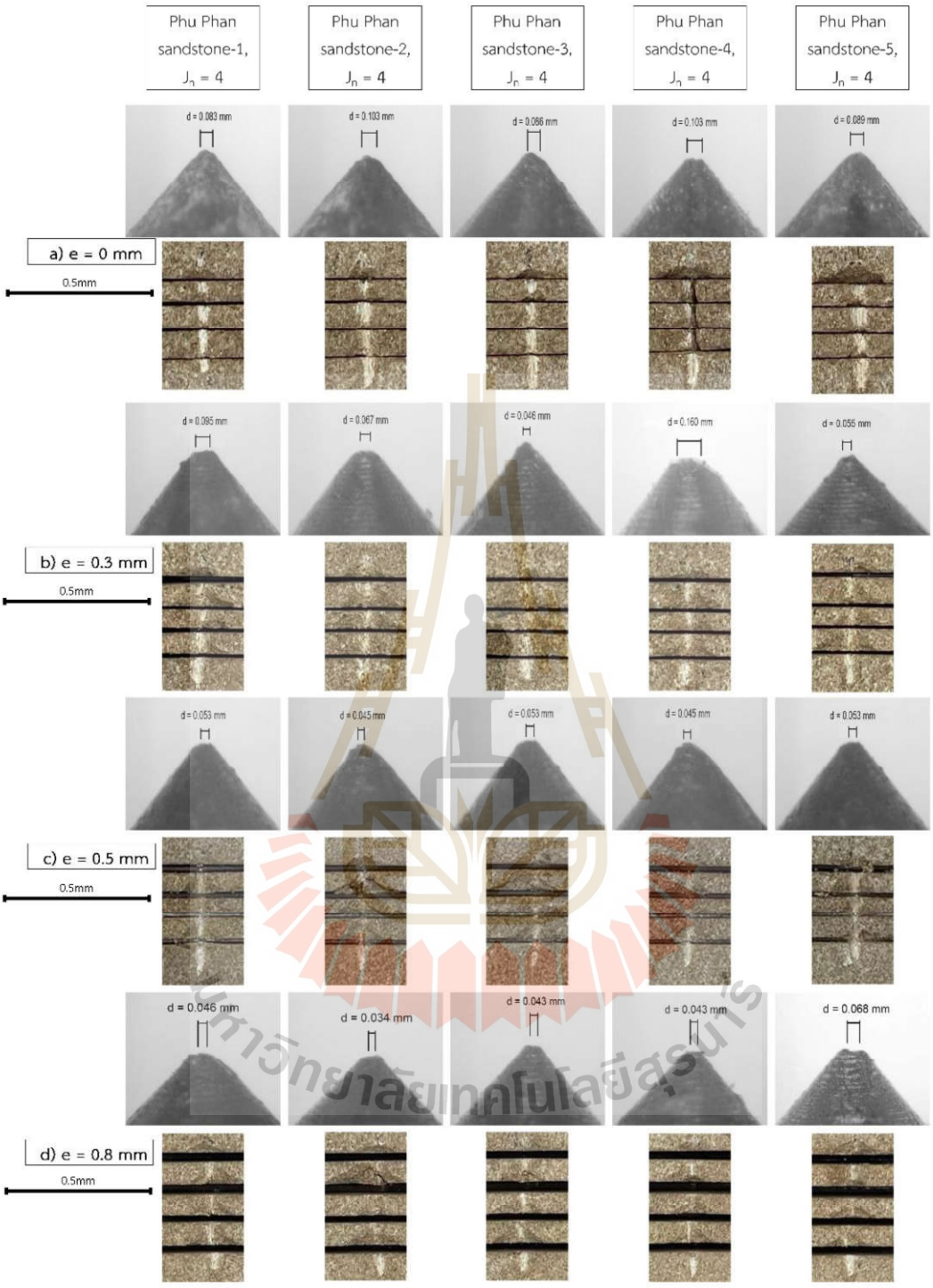

Figure E.2 CAI result for four joints with different aperture of Phu Phan sandstone for aperture of 0 mm (a), 0.3 mm (b), 0.5 mm (c) and 0.8 mm (d).

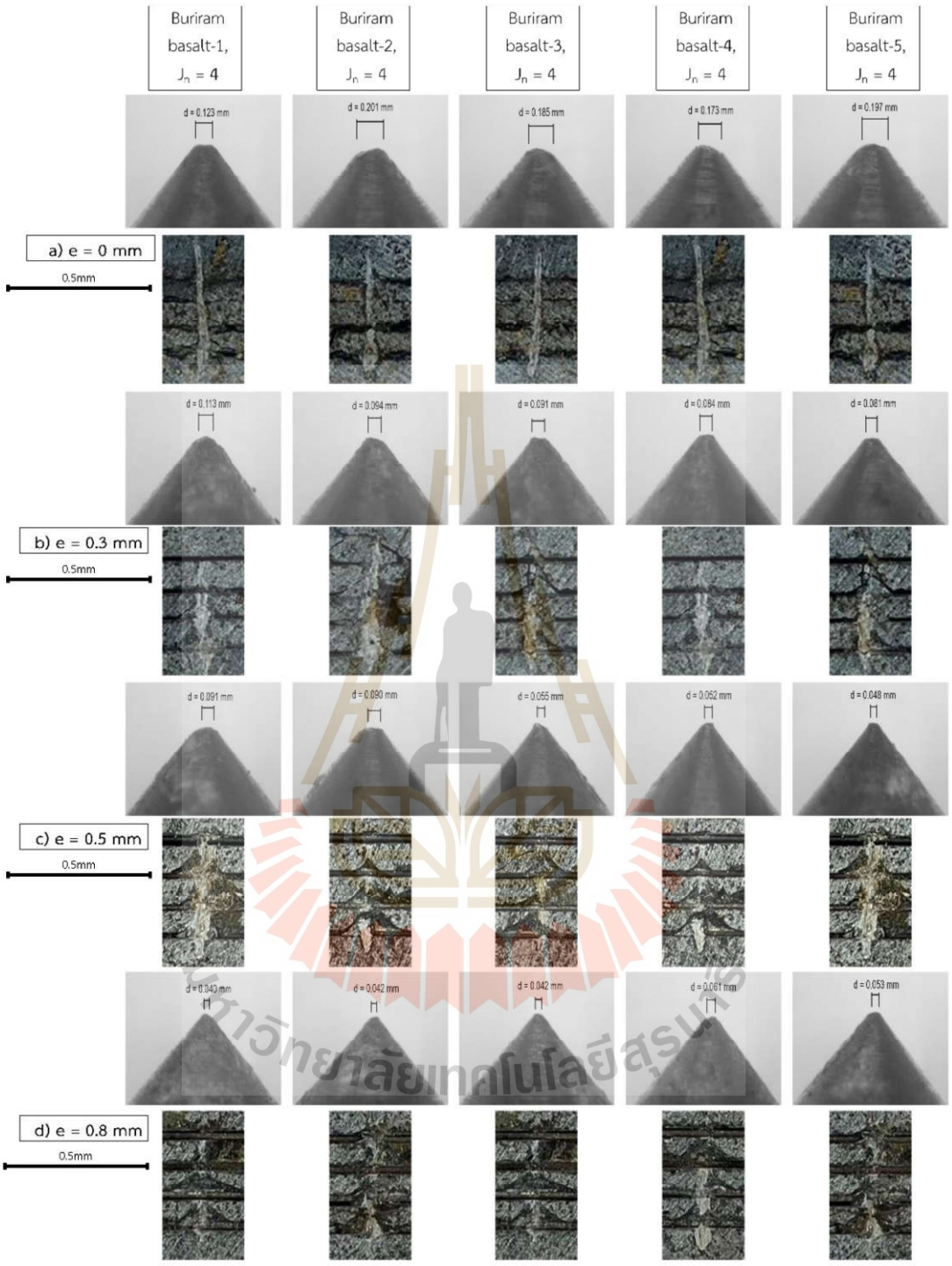

Figure E.3 CAI result for four joints with different aperture of Buriram basalt for aperture of 0 mm (a), 0.3 mm (b), 0.5 mm (c) and 0.8 mm (d).

APPENDIX F

LATERAL FORCE AS A FUNCTION OF SCRATCHING DISPLACEMENT

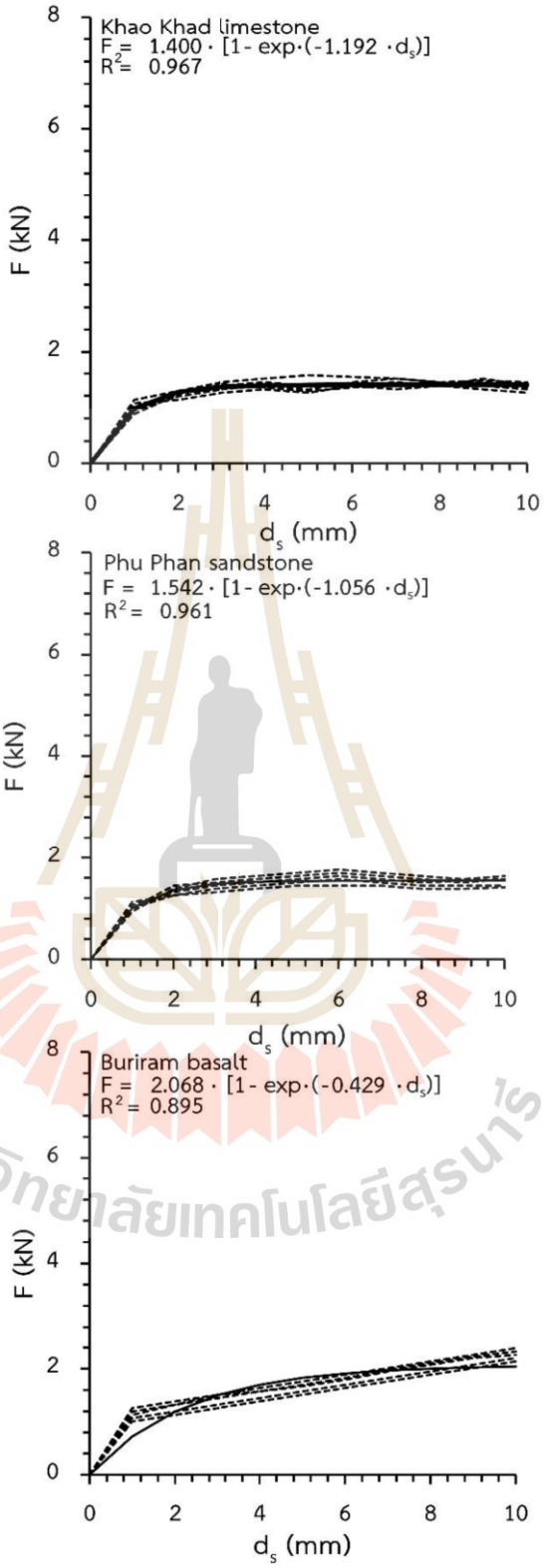

Figure F.1 Lateral force as a function of scratching displacement for Intact rock

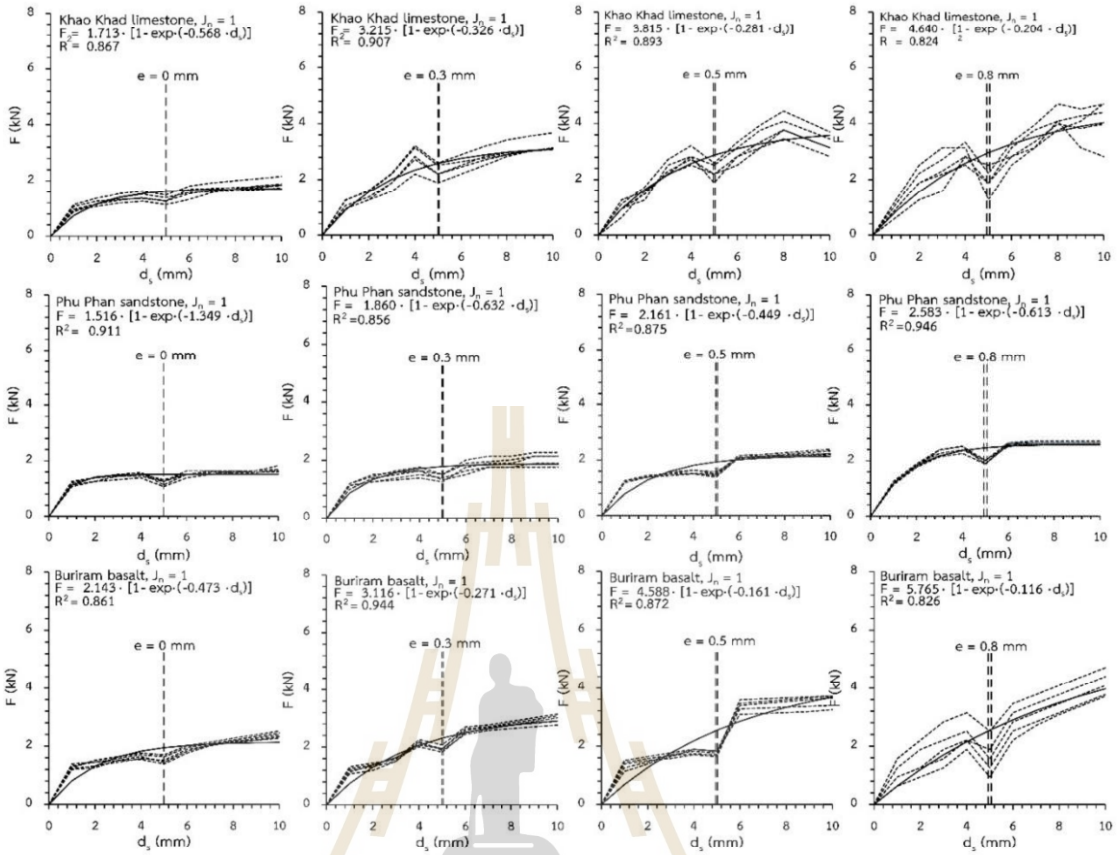

Figure F.2 Lateral force as a function of scratching displacement (d_s) for one joint specimens.

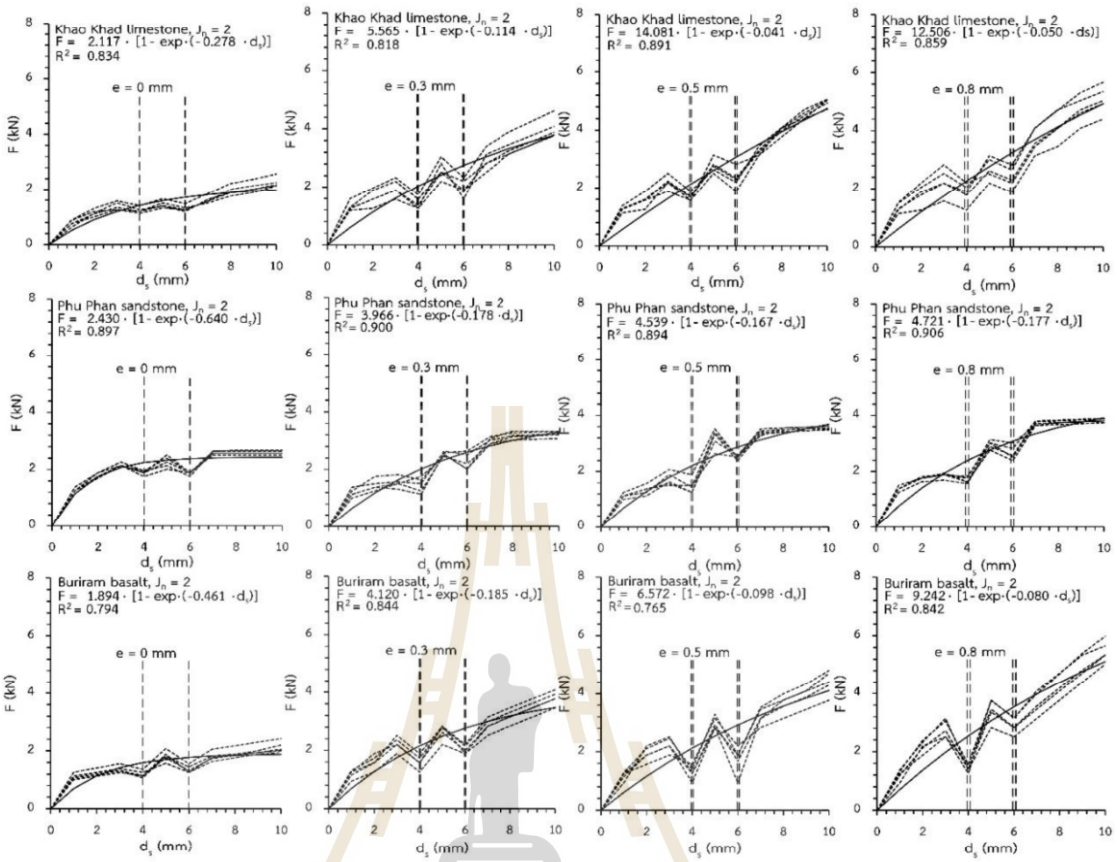

Figure F.3 Lateral force as a function of scratching displacement (d_s) for two joints specimens.

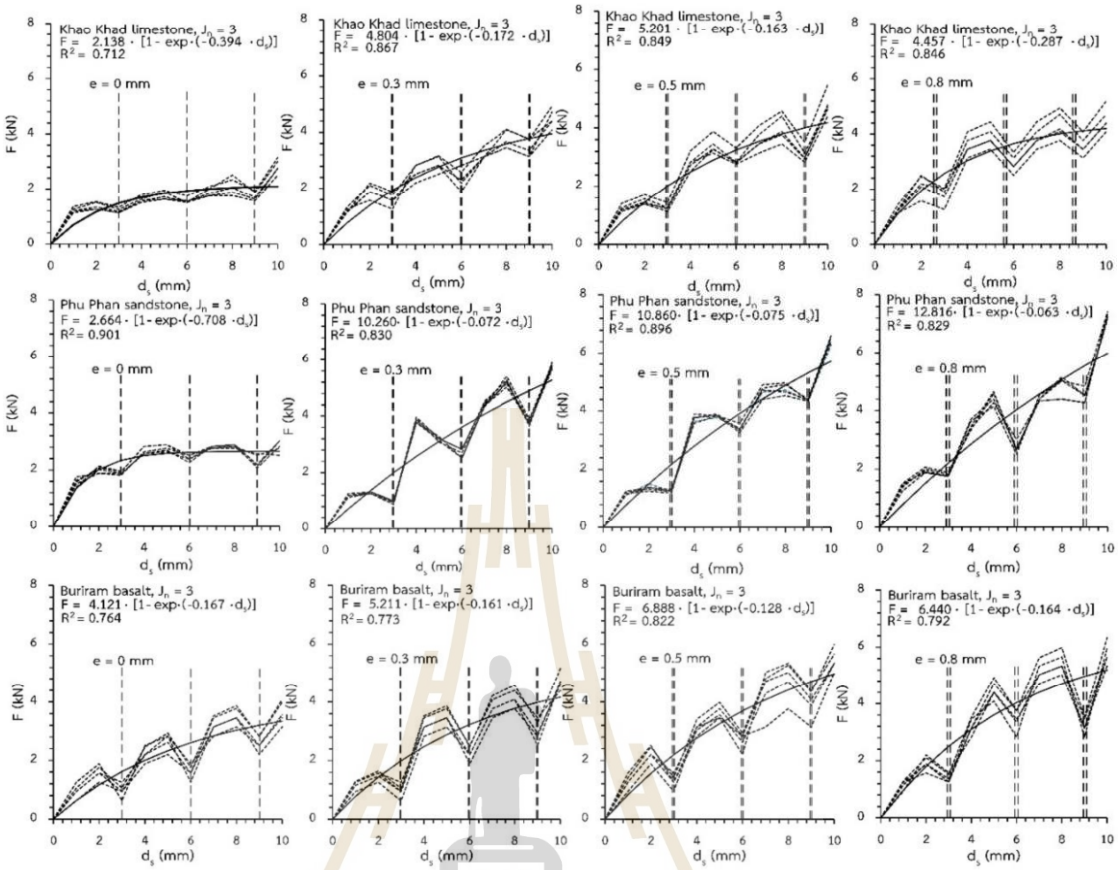

Figure F.4 Lateral force as a function of scratching displacement (d_s) for three joints specimens.

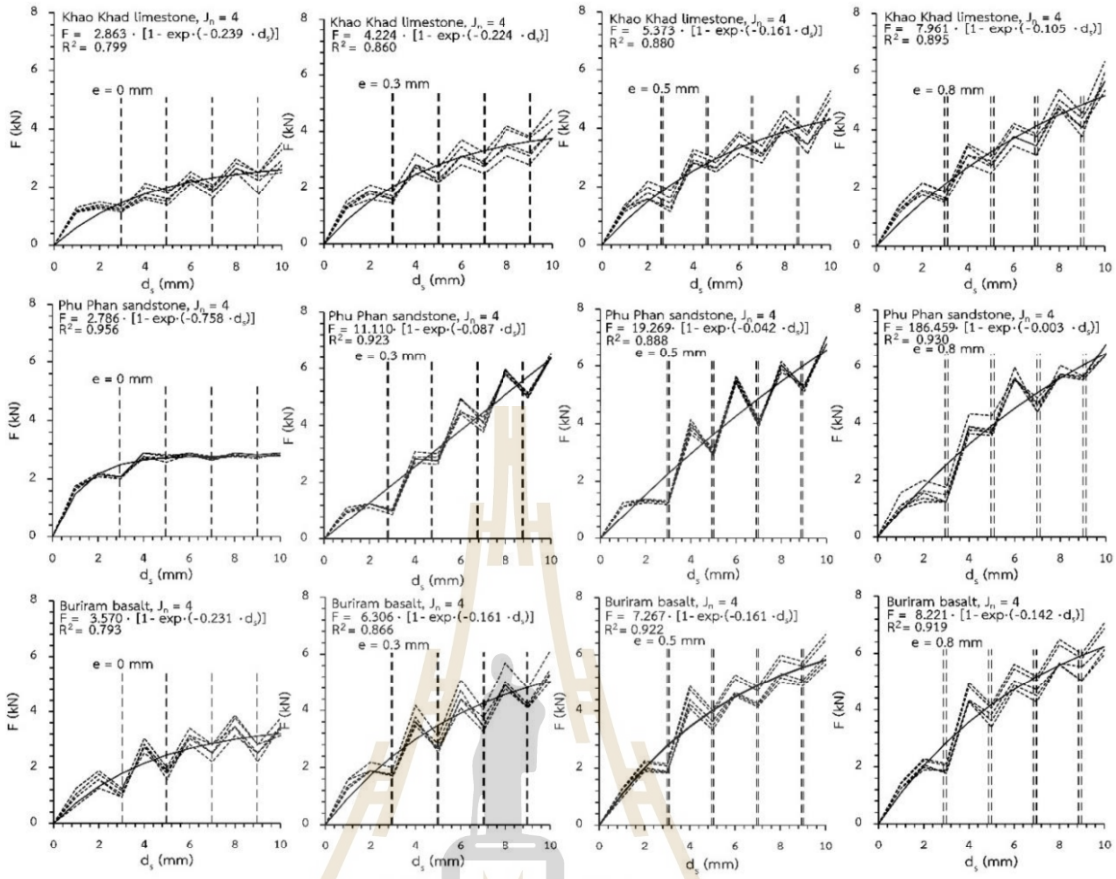

Figure F.5 Lateral force as a function of scratching displacement (d_s) for four joints specimens.

APPENDIX G

LASER - SCANNED IMAGES

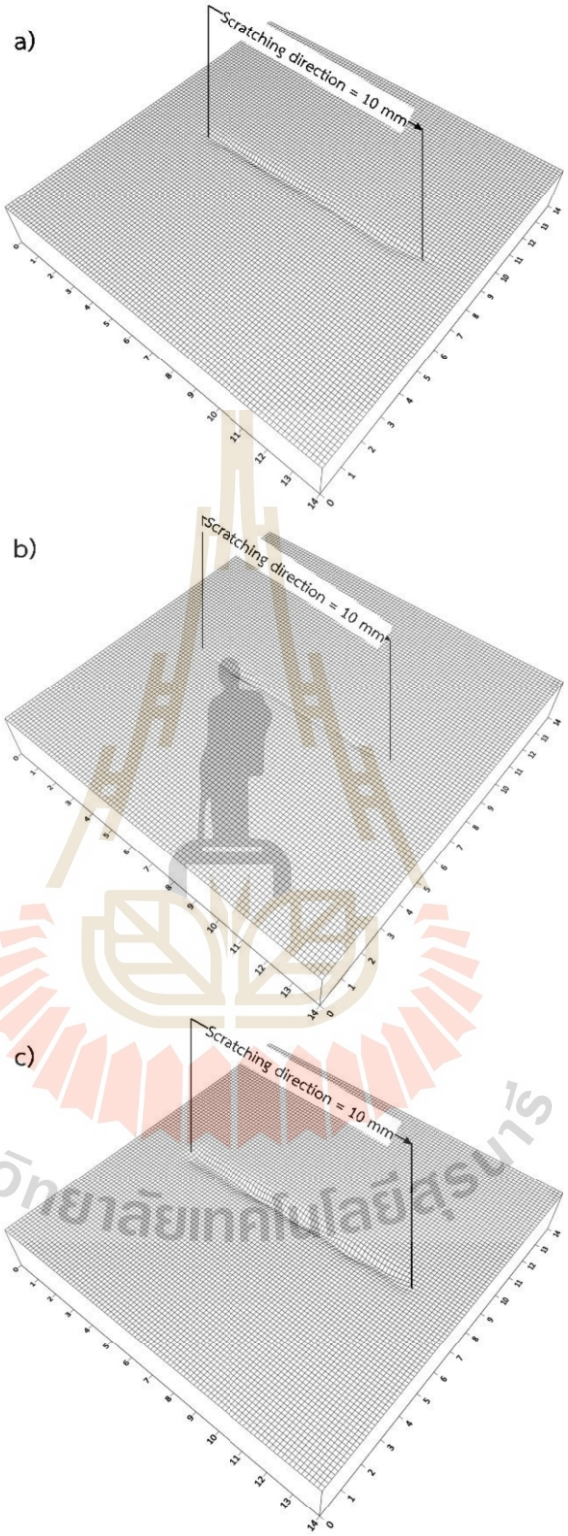

Figure G.1 Example of scratching groove profile on rock surfaces after CAI testing for intact rock for Khao Khad limestone (a), Phu Phan sandstone (b) and Buriram basalt (c). Arrow indicates scratching direction.

Khao Khad limestone, J_n = 1

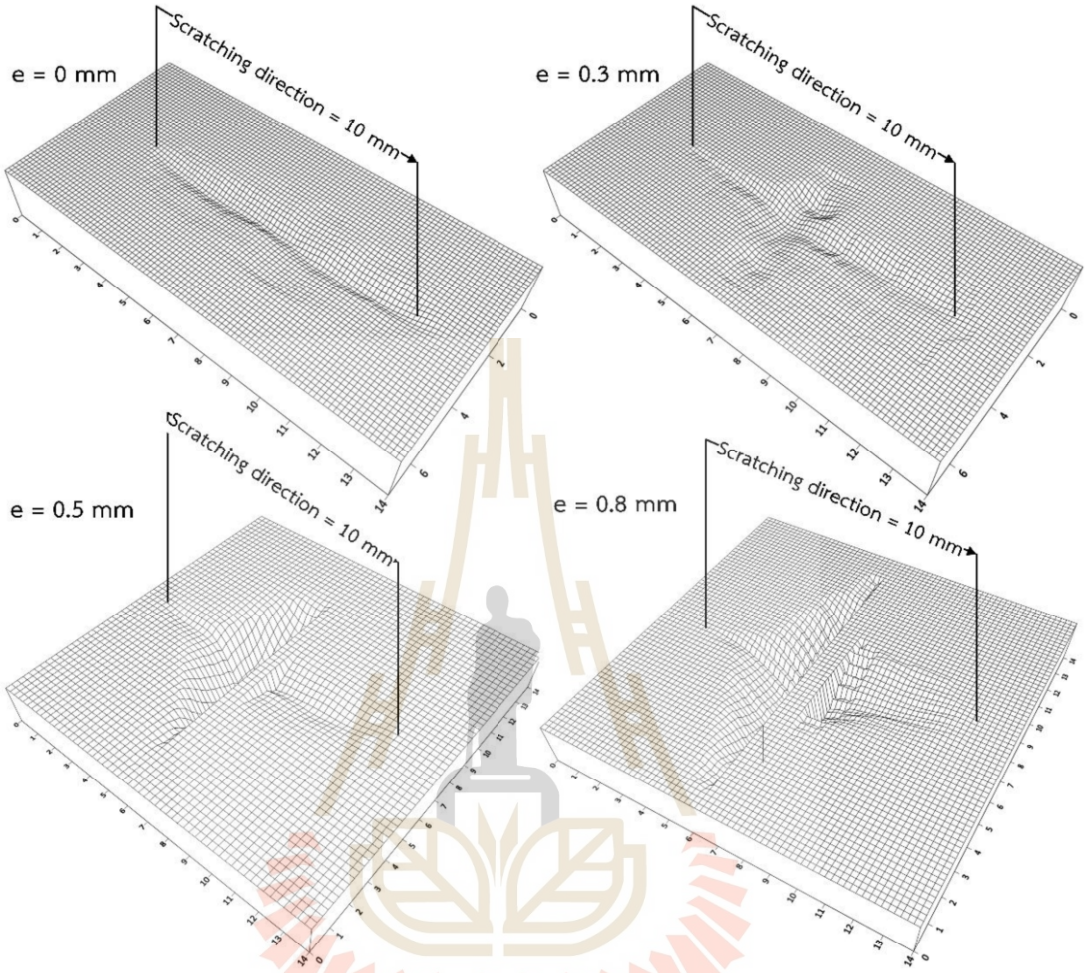

Figure G.2 Example of scratching groove profile on rock surfaces of Khao Khad limestone after CAI testing for one joint. Arrow indicates scratching direction.

Phu Phan sandstone, J_n = 1

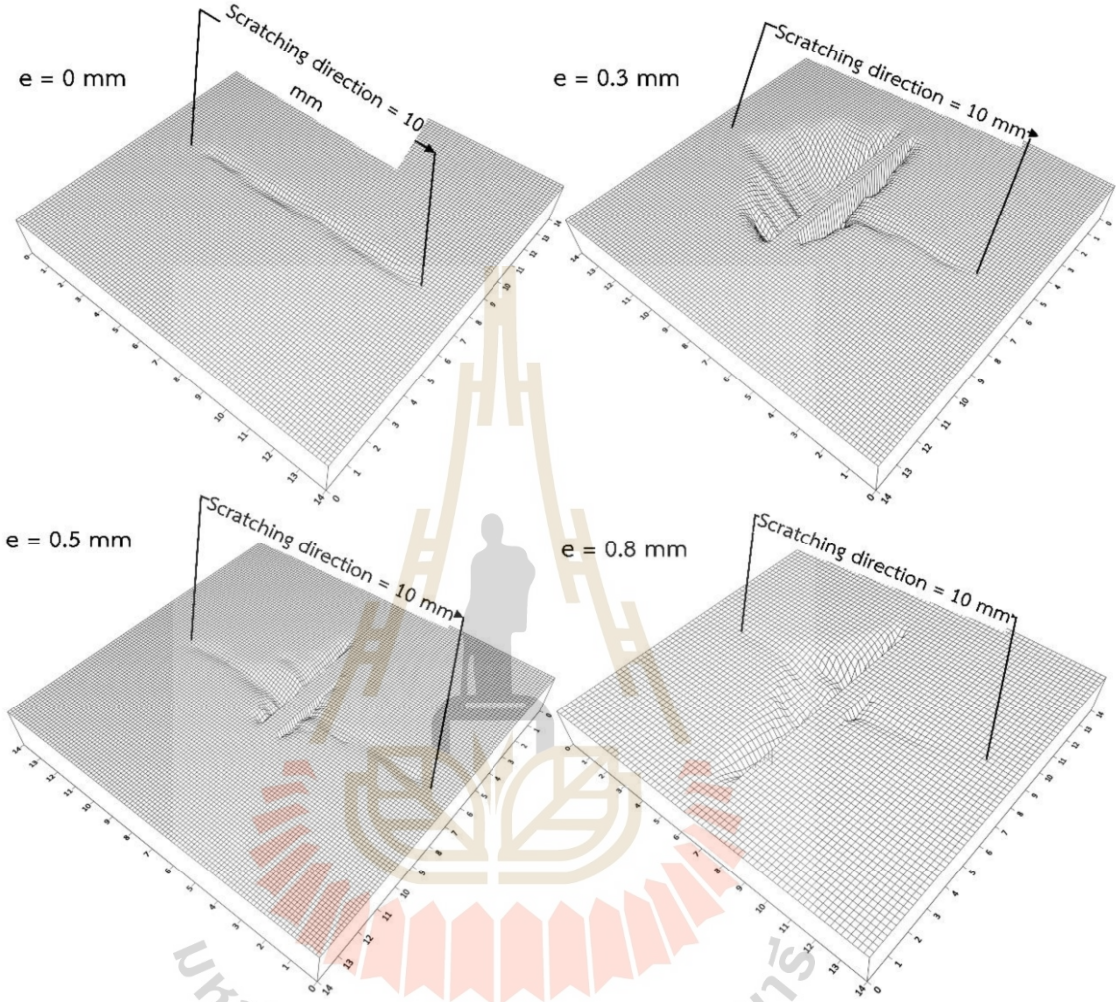

Figure G.3 Example of scratching groove profile on rock surfaces of Phu Phan sandstone after CAI testing for one joint. Arrow indicates scratching direction.

Buriram basalt, J_n = 1

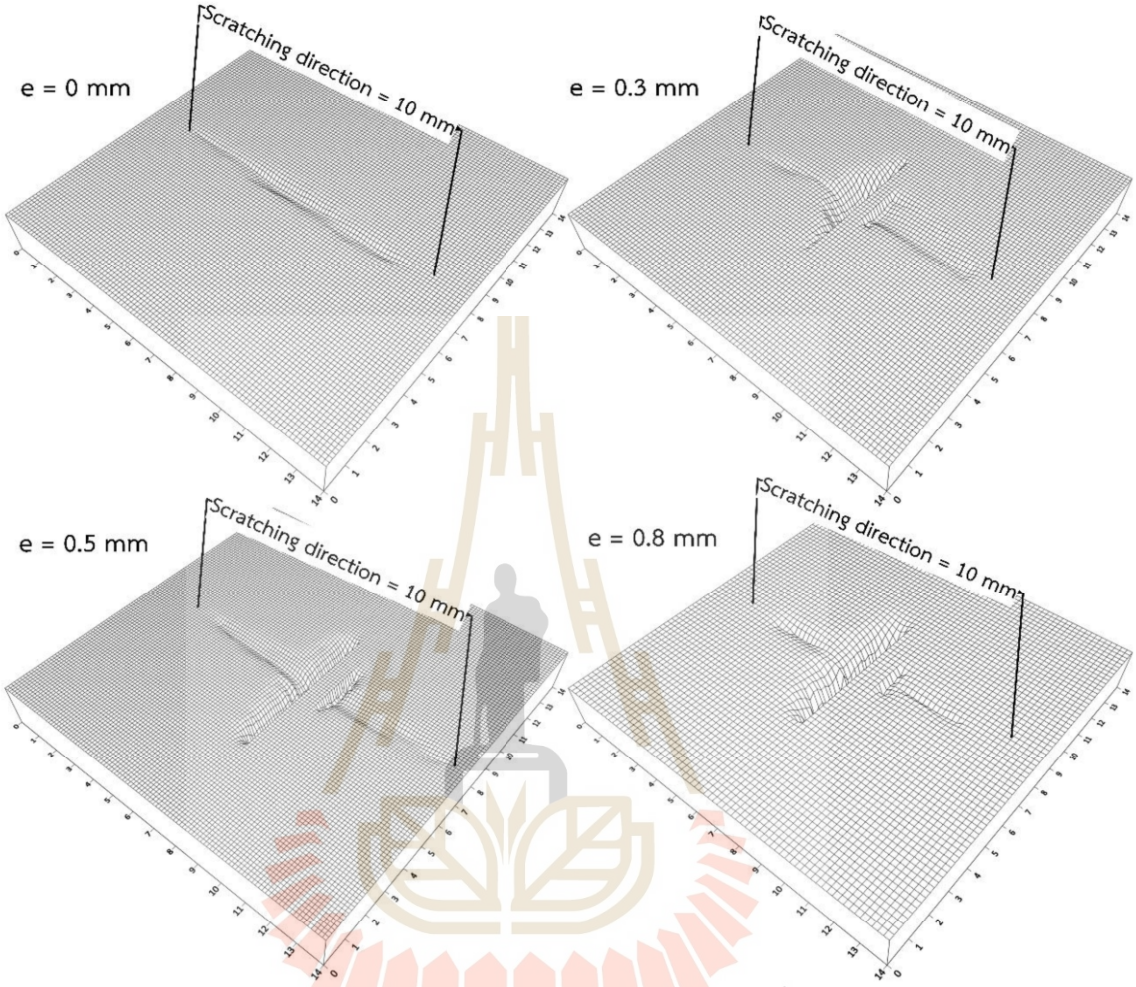

Figure G.4 Example of scratching groove profile on rock surfaces of Buriram basalt after CAI testing for one joint. Arrow indicates scratching direction.

Khao Khad limestone, J_n = 2

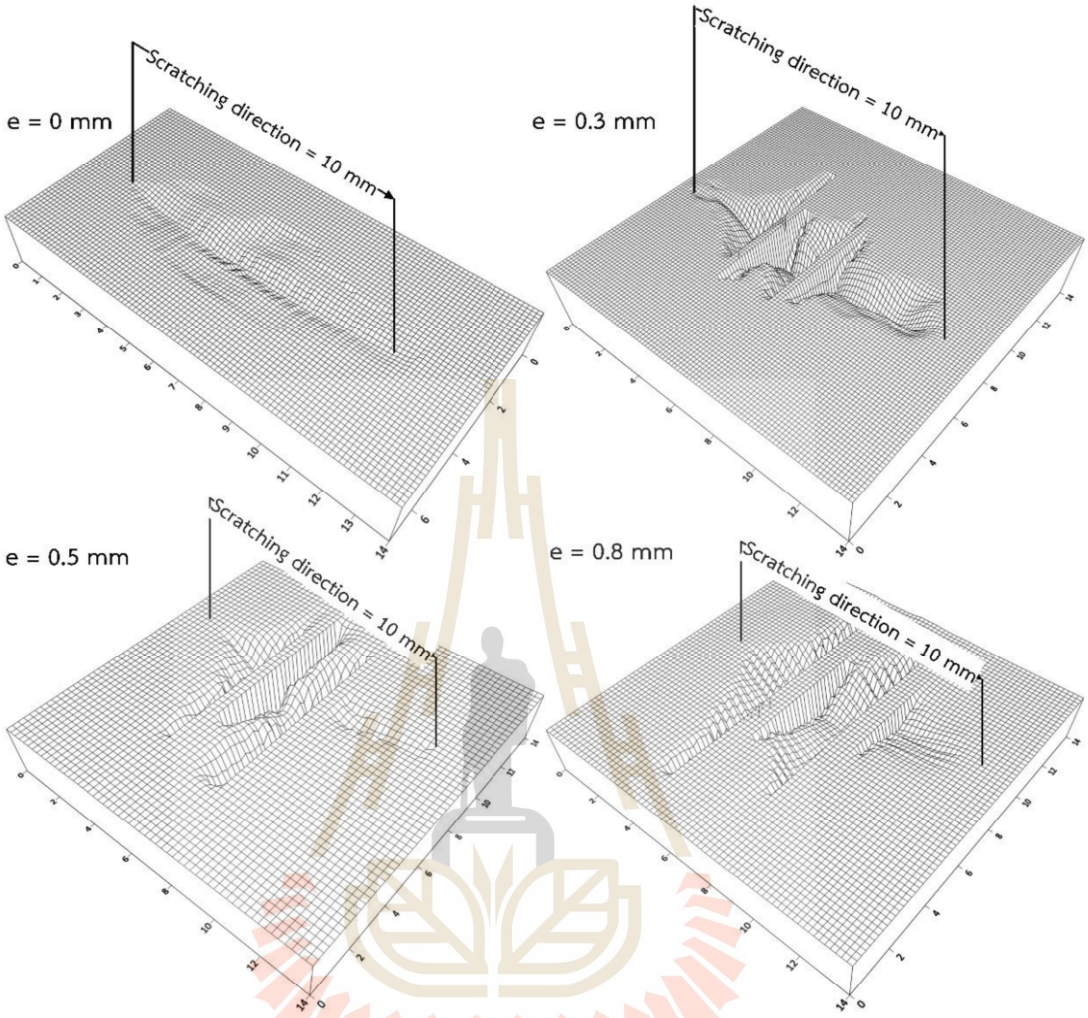

Figure G.5 Example of scratching groove profile on rock surfaces of Khao Khad limestone after CAI testing for two joints. Arrow indicates scratching direction.

Phu Phan sandstone, J_n = 2

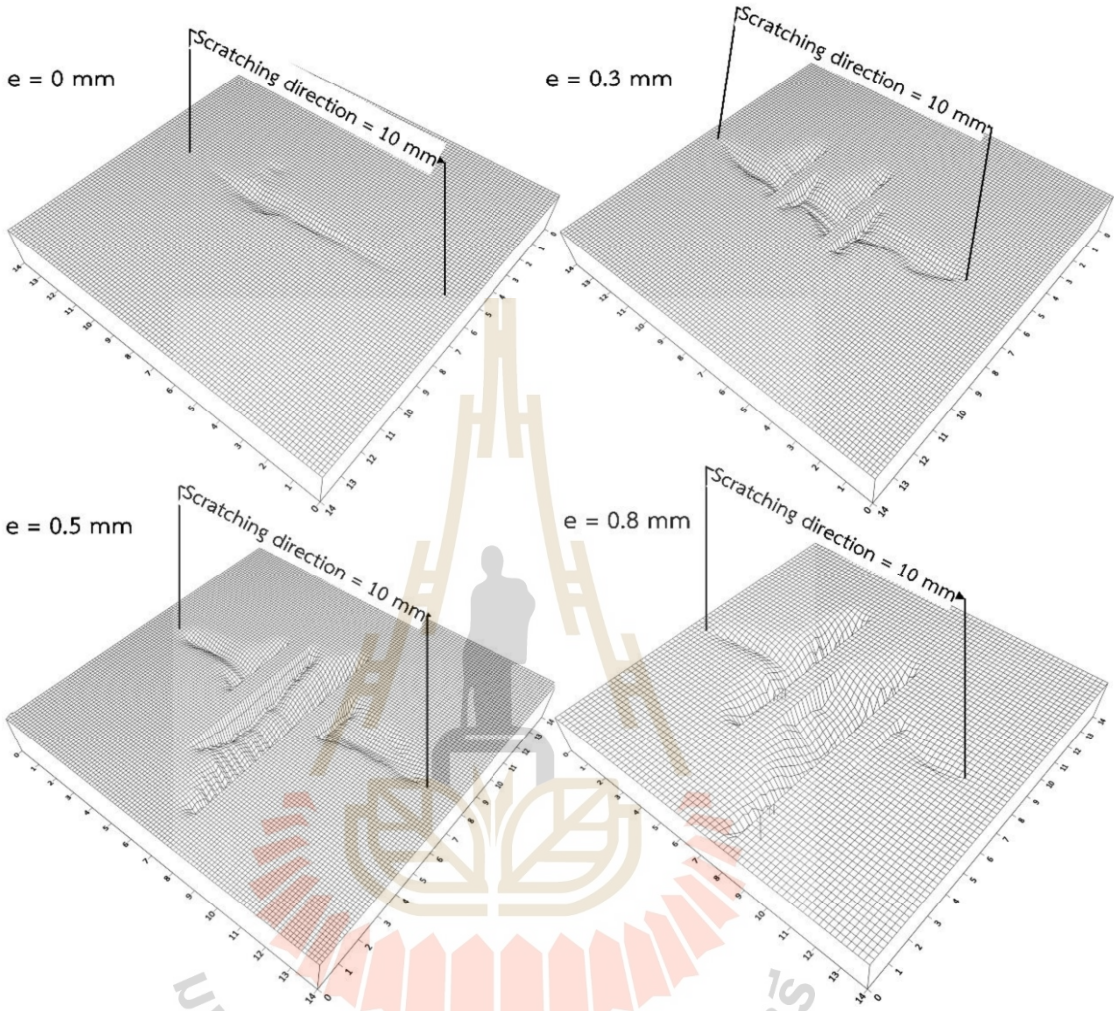

Figure G.6 Example of scratching groove profile on rock surfaces of Phu Phan sandstone after CAI testing for two joints. Arrow indicates scratching direction.

Buriram basalt, J_n = 2

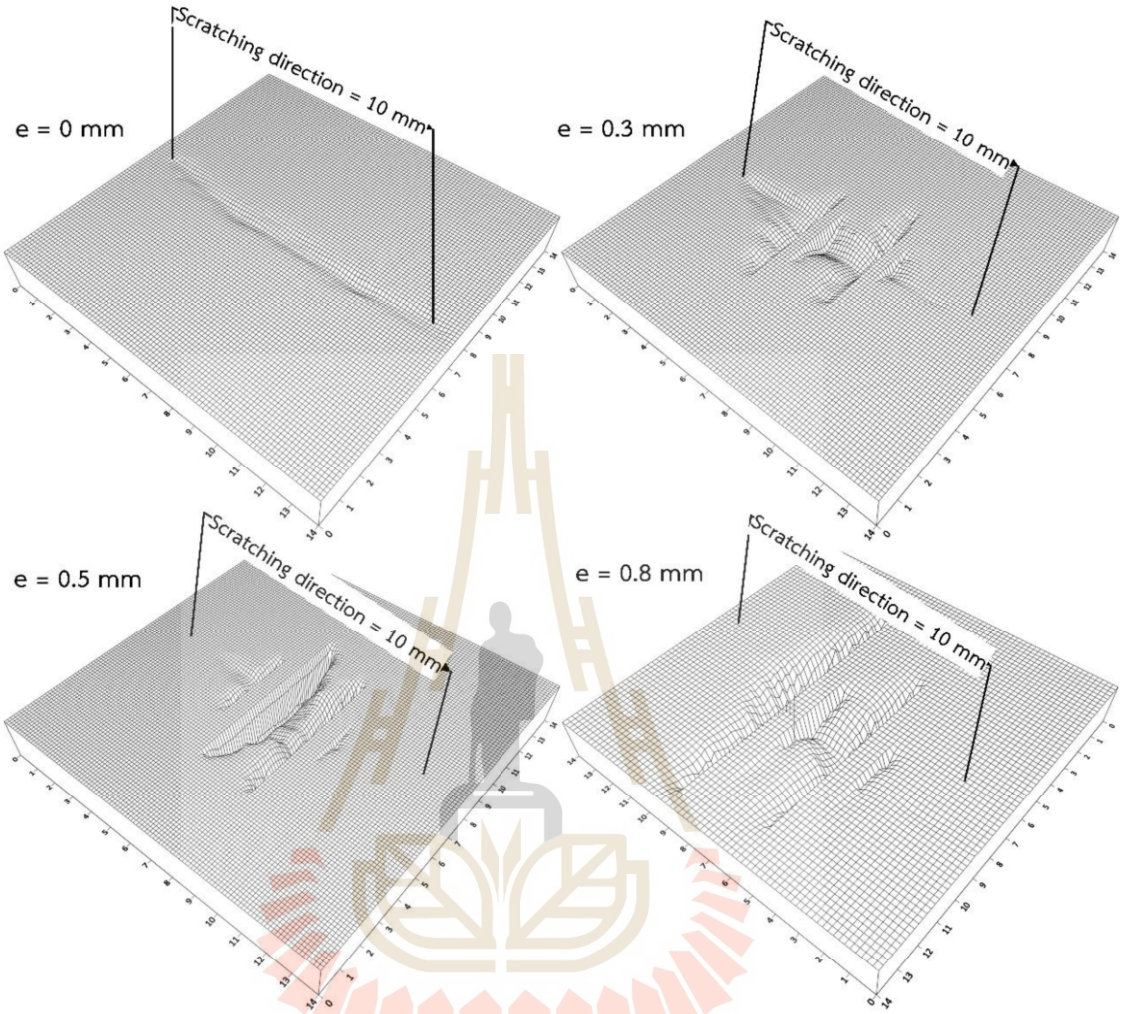

Figure G.7 Example of scratching groove profile on rock surfaces of Buriram basalt after CAI testing for two joints. Arrow indicates scratching direction.

Khao Khad limestone, J_n = 3

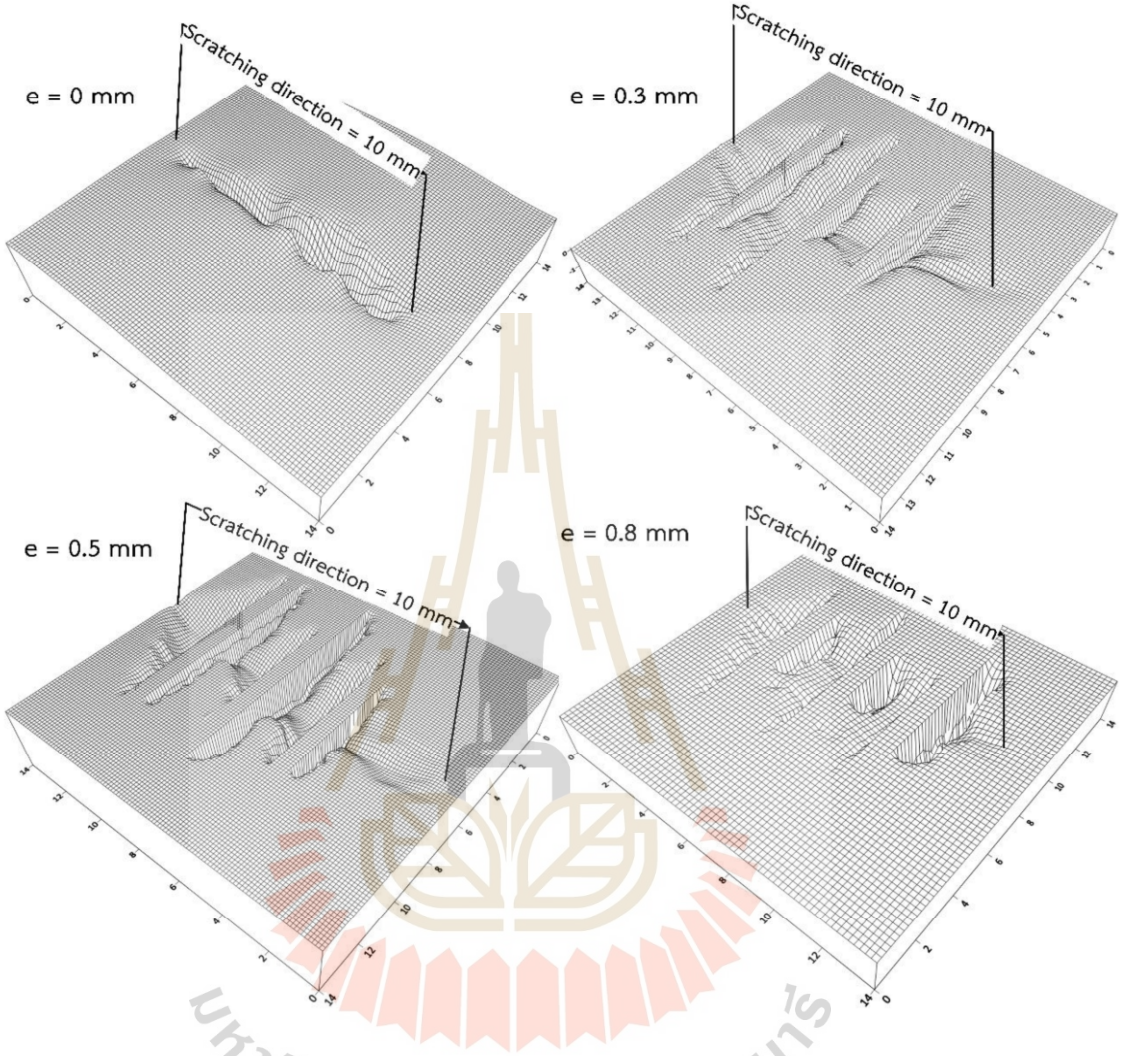

Figure G.8 Example of scratching groove profile on rock surfaces of Khao Khad limestone after CAI testing for three joints. Arrow indicates scratching direction.

Phu Phan sandstone, J_n = 3

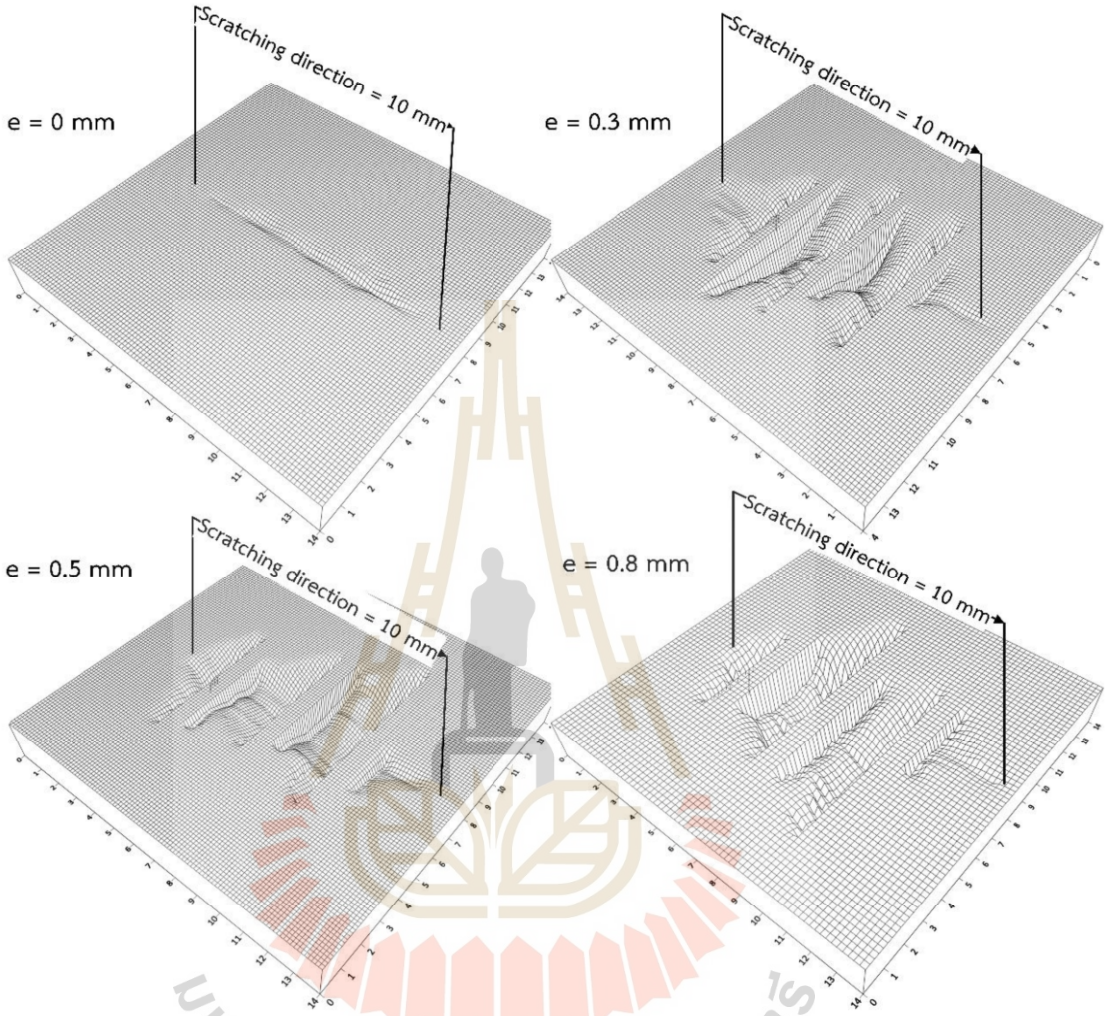

Figure G.9 Example of scratching groove profile on rock surfaces of Phu Phan sandstone after CAI testing for three joints. Arrow indicates scratching direction.

Buriram basalt, J_n = 3

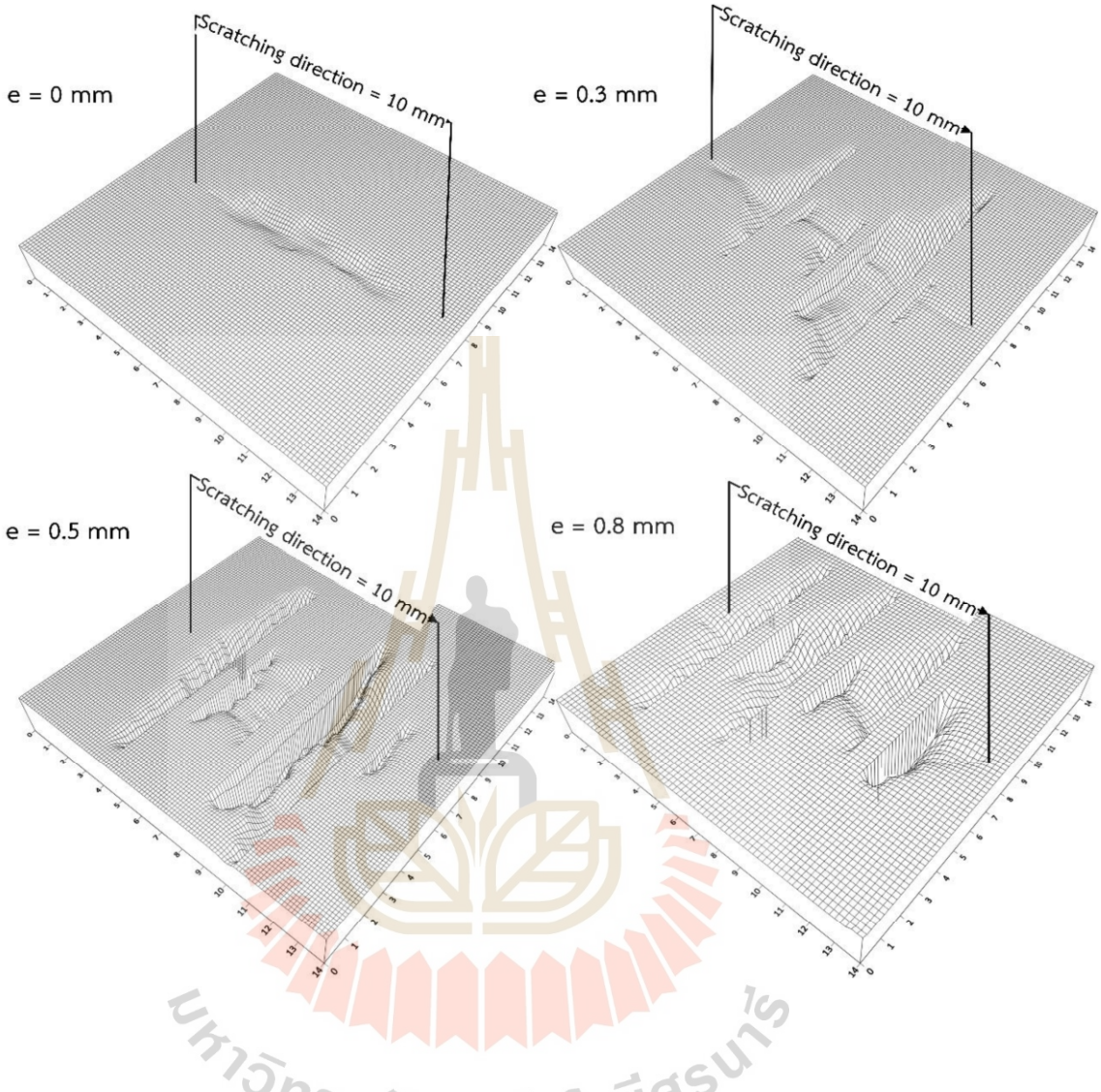

Figure G.10 Example of scratching groove profile on rock surfaces of Buriram basalt after CAI testing for three joints. Arrow indicates scratching direction.

Khao Khad limestone, J_n = 4

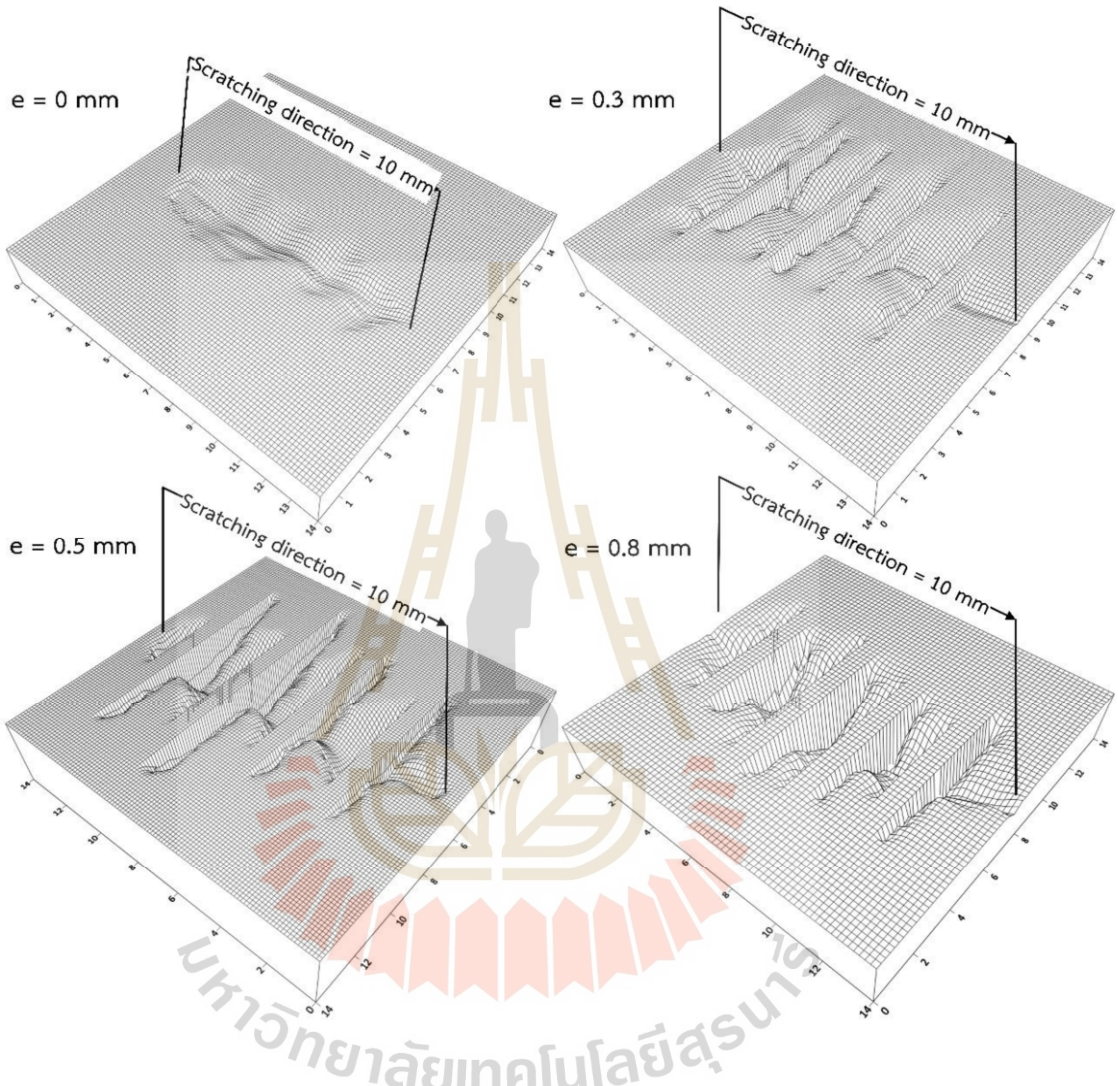

Figure G.11 Example of scratching groove profile on rock surfaces of Khao Khad limestone after CAI testing for four joints. Arrow indicates scratching direction.

Phu Phan sandstone, J_n = 4

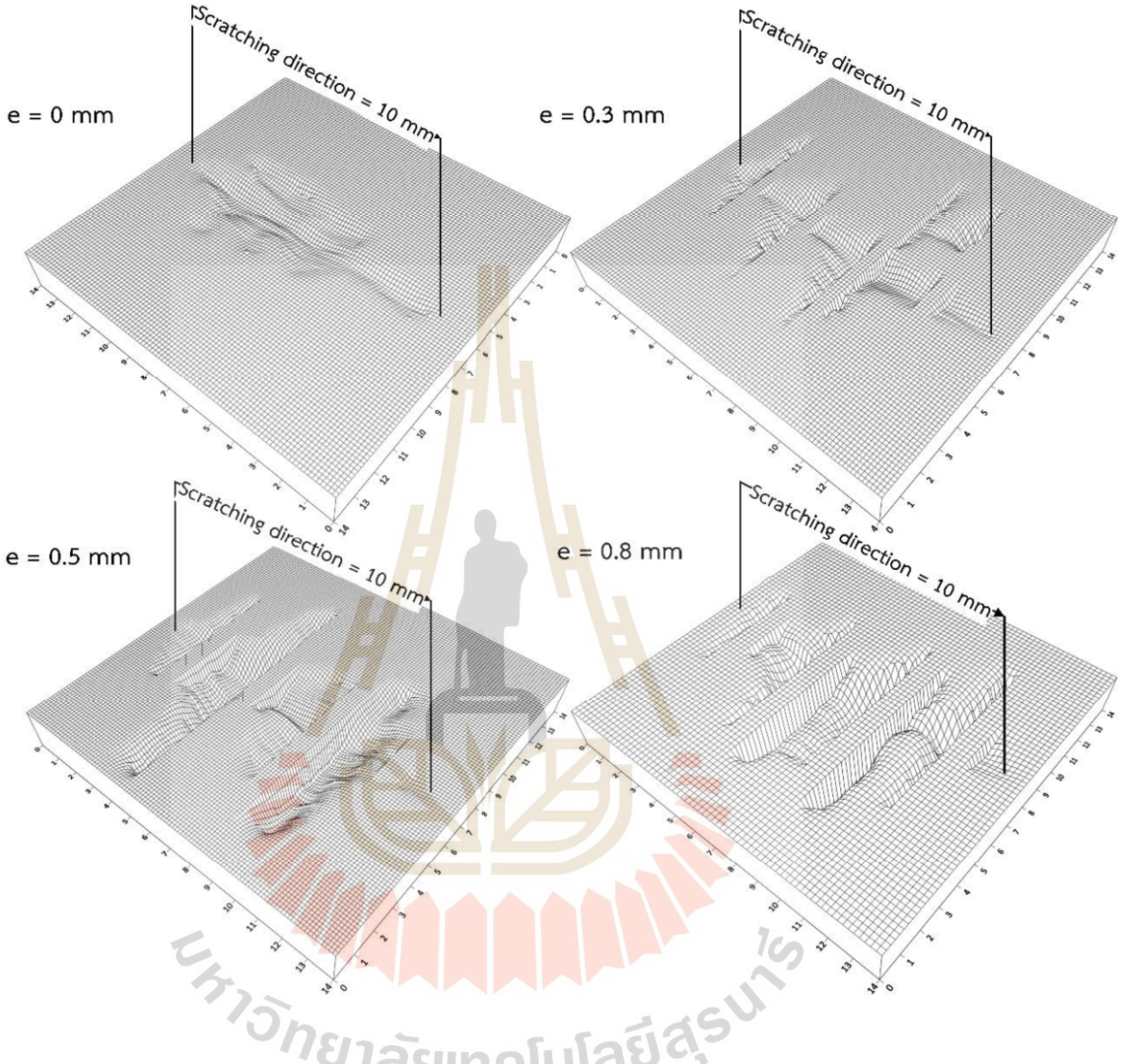

Figure G.12 Example of scratching groove profile on rock surfaces of Phu Phan sandstone after CAI testing for four joints. Arrow indicates scratching direction.

Buriram basalt, J_n = 4

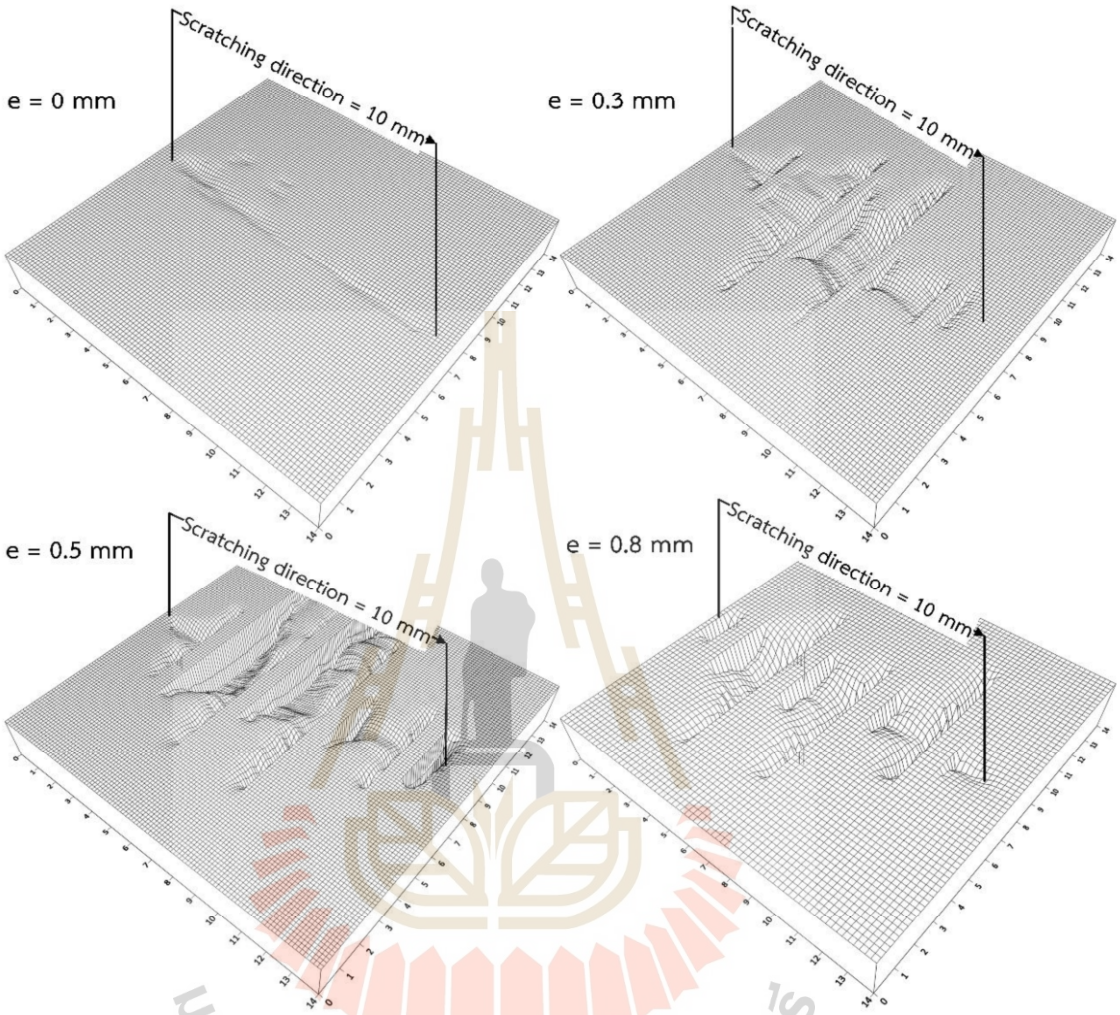

Figure G.13 Example of scratching groove profile on rock surfaces of Buriram basalt after CAI testing for four joints. Arrow indicates scratching direction.

APPENDIX H

LIST OF PUBLICATION

Effect of Rock Joint Frequency and Aperture on CERCHAR Abrasivity Index

Ratchapon Mingkhwan(✉), Thanittha Thongprapha, Laksikar Sitthimongkol, and Kittitep Fuenkajorn

Geomechanics Research Unit, Suranaree University of Technology, 111 University Avenue, Nakhon Ratchasima 30000, Thailand
M6500801@g.sut.ac.th

Abstract. The objective of this study is to investigate the effect of rock joints on the CERCHAR abrasivity index (CAI). Sandstone, limestone, and basalt with parallel fractures with joint numbers varying from 1, 2, 3, to 4, and joint apertures of 0, 0.3, 0.5, to 0.8 mm are tested. The joint spacing is kept constant at 2 mm. The results indicate that the CAI value decreases with increasing joint frequencies and apertures. The ploughing force exerted on the stylus pin is reduced when the pin tip reaches the fracture. This becomes more pronounced as the aperture becomes larger. As the number of joints increases and the separations widen, greater scratching force is increased. The ploughing volume increases as CAI decreases, suggesting that highly fractured rocks show less CAI and less energy to cut while yielding a higher ploughing volume as compared to rock with less fractures.

Keywords: joint number · joint separation · ploughing force · ploughing volume

1 Introduction

Rock abrasiveness is an important factor influencing the performance and longevity of excavation tools leading to significant costs associated with wear and tear. The effectiveness of excavation tools on-site is affected by various rock characteristics, making it essential to gather detailed information about the rock properties in the area before starting any work [1]. Rock abrasiveness is determined by the type of rock and the presence of abrasive minerals within it. As a result, several tests have been developed and widely used for rock identification [2]. Since a huge portion of excavation budget is spent on repair and costly replacement of rock cutting tools which results in time loss [3, 4].

CERCHAR abrasivity index (CAI) is a widely used test for evaluating the abrasion resistance of drill bits. Its popularity is attributed to the method's simplicity, speed, and low cost [5–7], which has driven extensive research to obtain various practical outcomes. The relationship of the CERCHAR abrasivity index (CAI) with various factors has been extensively researched, including testing length [8–10], velocity [11–13], surface conditions [9, 14], mineral and rock composition [15], orientation [16], temperature [17] and mechanical properties [4, 17–19].

T. Kang and Y. Lee (Eds.): ICCEA 2024, LNCE 640, pp. 368–376, 2025.
https://doi.org/10.1007/978-981-96-6115-2_31

Despite the extensive research conducted on the CAI, the current understanding does not fully account for all the variables that influence CAI. Specifically, the effects of number of joints and their aperture width in rock are critical but have not been thoroughly explored. This test introduces a new concept that is an important factor in affecting CAI when observing tool wear. For example when a drill bit encounters a rock formation with a greater number of joints or wide apertures, these structural features can significantly affect the drill bit performance, potentially leading to increased wear or altered drilling efficiency. Understanding these effects is essential for improving the accuracy of CAI as a predictive tool and for optimizing drilling operations in geologically complex environments.

The objective of this study is to assess the effect of rock joints on CAI. Number of joints and their apertures are considered. Three rock types have been tested. Methematical relations between CAI and joint characteristics are developed.

2 Sample Preparation

Three rock types have been used in this study including Khao Khad limestone, Phu Phan sandstone and Buriram basalt. They widely exposed in the northeast of Thailand. The rock specimens are cut and ground to produce saw-cut surface in accordance with the ASTM D7625–22 standard practice. Rectangular block specimen with nominal dimensions of 80 × 50 × 40 mm^3 are obtained with artificial fractures (saw-cut) normal to the test surfaces. The numbers of parallel joints are varied from 1 to 4, with joint apertures from 0 to 0.8 mm. The joint apertures are made by using filler gages placed between thin slaps of rock specimens to obtain a precise gap (aperture) between them. These thin slaps are then glued together while maintaining the desired joint apertures and spacing.

3 Test Method

The CERCHAR abrasivity test follows the ASTM D7625–22 standard practice with an apparatus similar to the West apparatus (Fig. 1). Five scratching lines are made perpendicular to joint aperture (Fig. 2).

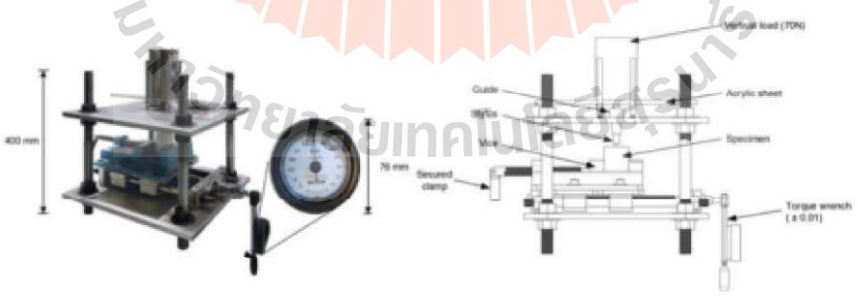

Fig. 1. Device based on West CERCHAR apparatus [20] with additional torque [13].

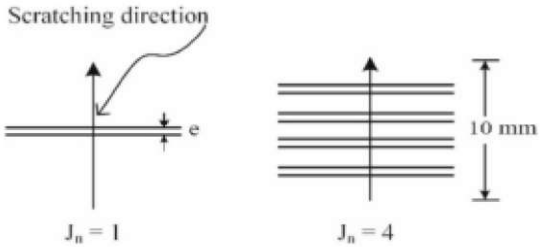

Fig. 2. Scratching direction perpendicular to joints with $J_n = 1$ to 4 and e = 0, 0.3, 0.5 to 0.8 mm.

The ploughing force during scratching is measured by a torque meter to calculate the scratching energy, which is affected by different joint characteristics. The force can be calculated using the following equation [13]:

$$F = 2\pi T/P \tag{1}$$

where F is ploughing force (N), T is torque (N•m) and P is screw pitch (0.001 m). The rock surface after CAI testing have been laser-scanned to observe groove shape and to calculate the groove volume. The measurements are made to the nearest 0.001 mm.

4 Test Results

4.1 Correlation Between CAI and Rock Joint Characteristics

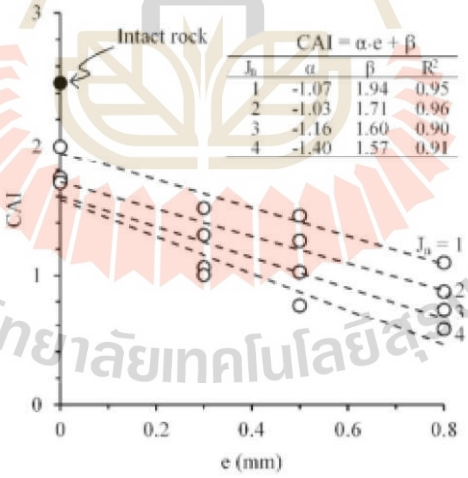

Fig. 3. CAI as a function of joint aperture (e) for different numbers of joints (J_n) for Buriram basalt.

Result of the CAI tests are shown in Table 1. The CAI value of Buriram basalt tends to decrease with increasing number of joints (J_n) and aperture (e) (Fig. 3). This is true for all rock types. This is because the stylus contacts the rock surface less frequently when larger gaps (apertures) are present within a 10 mm scratching length, leading to less abrasion. A linear equation is proposed to present relationship between CAI and joint aperture, as follows;

$$CAI = \alpha \cdot e + \beta \tag{2}$$

where α and β are empirical constants, and e is joint aperture. Good correlations are obtained ($R^2 > 0.9$). Table 1 gives these empirical constants for all tested rocks.

4.2 Correlation Between Force and Rock Joint Characteristics

Figure 4 shows example of scratching force as a function of distance for limestone. The force (F) increases with scratching displacement (d_s) and number of joints. Rock with higher number of joints and aperture requires greater ploughing force as compared to those with fewer joints. Joint apertures show more effect on the ploughing force than does number of joints. The correlation between F-ds can be described by an exponential equation [15], as follows:

$$F = a \cdot \left[1 - \exp \cdot (-b \cdot d_s)\right] \tag{3}$$

where a and b are empirical constants, good correlation is obtained ($R^2 > 0.9$). Table 1 summarizes the result for the three rock types.

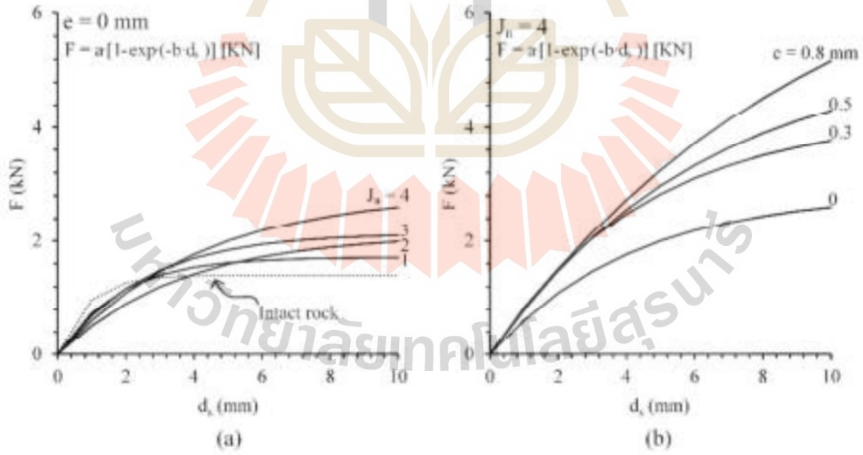

Fig. 4. Scratching force as a function of distance for joint aperture (e) = 0 mm under different numbers of joints (a), and under $J_n = 4$ with different apertures (b) for Khao Khad limestone.

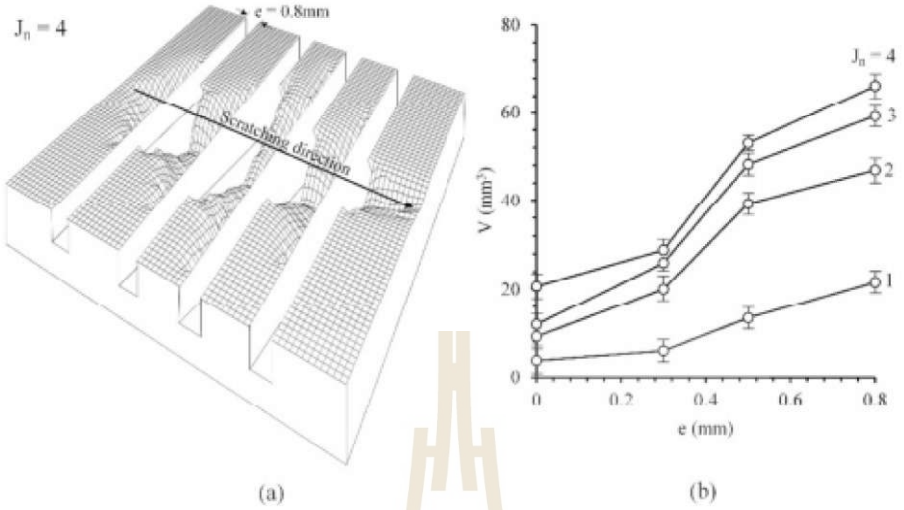

Fig. 5. Example of scratching groove profile of sandstone with $J_n = 4$ (a), and groove volume as a function of joint aperture with different J_n values (b) for sandstone.

4.3 Correlation Between Groove Volume and Rock Joint Characteristics

Figure 5a shows that the groove volume of material scratched increases as the stylus approaches joints. This increase is attributed to the reduced rock surface area before the material fails under the applied load force, leading to a larger groove volume of material being removed along the joint. Figure 5b shows that the groove volume of the scratched area increases with joint aperture (e). A larger e, which may correspond to increased Jn or e, results in a greater groove volume of material being scratched out.

The CAI values decrease as a result of both J_n and e. This reduction is attributed to the stylus tip entering the joint apertures during the test, which led to a smaller abrasion of the stylus. The stylus tip did not maintain contact with the entire rock surface over the 10 mm distance, resulting in reduced overall abrasion.

Sandstone and basalt show higher CAI values than limestone. This may be due to the dependence of CAI on rock strength, as indicated by previous studies [14, 15], which report strengths of 81.43 MPa for sandstone, 79.17 MPa for basalt and 54.61 MPa for limestone. Hard rock gives greater CAI values and more affected by joint characteristics than softer ones.

The force measured during the CAI increases with Jn and e. Higher numbers of joints and larger apertures required higher force to scratch the rock surface. This is attributed to the stylus encountering the gaps created by larger apertures, with additional resistance. This is because when the stylus passes through a large gap, it drops and requires more force to step up to continue scratching.

Table 1. CERCHAR abrasivity index, force and groove volume for all rocks.

Rock type	J_n	e	CAI	CAI = α•e + β		F = a · [1 - exp · (-b · d_s)]		V
		(mm)		α (mm^{-1})	β	a (N)	b (mm^{-1})	(mm^3)
Khao Khad limestone	0	–	1.75			1.40	1.19	1.14
		0	1.47			1.78	0.56	1.12
	1	0.3	1.37	−0.65	1.51	3.21	0.32	3.01
		0.5	1.17			3.81	0.28	11.78
		0.8	0.96			4.64	0.20	16.05
		0	1.36			2.11	0.27	1.92
	2	0.3	1.13	−0.52	1.32	5.56	0.11	10.36
		0.5	1.02			14.08	0.04	21.05
		0.8	0.94			12.50	0.05	32.74
		0	1.25			2.13	0.39	5.25
	3	0.3	1.10	−0.63	1.27	4.80	0.17	16.90
		0.5	0.95			5.20	0.16	40.44
		0.8	0.75			4.45	0.28	50.99
		0	0.97			2.86	0.23	14.71
	4	0.3	0.95	−0.35	1.00	4.22	0.22	20.26
		0.5	0.80			5.37	0.16	47.65
		0.8	0.71			7.96	0.10	54.63
Phu Phan sandstone	0	–	2.27			1.54	1.05	1.58
		0	1.63			1.51	1.34	3.68
	1	0.3	1.56	−0.80	1.67	1.86	0.63	5.89
		0.5	1.20			2.16	0.44	13.34
		0.8	1.04			2.58	0.61	21.61
		0	1.41			2.43	0.64	9.09
	2	0.3	1.08	−0.71	1.36	3.96	0.17	20.03
		0.5	0.96			4.53	0.16	39.21
		0.8	0.83			4.72	0.17	46.92
		0	1.34			2.66	0.70	11.87
	3	0.3	0.95	−0.73	1.27	10.26	0.07	25.95
		0.5	0.88			10.86	0.07	48.20

(*continued*)

Table 1. (*continued*)

Rock type	J_n	e	CAI	CAI = α•e + β		F = a · [1 - exp · (-b · d_s)]		V
		(mm)		α (mm^{-1})	β	a (N)	b (mm^{-1})	(mm^3)
		0.8	0.73			12.81	0.06	59.19
		0	1.23			2.78	0.75	20.67
	4	0.3	0.72	−0.81	1.12	11.11	0.03	28.81
		0.5	0.69			19.26	0.04	52.99
		0.8	0.57			186.45	0.09	66.31
Buriram basalt	0	–	2.47			2.06	0.42	3.08
		0	1.99			2.14	0.47	0.85
	1	0.3	1.51	−1.07	1.94	3.11	0.27	2.87
		0.5	1.45			4.58	0.16	10.75
		0.8	1.09			5.76	0.12	13.78
		0	1.74			1.89	0.46	2.49
	2	0.3	1.0	−1.03	1.71	4.12	0.18	11.02
		0.5	1.26			6.57	0.09	29.16
		0.8	1.87			9.24	0.08	38.15
		0	1.71			4.12	0.16	3.89
	3	0.3	1.06	−1.16	1.60	5.21	0.16	14.87
		0.5	1.02			6.88	0.12	34.60
		0.8	0.87			6.44	0.16	47.72
		0	1.70			3.57	0.23	13.85
	4	0.3	1.00	−1.40	1.57	6.30	0.16	18.37
		0.5	0.77			7.26	0.16	42.57
		0.8	0.57			8.22	0.14	51.21

5 Discussions

The results obtained here are limited to the condition at which the scratching direction is only normal to the joint lines with one joint set. The effect of the angles between scratching direction and joint line has not been investigated.

6 Conclusion

The results obtained here can be concluded as follows.

- Number of joint and aperture can decrease the wear of stylus pin (CAI) while

- The effects of joint aperture and joint number on CAI and ploughing force pronounce more in strong rock (basalt) than in soft rock (limestone).
- The groove volume increases more rapidly for larger numbers of joints, as compared to smaller number of joints.
- The effect of joint aperture on groove volume is more significant in soft rock than in the stronger one.

References

Thuro, K., Käsling, H.: Classification of the abrasiveness of soil and rock. Geomechanics Tunnelling. **2**(2), 179–188 (2009)

Ghasemi, A.: Study of CERCHAR abrasivity index and potential modifications for more consistent measurement of rock abrasion. Master Thesis, Pennsylvania State University (2010)

Fowell, R.J., Bakar, A.M.Z.: A review of the CERCHAR and LCPC rock abrasivity measurement methods. In: Proceeding of the 11th Congress of the International Society for Rock Mechanics, pp. 155–160 (2007)

Hamzaban, M.T., Memarian, H., Rostami, J.: Continuous monitoring of pin tip wear and penetration into rock surface using a new Cerchar abrasivity testing device. Rock Mech. Rock Eng. **47**(2), 689–701 (2014)

Prieto, L.A.: The CERCHAR abrasivity index's applicability to dredging rock. In: Proceedings of Western Dredging Association (WEDA XXXII) Technical Conference and Texas A&M University (TAMU 43) Dredging Seminar; San Antonio, Texas, pp. 212–9 .June 10–13 (2012)

Ko, T.Y., Kim, T.K., Son, Y., Jeon, S.: Effect of geomechanical properties on CERCHAR abrasivity Index (CAI) and its application to TBM tunnelling. Tunnel Underground Space Technol. **57**, 99–111 (2016)

Hamzaban, M.T., Karami, B., Rostami, J.: Effect of pin speed on CERCHAR abrasion test results. J. Test. Eval. **47**(1), 121–39 (2019)

Al-Ameen, S.I., Waller, M.D.: The influence of rock strength and abrasive mineral content on the Cerchar abrasive index. Eng. Geol. **36**(3–4), 293–301 (1994)

Plinninger, R., Käsling, H., Thuro, K., Spaun, G.: Testing conditions and geomechanical properties influencing the CERCHAR abrasiveness index (CAI) value. Int. J. Rock Mech. Min. Sci. **40**(2), 259–263 (2003)

Yaralı, O., Duru, H.: Investigation into effect of scratch length and surface condition on Cerchar abrasivity index. Tunn. Undergr. Space Technol. **60**(36), 111–120 (2016)

Kotsombat, T., Thongprapha, T., Fuenkajorn, K.: Scratching rate effects on cerchar abrasiveness index of sandstones. In: Academicsera International Conference, Chiang Mai, Thailand, pp. 6–9 (2020)

Plinninger, R. J., Kasling, H., Thuro, K.: Wear prediction in hardrock excavation using the CERCHAR abrasiveness index (CAI). EUROCK 2004 & 53rd Geomechanics Colloquium. Schubert (ed.). pp. 1–6 (2004)

Rostami, J., Ghasemi, A., Alavi Gharahbagh, E., Dogruoz, C., Dahl, F.: Study of dominant factors affecting Cerchar abrasivity index. Rock Mech. Rock Eng. **47**, 1905–1919 (2014)

Thanadkha, P., Fuenkajorn, K.: Correlation between cerchar abrasivity index of smooth and rough rock fractures. In: Academicsera International Conference, Kuala Lumpur, Malaysia, pp. 8–12 (2022)

Kathancharoen, N., Fuenkajorn, K.: Effects of mechanical and mineralogical properties on cerchar abrasivity index and specific energy of some Thai rocks. Eng. Appl. Sci. Res. **50**(5), 478–489 (2023)

Alber, M., Yarali, O., Dahl, F., et al.: ISRM suggested method for determining the abrasivity of rock by the CERCHAR abrasivity test. In: Ulusay R (ed) The ISRM suggested methods for rock characterization, testing and monitoring, Springer, 2007–2014, Publishing, Cham, pp. 101–106 (2015)

Ji, Y., Wang, L., Zheng, Y., Wu, W.: Temperature-dependent abrasivity of Bukit Timah granite and implications for drill bit wear in thermomechanical drilling. Acta Geotech (2020)

Capik, M., Yilmaz, A.O.: Correlation between Cerchar abrasivity index, rock properties, and drill bit lifetime. Arab. J. Geosci. **10**(15), 1–12 (2017)

Alber, M.: Stress dependency of the Cerchar abrasivity index (CAI) and its effects on wear of selected rock cutting tools. Tunn. Undergr. Space Technol. **23**(4), 351–359 (2008)

Deliormanlı, A.H.: Cerchar abrasivity index (CAI) and its relation to strength and abrasion test methods for marble stones. Constr. Build. Mater. **30**, 16–21 (2012)

West, G.: Rock abrasiveness testing for tunnelling. Int. J. Rock Mech. Min. Sci. Geomech. Abstracts **26**(2), 151–160 (1989)

BIOGRAPHY

Mr. Ratchapon Mingkhwan was born on November 17, 1999 in Chanthaburi, Thailand. He received his Bachelor's Degree in Engineering (Geological Engineering) from Suranaree University of Technology in 2021. For his post-graduate, he continued to study with a Master of Degree Program in the Geological Engineering Program, Institute of Engineering, Suranaree university of Technology. During graduation, 2018-2022, he was a part time worker in position of research associate at the Geomechanics Research Unit, Institute of Engineering, Suranaree University of Technology.